

THERMOECONOMICS OF LITHIUM BROMIDE/WATER ABSORPTION  
CHILLERS AND HEAT TRANSFORMERS

By

SHUN-FU LEE

A DISSERTATION PRESENTED TO THE GRADUATE SCHOOL  
OF THE UNIVERSITY OF FLORIDA IN PARTIAL FULFILLMENT  
OF THE REQUIREMENTS FOR THE DEGREE OF  
DOCTOR OF PHILOSOPHY

UNIVERSITY OF FLORIDA

1999

## ACKNOWLEDGMENTS

My sincerest gratitude goes to all of those who have been directly and indirectly involved. First, I would like to thank my advisor Dr. S. A. Sherif for his constant encouragement, assistance, and patient guidance. He encouraged me throughout my study. I would also like to thank Dr. D. Y. Goswami, Dr. C. K. Hsieh, and Dr. H. A. Ingley for their suggestions, and Dr. C. D. Baird for the time and effort he devoted to the dissertation review. Support from the Department of Mechanical Engineering at the University of Florida is also gratefully acknowledged.

Most importantly, my deep appreciation goes to my family for their abundant love, support, and inspiration they have always provided. Finally, I would like to acknowledge my wife, Hsiao-Yun, for her love, encouragement, and tolerance. This would not have been possible solely by myself.

## TABLE OF CONTENTS

	<u>Page</u>
ACKNOWLEDGMENTS .....	ii
ABSTRACT.....	vi
 CHAPTERS	
1 INTRODUCTION .....	1
1.1 Background .....	1
1.2 Literature Survey .....	7
1.2.1 Studies of Working Fluid Pairs.....	8
1.2.2 Studies of Various Absorption Systems .....	9
1.2.3 Studies of Applications and Economics of Absorption Systems.....	11
1.3 Objectives of Research.....	11
2 THERMODYNAMIC ANALYSIS OF ABSORPTION SYSTEMS AND METHODOLOGY OF SIMULATION.....	14
2.1 Background .....	14
2.2 Thermodynamic Principles .....	15
2.2.1 First Law Analysis .....	16
2.2.2 Second Law Analysis.....	17
2.3 Thermal Properties of Working Fluids .....	20
2.3.1 Thermal Properties of Lithium Bromide/Water Solution .....	20
2.3.2 Thermal Properties of Water and Vapor .....	24
2.4 Component Models.....	27
2.4.1 Absorber.....	27
2.4.2 Generator.....	29
2.4.3 Condenser .....	29
2.4.4 Evaporator.....	30
2.4.5 Solution Heat Exchanger .....	31
2.4.6 Throttling Valve.....	31
2.4.7 Mixer.....	31
2.4.8 Splitter.....	32
2.4.9 Solution Pump.....	32
2.5 Methodology of Simulation and Assumptions .....	32

3	ABSORPTION CHILLERS AND HEAT PUMPS .....	36
3.1	Ideal Absorption Chiller and Heat Pump Cycles .....	37
3.2	Single-Effect Absorption Chillers .....	39
3.2.1	Description of Single-Effect Absorption Chillers .....	39
3.2.2	Thermodynamic Analysis of Single-Effect Absorption Chillers .....	42
3.2.3	Discussion .....	43
3.3	Double-Effect Absorption Chillers .....	47
3.3.1	Description of Double-Effect Absorption Chillers .....	47
3.3.2	Thermodynamic Analysis of Double-Effect Absorption Chillers .....	53
3.3.3	Discussion .....	55
3.4	Triple-Effect Absorption Chillers .....	60
3.4.1	Description of Triple-Effect Absorption Chillers .....	60
3.4.2	Thermodynamic Analysis of Triple-Effect Absorption Chillers .....	65
3.4.3	Discussion .....	65
3.5	Absorption Heat Pumps for Heating .....	76
3.5.1	Description of Absorption Heat Pumps for Heating .....	76
3.5.2	Thermodynamic Analysis of Absorption Heat Pumps for Heating .....	77
3.5.3	Discussion .....	80
3.6	Conclusions .....	83
4	ABSORPTION HEAT TRANSFORMERS .....	85
4.1	Ideal Absorption Heat Transformer Cycle .....	86
4.2	Single-Stage Absorption Heat Transformers .....	88
4.2.1	Description of Single-Stage Absorption Heat Transformers .....	88
4.2.2	Thermodynamic Analysis of Single-Stage Absorption Heat Transformers .....	89
4.3	Multi-Stage Absorption Heat Transformers .....	91
4.3.1	Description of Double- and Triple-Stage Absorption Heat Transformers .....	92
4.3.2	Thermodynamic Analysis of Double- and triple-Stage Absorption Heat Transformers .....	95
4.4	Results and Discussion .....	98
4.4.1	Effect of Heat Temperatures and Temperature Boost on AHTs .....	98
4.4.2	Effect of Cooling Temperatures and Temperature Boost on AHTs .....	104
4.5	Conclusions .....	106
5	THERMOECONOMIC ANALYSIS OF ABSORPTION CHILLERS AND HEAT TRANSFORMERS .....	110
5.1	Concepts of Thermoeconomics .....	110
5.2	Thermoeconomic Optimization .....	112
5.3	Applications of Thermoeconomics to Absorption Chillers .....	113
5.3.1	Energy and Cost Evaluation of Absorption Chillers .....	113
5.3.2	Results and Discussion .....	122
5.4	Applications of Thermoeconomics to Absorption Heat Transformers .....	132
5.4.1	Energy and Cost Evaluation of Absorption Heat Transformers .....	132

5.4.2 Results and Discussion .....	144
5.5 Conclusions.....	155
6 CONCLUSIONS AND RECOMMENDATIONS .....	157
6.1 Conclusions.....	157
6.2 Recommendations.....	160
APPENDIX	
A. SAMPLE OUTPUT DATA OF SINGLE-EFFECT ABSORPTION CHILLER .....	162
REFERENCES .....	163
BIOGRAPHICAL SKETCH .....	172

Abstract of Dissertation Presented to the Graduate School  
of the University of Florida in Partial Fulfillment of the  
Requirements for the Degree of Doctor of Philosophy

THERMOECONOMICS OF LITHIUM BROMIDE/WATER ABSORPTION  
CHILLERS AND HEAT TRANSFORMERS

By

Shun-Fu Lee

December, 1999

Chairman: Dr. S. A. Sherif

Major Department: Mechanical Engineering

Thermoeconomics is a discipline that combines both thermodynamic and economic analysis for thermal systems. One of the objectives of thermoeconomics is to minimize the product cost of a thermal system for a given capacity or to maximize the product capacity for a given total cost. The second law of thermodynamics in conjunction with the first law gives a premium to the consideration of the quality of energy over the quantity involved in a thermal system, and can lead the way to improving the system's performance. Economic analysis includes both initial capital and total operating costs of a thermal system to evaluate exergetic life cycle cost.

Absorption systems have a wide application range from cooling to heating to temperature boosting. In this study, performance comparisons of various absorption systems using a lithium bromide/water ( $\text{LiBr}/\text{H}_2\text{O}$ ) solution as the working fluid were conducted and analyzed on the basis of the first and second laws of thermodynamics. These systems include single-, double-, and triple-effect absorption chillers for cooling,

absorption heat pumps for heating, and single-, double-, and triple-stage absorption heat transformers for waste heat temperature boosting applications. Simulation of these systems was employed first to evaluate the first law performances, while the thermal properties, entropy, and exergy of the working fluids were also calculated to analyze the second law efficiencies under different operating conditions.

In addition to performance comparisons, applications of thermoeconomics are also directed to the three absorption chillers as well as the three absorption heat transformers to evaluate the capital and operating costs of the systems and their auxiliary equipment over a wide range of heat source temperatures and temperature boost values. The objective is to investigate the optimal selections for specific operating conditions on the basis of life cycle costs. The life cycle costs of relative electric-powered vapor-compression systems are also evaluated for comparison purposes. Results of the thermoeconomic analysis are shown to provide guidelines for designing and selecting cost-efficient absorption chillers and heat transformers.

## CHAPTER 1 INTRODUCTION

### 1.1 Background

Heat pumping technologies include not only heat pumps but also all technologies that have abilities to pump heat from a low temperature source to a higher one.

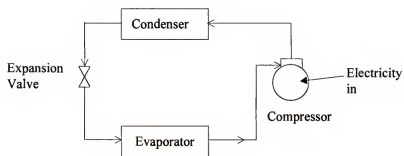
Therefore, besides the heat pumps for heating purposes, heat pumping technologies generally include all aspects of air-conditioning (cooling and heating), refrigeration, and heat recuperation systems. These systems are very important to our daily life in modern society. Air-conditioning systems provide a comfort environment in residential houses, commercial buildings, working factories, and institutions, and thus contribute to a higher productivity and well-being for human beings. Refrigeration systems provide the needs in food storage and distribution and in industrial and commercial applications. And heat recuperation systems can recover and upgrade waste heat from industrial processes or power plants to a higher temperature level, thus increasing energy efficiencies and reducing the need for primary energy (e.g. oil and natural gas). The types of primary energy input, whether heat or work, change the details of the technologies that provide the heat pumping function. Also, the developments of heat pumping technologies have faced three important issues: global environment (the ozone layer and global warming issues), energy efficiency, and economy (Granryd 1996). These three issues may change the considerations of engineers and designers while developing and applying desirable heat pump systems and their working fluids.

There are many different types of heat pump systems for cooling applications. The most important of those systems is based on two cycles: vapor-compression and

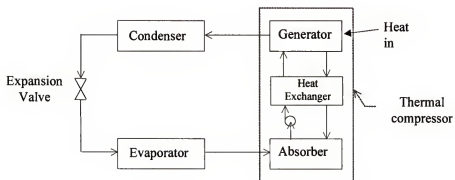


absorption cycles. Apart from those, other cycles such as thermoelectric, Stirling, and vapor ejection cycles are also considered for special purposes.

Heat-driven absorption systems, which once dominated the refrigeration and air-conditioning market, have lost competition to their electricity-powered vapor-compression counterparts since 1940. The main reason for that is the higher capital costs and lower energy efficiency of the absorption systems. However, absorption systems can become more attractive when some factors such as total energy utilization, electricity demand side management, and depletion of ozone layer, are to be considered. Energy consumption in power plants, industrial facilities, and residential and commercial buildings has increased dramatically in recent years, and much of this energy has not been used properly. It is necessary to investigate various techniques and applications to improve the overall energy efficiency of the power plants and industrial facilities. On the other hand, many utility companies in some countries or areas with hot and humid climates experience an increasing electric demand during summer peak periods, which will soon reach the limit of the existing supply capacity. And the power consumption of air-conditioning systems for building cooling is a major contributor to creating these peaks. In order to meet the fast growing demand for power, utility companies around the world may have to build more new generation stations. However the cost of construction of new power plants has been increasing in recent years, and, on the other hand, more power plants would result in more emissions of CO<sub>2</sub> (the main contributive gas to the global warming effect) to the environment in the process of electricity generation based on fossil fuels. Demand side management to lessen the demand for cooling is a more economical way than constructing new power plants. Application of heat-driven absorption chillers is one effective way to reduce peak demand for air-conditioning usage. Therefore, many power companies in large market areas are currently offering rebates to their customers to encourage installation of absorption chillers for building cooling.



(a)



(b)

Figure 1-1. (a) Schematic of a basic vapor-compression system;  
(b) Schematic of a basic absorption system.

In addition, the chlorofluorocarbons (CFCs) and hydrochlorofluorocarbons (HCFCs) refrigerants used in electric-powered vapor-compression heat pump systems are the main factor for the depletion of the earth's protective stratospheric ozone layer. The Montreal protocol is the first international treaty signed to control the production of these ozone-depleting substances. The Copenhagen Amendment called for a complete cessation of the production of CFCs by January 1, 1996, and a complete cession of production of HCFCs by January 2030 (ASHRAE 1997). In addition to these international agreements, these ozone-depleting refrigerants may face more stringent regulations by individual countries. The bans on certain CFCs and HCFCs have encouraged engineers and researchers to switch more attentions to absorption heat pump systems.

Figure 1-1 shows schematics of a basic vapor-compression system and a basic absorption heat pump system for cooling/heating applications. It is clear that the most power consuming component, the compressor in the vapor-compression system has been replaced by a "thermal compressor" consisting of a generator, an absorber, a heat exchanger, and a solution pump in the absorption system with heat source supplied to the generator. Still, cooling capacity is obtained from the evaporator for cooling or heating capacity is delivered by the condenser for heating in both systems.

Absorption heat pump systems that use non-CFC and non-HCFC working fluids in their cycles are able to utilize low-grade energy "heat" as their primary energy sources to drive the systems and create chilled water for cooling, hot water for heating, or upgrade waste heat for temperature boosting. Some manufacturers provide absorption machines able to produce both chilled and hot water simultaneously. Since only a small amount of electricity is required by solution and refrigerant pumps to operate the systems, these absorption systems can reduce the power demands for air-conditioning of buildings during peak periods in the summer time. A variety of heat sources such as solar energy, geothermal energy, steam, hot water or exhausted gas from power plants or cogeneration

systems, and waste heat from industrial processes can be directly or indirectly applied to absorption systems. In situations without those thermal sources being available, absorption heat pump systems can utilize the combustion energy from natural gas directly. Direct-fired absorption systems have been commercially developed for building cooling/heating by many major manufacturers, such as Carrier, Trane, York, Hitachi, Mitsubishi, and Ebara, in the United States and Japan. Therefore, besides the ability to reduce power consumption for cooling during the summer time, absorption systems also have potential to take advantage of a lower price of natural gas in the summer time, and to balance the annual needs for natural gas since natural gas is consumed mostly for building heating in the winter time.

Furthermore, very large quantities of waste heat at low temperatures are rejected daily from power plants and industrial processes around the world. These energy losses not only result in a lower efficiency but also cause thermal pollution to the regional and global environments. In order to make effective recovery of this waste heat and improve energy efficiency, it is usually necessary to upgrade the waste heat to higher process temperatures for recuperation. There are many different types of industrial heat pumps applied for heat recuperation purposes. The most important heat pump systems that are in use or have been proposed are based on the following cycles (IEA 1995):

Closed-cycles:

- Electrical or mechanical compression cycle;
- Absorption cycle;

Open-cycles:

- Steam or gas compression cycle (mechanical vapor recompression)
- Ejector heat pump (thermal vapor recompression).

The closed electrical compression cycle is the simplest and most common cycle for industrial heat pumps. Absorption cycles are also favored for such temperature boost applications, because they have the advantage of using a part of the waste heat to power

the systems themselves while upgrading the temperature and only consuming little electric power. These absorption systems have received growing attention in the United States, Japan, and some countries in Europe in recent years, and are often referred to as absorption heat transformers (AHT) or temperature boosters.

As a result of these factors and applications, absorption chillers, heat pumps, and heat transformers have regained interest in the past two decades due to the advantages in reduction of power demands, improvement of overall energy efficiency, and the avoidance of CFC and HCFC refrigerants. Many studies on absorption heat pump systems have been continuing by engineers in manufacturing companies and researchers in academia.

However, a combination of improving energy efficiency and investigating optimization of thermal systems is not purely a technique issue. There are several factors involved in employing and designing thermal systems for which energy resources are utilized. Many of these factors are basically economic issues and the decision-making process is usually dominated by cost considerations. Total ownership costs of a thermal system must include both initial and operating costs. Usually the initial costs refer to the capital costs of purchases for the thermal system and auxiliary components. The operating costs include the cost of the driving energy sources as well as maintenance costs over the life cycle of the thermal system. Life cycle costing includes all cost factors (e.g. capital costs, operation, and estimated energy use) and can be used to evaluate the total costs of the systems over a period of years. Therefore, the purpose of this study is to provide life cycle cost guidelines for the absorption systems considered by employing the principles of thermoeconomics.

Thermoeconomics (or exergoeconomics) as reported in Tsatsaronis (1993) combines the principles of thermodynamic analysis and economic optimization for the purpose of rational decision-making in the development, design, and operation of complex thermal systems such as power plants and heat pump systems. Thermodynamic

analysis of a thermal system is usually biased to purely thermodynamic measures like energy efficiency, entropy generation, irreversibilities, and exergetic efficiency. Meanwhile, economic considerations require a proper balance between appropriate thermodynamic measures and capital expenditures in order to achieve either a minimum unit product cost or a maximum product capacity for the thermal system. The development of thermoeconomics was first presented by Tribus and Evans (1962) for sea water desalination processes. Since then, many investigators such as Valero et al. (1994) have successfully applied this to power plants and cogeneration systems, and found that thermoeconomics is a good tool for optimization studies of thermal systems. Tozer and James (1995, 1997b) used thermoeconomics to determine life cycle costs of single- and double-effect absorption chillers applied to combined heat and power (CHP) systems with various forms of energy sources.

## 1.2 Literature Survey

In 1810, an absorption system was first developed by John Leslie in Scotland, but it was operated intermittently. A French named Ferdinand Carre built the first continuously operating ammonia/water ( $\text{NH}_3/\text{H}_2\text{O}$ ) absorption heat pump system in 1859. The U.S. Carrier Company began its study for a lithium-bromide/water ( $\text{LiBr}/\text{H}_2\text{O}$ ) absorption system in 1938, and the first commercialized system was manufactured in 1945. Energy-efficient, steam-driven or direct-fired absorption heat pump systems have been developed and produced by the major HVAC manufacturers in the United States and Japan, with models that provide cooling, heating, temperature boosting (sometimes also called temperature lift or heat recuperation), and, in some cases, simultaneous cooling and heating.

The primary research issues for absorption heat pump systems include (1) thermodynamic properties and characteristics of new suitable working fluid pairs and

additives; (2) thermodynamic performance analysis of various operating models; and (3) new advanced operating cycles. There are other issues for absorption systems such as economic analysis and the coordination of the systems with cogeneration plants or other industrial processes.

### 1.2.1 Studies of Working Fluid Pairs

Thermodynamic performance and efficiency of an absorption heat pump system are highly dependent on the properties of the working fluids. Many working fluid pairs have been considered for absorption systems. Most of commercialized absorption heat pump systems use lithium bromide/water ( $\text{LiBr}/\text{H}_2\text{O}$ ) or ammonia/water ( $\text{NH}_3/\text{H}_2\text{O}$ ) as their working fluid pairs. Both fluid pairs have the advantage of using refrigerants with high latent heat, and some other advantages of desirable properties. But each of these two working pairs has application limits and exhibits problems at high temperatures. Lithium bromide/water cannot be operated below the freezing point of water. It may cause excessive corrosion of component materials at high temperatures and also has to consider crystallization limits. On the other hand, the high operating pressure (up to 2500 kPa) at high temperatures and the toxic nature of ammonia make ammonia/water systems undesirable in some applications.

A high temperature working fluid called Alkitrane, an aqueous ternary nitrate consisting of  $\text{LiNO}_3$ ,  $\text{KNO}_3$ , and  $\text{NaNO}_3$  in the mass fraction 53/28/19, was reported by Davidson and Erickson (1986) and by Ally (1987). In 1990, Iyoki and Uemura theoretically analyzed the performance characteristics of lithium bromide-zinc chloride-calcium bromide/water ( $\text{LiBr}-\text{ZnCl}_2-\text{CaBr}/\text{H}_2\text{O}$ ) absorption systems and found that this new working pair is suitable for an air-cooled single-effect absorption chiller, a high temperature double-effect absorption heat pump, and a two-stage absorption heat transformer. Herold et al. (1991) discussed optimization for each of the components of

an absorption heat pump using an aqueous ternary hydroxide ( $\text{NaOH}+\text{KOH}+\text{CsOH}$ ) working fluid. Sawada et al. (1994) developed a new working fluid, trifluoroethanol (TFE) as refrigerant and N-methyl-2-pyrrolidone (NMP) as absorbent, to operate absorption systems below the freezing point and at high temperatures. In order to realize the high temperature application of lithium bromide/water systems, an organic inhibitor BTA (Inoue et al. 1994b) was found to decrease the corrosion rates of materials and components.

### 1.2.2 Studies of Various Absorption Systems

All current residential and commercial absorption heat pump systems are based on the single-effect and double-effect cycles. Many studies have been performed in the last two decades to analyze the performance under different operating conditions and employing advanced cycles. Eisa et al. (1986) classified more than 400 references of absorption heat pump systems on the basis of cooling and heating, and on the basis of lithium bromide/water, ammonia/water, and other working fluid pairs.

Single-effect absorption systems are severely limited in their ability to utilize high-temperature heat sources, but they are suitable with a heat source temperature between  $70^{\circ}\text{C}$  and  $100^{\circ}\text{C}$  (Perez-Blanco and Grossman 1981; Eisa and Holland 1986; Siddiqui 1993;). A modified single-effect cycle, called a generator-absorber heat exchange (GAX) absorption cycle, has the potential to achieve a higher coefficient of performance in a simple and cost-effective machine. In recent years, several advanced GAX cycles have been proposed by Alefeld (1985), Erickson (1991, 1992), Garimella et al. (1994), Rame and Erickson (1994), and Grossman et al. (1995b).

The double-effect system represents a significant improvement in performance over the basic single-effect system. Typical gas-fired double-effect absorption chillers that have been commercialized have coefficients of performance of 1.1 to 1.3. Many



studies (Vliet et al. 1982; Alefeld 1985; Alefeld and Ziegler 1985a and 1985b; Ziegler and Alefeld 1987; Gommed and Grossman 1990; Meacham et al. 1993) have analyzed the different operating characteristics of the systems.

In order to further improve utilization of the high-temperature heat source available from natural gas or cogeneration systems, many advanced triple-effect systems have been proposed that are capable of substantial performance improvement over the single- and double-effect systems (Miyoshi et al. 1985; Oouchi et al. 1985; DeVault 1988; DeVault and Biermann 1993; Alefeld and Radermacher 1994; Ziegler and Alefeld 1994; Inoue et al. 1994a). Alefeld and Radermacher (1994) and Grossman et al. (1994) have proposed several potential triple-effect absorption systems for cooling applications.

In the study of recuperation of waste heat, Grossman (1982) simulated the improved single-stage temperature-boosting absorption heat pumps by adiabatic absorption and desorption. Ciambelli and Tufano investigated two-stage (1988a) and double (1988b) absorption heat transformers using sulphuric acid/water as the working pair mixture. Patil et al. (1991) analyzed the influence of operating temperatures on the performances of absorption heat transformers operating on water-lithium iodide. Rivera et al. (1994a, 1994b) presented a thermodynamic analysis on the performance of single-stage, two-stage, and double absorption heat transformers using lithium bromide/water as the working fluid. A ternary working fluid (lithium bromide/zinc chloride/calcium bromide-water) was presented by Iyoki and Uemura (1990) who compared the theoretical performance of those heat transformers with the performance of the heat transformers operating with water/lithium bromide, water/ammonia, and water/methanol, and found that this new working fluid pair is suitable for a single-effect absorption chiller, a double-effect absorption heat pump, and a two-stage absorption heat transformer. And Alefeld and Radermacher (1994) also proposed various possible configurations of multi-stage absorption heat transformers for temperature lifting applications.

### 1.2.3 Studies of Applications and Economics of Absorption Systems

Absorption systems can also integrate easily with other systems, plants, and equipment where heat is available for various purposes. Applications of absorption heat pump systems integrated with cogeneration systems where thermal energy available as waste heat were presented by Hufford (1991, 1992). In his studies, waste heat is either converted to chilled water by a double-effect absorption system or upgraded to a higher temperature to enhance the generation process itself. Mohanty and Paloso (1995) employed an absorption chiller that uses the heat of exhaust gas from a gas turbine to cool the turbine's intake air and increase turbine capacity. A variety of heat recovery applications for absorption machines to generate cooling is listed in Dorgan et al. (1995).

In the economic analysis area, Herold et al. (1991) studied capacity maximization by varying the primary heat exchanger UAs of an absorption heat pump using an aqueous ternary hydroxide working fluid. Siddiqui (1993, 1994) analyzed the operating costs in absorption cooling and heating systems using various working pairs and different energy sources for optimizing the generator and condenser temperatures. Summerer (1996) evaluated absorption cycles with respect to COP and economics. He considered the first cost of the machines and the distribution of the heat exchanger surface area between the respective components to determine the optimal COP. Tozer and James (1995, 1997b) used thermoeconomics to evaluate life cycle costs of single- and double-effect absorption chillers with various forms of energy sources from a combined heat and power (CHP) system.

### 1.3 Objectives of Research

During the past three decades, there has been a growing interest in applying the second law of thermodynamics to thermal systems for performance analysis and economic considerations. Thermodynamic second law analysis based on exergy (or

availability) in conjunction with first law analysis gives a premium to the consideration of the quality of energy over the quantity involved in a process or a system. A detailed thermodynamic analysis leads the way to improving the performance of thermal systems and their components. The analysis can be applied as a tool for understanding and improvement of absorption heat pump systems.

As mentioned earlier, absorption heat pump systems have a wide application range from water-cooling units used for air-conditioning and refrigeration applications, to heat pumps and heat transformers for heating and heat recuperation. However, most research on second law analysis of absorption systems has focused on single-effect chillers and single-stage heat transformers. Alefeld (1989), Anand et al. (1984), and Aphornratana and Eames (1995) studied the effect of operating parameters of single-effect LiBr/H<sub>2</sub>O absorption chillers based on the second law analysis. Bosnjakovic et al. (1986) analyzed an ammonia/water absorption heat pump for heating. In the area of second law analysis of absorption heat transformers, Herold and Moran (1985, 1987) analyzed single-stage absorption heat transformers using LiBr/H<sub>2</sub>O and NH<sub>3</sub>/H<sub>2</sub>O. There appears to be a lack of literature dealing with second law analysis of multi-effect absorption chillers and multi-stage absorption heat transformers. To obtain a clear perspective of future possibilities for absorption chillers, heat pumps, and heat transformers, it is necessary to evaluate the thermodynamic performance of various types of absorption systems. Adopting this viewpoint, the present study analyzes several lithium bromide/water absorption systems on the basis of both the first and second laws of thermodynamics. The principles involved, thermal properties of the working fluid pair (lithium bromide/water solution), component model of absorption systems, and methodology of simulation are all described in Chapter 2. Chapter 3 evaluates and compares the coefficient of performance and the thermodynamic and exergetic efficiencies of single-, double-, and triple-effect absorption chillers for cooling and absorption heat pumps for heating applications under different operating conditions

including the heat source temperatures, supply cooling water temperatures, and supply chilled and hot water temperatures. The thermodynamic performance of the single-, double-, and triple-stage absorption heat transformers for heat recuperation is evaluated and compared in Chapter 4 under different operating conditions including the waste heat source temperatures, cooling water temperatures, and the magnitude of temperature boost. The results obtained here should provide some theoretical bases for the optimal operation and design of real absorption systems.

In addition to the thermodynamic performance of a thermal system, an engineering designer also needs to consider the economic factors while designing a thermal system. Therefore, in Chapter 5, applications of thermoeconomics is directed to single-, double-, and triple-effect lithium bromide/water ( $\text{LiBr}/\text{H}_2\text{O}$ ) absorption systems for cooling applications to evaluate the capital and operating costs of the systems and their auxiliary equipment over a wide range of heat source temperatures. The objective is to investigate the optimal selections for specific operating conditions on the basis of life cycle costs. The life cycle cost of an electric vapor-compression chiller is also evaluated for comparison purposes.

The application of thermoeconomics is also directed to single-, double-, and triple-stage  $\text{LiBr}/\text{H}_2\text{O}$  absorption heat transformers for waste heat recovery applications to evaluate the capital and total operating costs of the systems over a wide range of temperature boost values. Life cycle costs of electric-powered one- and two-stage vapor-compression heat transformers using R-113, R-114, and R-134a as refrigerants are also evaluated for comparison purposes. Both the absorption and vapor-compression heat transformers are evaluated and compared with other systems that upgrade waste heat by burning of natural gas. Results of the thermoeconomic analysis are shown to provide guidelines for designing and selecting cost-efficient absorption chillers and heat transformers.

## CHAPTER 2

### THERMODYNAMIC ANALYSIS OF ABSORPTION SYSTEMS AND METHODOLOGY OF SIMULATION

#### 2.1 Background

In recent years, there has been a growing interest in the use of principles of the second law of thermodynamics for analyzing and evaluating thermal systems as well as their technologies. Especially, second law analysis, when performed on processes or on energy systems, helps designers and engineers understand and determine the irreversibilities associated with inefficient processes. The development of new techniques such as better component designs, operating conditions, and advanced systems that minimize the irreversible production of entropy and improve system's performance then becomes possible. The importance of that type of analysis is that it combines the first and second laws of thermodynamics to show the direct relationship that exists between the entropy generated (irreversibilities) by inefficient processes and the resulting inadequate utilization of energy.

For a complete energy system's analysis and optimization, exergy analysis, not energy analysis, is the appropriate tool. Exergy is the common denominator since all forms of available energy involved in the system are equivalent to each other as measures of departure from equilibrium. Exergy (also called available energy, useful energy, essergy, availability, and others) is defined as the maximum useful work attainable from an energy carrier at a given state in any process that brings the energy carrier into equilibrium with its environment. Tsatsaronis (1993) indicated that exergy not only is an objective thermodynamic measure of the energy carrier, but is also relevant to economic decision making. These economic issues will be discussed in Chapter 5.

It is important to recognize that exergy analysis is intended to complement, not to replace, energy analysis. Exergy balances, when combined with mass balances and other physical principles, help determine the performance of the desired thermal system. The optimal system is a system that satisfies the imposed constraints (such as thermal and/or economic) and minimizes exergy losses. More importantly, unlike first law analysis, second law analysis pinpoints and quantifies the useful consumption (destruction) and unrecoverable losses of exergy in the system. Therefore, determination of these exergy consumptions and losses obtained through exergy analysis leads the direction to improving the performance of thermal systems.

## 2.2 Thermodynamic Principles

The interactions between thermal systems and their environments are described via work, heat transfer, and material flow streams. In performing a thermodynamic analysis for an absorption heat transformer, the principle of mass conservation and the first and second laws of thermodynamics are applied to individual components of the system. Each component can be treated as a control volume with inlet and outlet streams as illustrated in Figure 2-1. In the system, mass conservation includes the mass balance of the total mass and each material species (e.g. refrigerant and absorbent in an absorption chiller). The governing equations for a steady-state and steady-flow system are

Conservation of total mass:

$$\sum (m)_{out} - \sum (m)_{in} = 0 \quad (2.1)$$

Conservation of mass for refrigerant or absorbent:

$$\sum (mX)_{out} - \sum (mX)_{in} = 0 \quad (2.2)$$

where  $m$  is the mass flow rate and  $X$  is the concentration of LiBr (absorbent) in the solution.

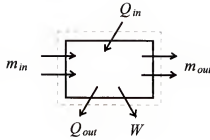


Figure 2-1. Schematic of a control volume with inlet and outlet flows

### 2.2.1 First Law Analysis

The first law of thermodynamics readily yields the energy balance of each component of the absorption system.

$$\sum (mh)_{out} - \sum (mh)_{in} + [\sum Q_{out} - \sum Q_{in}] + W = 0 \quad (2.3)$$

where the  $Q$ 's are the heat transfer rates between the control volume and its environment, and  $W$  is positive if work is done by the system.

First law analysis of the absorption system leads to computing a coefficient of performance (COP), which is defined as the ratio of the useful energy obtained from the system to the primary energy input to the system.

$$COP_{cycle} = \frac{\text{useful energy output}}{\text{primary energy input}} \quad (2.4)$$

For an absorption chiller, the numerator of Equation (2.4) is the cooling capacity obtained from the evaporator, and the denominator is the heat from a heat source supplied to the generator. Meanwhile, for an absorption heat transformer, the useful energy output is the upgraded heat obtained from the absorber and the primary energy input is the waste heat added to the evaporator and generator.

### 2.2.2 Second Law Analysis

The second law calculates system performance based on exergy. Exergy is defined as the maximum useful work attainable from an energy carrier at a given state in any process that brings the energy carrier into equilibrium with its environment (Moran 1989). If a large reference environment is at temperature  $T_o$ , then the exergy of a material stream with  $n$  components is defined as

$$\varepsilon = h - T_o s - \sum_i^n x_i \mu_{i0} + KE + GE \quad (2.5)$$

where  $\varepsilon$  is the exergy of the fluid at temperature  $T$ ;  $h$  and  $s$  are the specific enthalpy and entropy of the fluid;  $x_i$  is mole fraction of the  $i$ th component;  $\mu_{i0}$  is the chemical potential of the  $i$ th component at the reference temperature; and  $KE$ ,  $GE$  are the kinetic and gravitational exergies (El-Sayed and Evans 1970). The last two terms are neglected in this study.

The chemical potential  $\mu_{i0}$  can be obtained by substituting the molar Gibbs free energy  $G_o$  of the fluid at  $T_o$  in Equation (2.5) (Ishida and Kawamura 1982),

$$G_o = \sum_{i=1}^n x_i \mu_{i0} \quad (2.6)$$

to give

$$\varepsilon = h - T_o s - G_o \quad (2.7a)$$

Introducing an intermediate state at  $T_o$ ,  $P_o$ ,  $KE=0$ ,  $GE=0$ , and  $x_j$  unchanged, the exergy of the material stream in Equation (2.7a) becomes zero.

$$\varepsilon^0 = h^0 - T_o s^0 - G_o^0 = 0 \quad (2.7b)$$

where the superscript "o" refers to the state of the stream at  $T_o$ ,  $P_o$  with composition unchanged. Equation (2.7a) may be written as

$$\varepsilon = (h - h^0) - T_o (s - s^0) - (G_o - G_o^0) \quad (2.7c)$$

If the intermediate state is selected as the same as the large environment at  $T_o$ , then the terms in the last brackets in Equation (2.7c) vanish and Equation (2.7c) becomes

$$\varepsilon = (h - h_o) - T_o (s - s_o) \quad (2.7d)$$



Also, the exergy that is associated with the transfer by heat interaction is given by

$$E_Q = Q(1 - \frac{T_0}{T}) \quad (2.8)$$

where  $T$  is the temperature of the system in which the heat transfer occurs. If heat loss from the control volume to its surrounding is assumed zero, then this exergy amount is negligible. And the interaction of mechanical work and electrical energy is directly transferred into exergy:  $E_w = W$ , but the work inputs to the solution pumps are very small when compared with the primary energy input to the generator and evaporator of absorption systems and thus are negligible.

A natural entropy measure of internal irreversible losses is provided by the strength of an inequality sign. This leads to the definition of entropy generation for any thermodynamic process as

$$S_{gen} = \sum (ms)_{out} - \sum (ms)_{in} - [\sum (Q/T)_{in} - \sum (Q/T)_{out}] \geq 0 \quad (2.9)$$

A second measure of internal irreversible losses, particularly of interest to the system analyst, is defined as the product of the entropy generation in Equation (2.9) and the reference temperature. This is denoted by  $I_{irr}$

$$I_{irr} = T_0 S_{gen} \quad (2.10)$$

and is called irreversibility.

An expression of exergy balance that provides a different insight into a thermodynamic process in a control volume (each component) can be derived as

$$\Delta E = \sum (m\varepsilon)_{out} - \sum (m\varepsilon)_{in} + [\sum (Q(1 - \frac{T_0}{T}))_{out} - \sum Q(1 - \frac{T_0}{T})_{in}] + \sum W \quad (2.11)$$

$\Delta E$  is the lost exergy or the irreversibility that occurred in the process. The first two terms of the right hand side are the exergy of the inlet and outlet streams of the control volume. The third and fourth terms are the exergy associated with the heat transferred from the source maintained at a temperature  $T$ , and sometimes are called "equivalent work." The last term is the exergy of mechanical work added to the control volume, and is negligible for absorption systems unless solution and refrigerant pumps are considered.

The second law efficiency for an absorption system may be measured in three manners (Abrahamsson et al. 1994). The first method is through thermodynamic efficiency, which is the ratio of the coefficient of performance of the real cycle to the Carnot COP of an ideal cycle,

$$E_{th} = \frac{COP}{COP_{Carnot}} \quad (2.12)$$

The Carnot COP of an ideal cycle for cooling, heating, and temperature boosting applications will be discussed in Sections 3.1 and 4.1, respectively.

The thermodynamic efficiency provides an expression for the performance of absorption systems but does not describe the complete picture. The quality of the output energy is not specifically addressed by these performance measures. The second manner with which the second law efficiency can be measured is called the exergetic efficiency,  $E_{ex}$ , and is defined as the ratio of the useful exergy gained from a system to that supplied to the system. Therefore, the exergetic efficiency of the single-effect chiller, for example, is the ratio of the chilled water exergy at the evaporator to the heat source exergy at the generator, and can be expressed as

$$E_{ex} = \frac{\text{useful exergy}}{\text{supplied exergy}} = \frac{\Delta E_{\text{chilled water}}}{\Delta E_{\text{heat source}}} \quad (2.13)$$

The third measure of the second law efficiency is called the exergy index and is considered to be an adequate indicator of efficiency for the absorption systems in this study. Exergy index is the ratio of the exergy produced and exergy lost,

$$I_{ex} = \frac{\sum \Delta E_{\text{useful}}}{\sum \Delta E_{\text{supplied}} - \sum \Delta E_{\text{useful}}} \quad (2.14)$$

The first two second law efficiency measures are widely accepted and will be analyzed and compared later for the various absorption heat pump systems examined in this study.

## 2.3 Thermal Properties of Working Fluids

The performance, efficiency, and operating conditions of an absorption system are determined by the properties of the working fluid pair it uses. These properties include chemical, physical, and thermal properties. Both the capital and operating costs of the absorption systems are also dependent on the properties of working fluids. The lithium bromide/water solution is one of the most used fluid pairs for absorption systems for cooling, heating, and heat recuperation applications. The chemical and physical properties of lithium bromide/water solution are described in detail in the literature by Takada (1982) and Herold et al. (1996). The thermal properties including temperature, pressure concentration, enthalpy, entropy, and exergy, are crucial for absorption systems in their operation, application, and performance. These properties will be discussed in this section.

### 2.3.1 Thermal Properties of Lithium Bromide/Water Solution

#### Enthalpy of LiBr/H<sub>2</sub>O solution

The equilibrium equations of enthalpy, temperature, concentration, and vapor pressure of the lithium bromide/water solution within a general operating range for the absorption systems using this working pair are described by McNeely (1979) for use in computer programs. The relationships of temperature, concentration, and pressure are given by

$$T = AT' + B \quad (2.15)$$

$$\text{and} \quad \ln P = C + D/(T' + 459.72) + E/(T' + 459.72)^2 \quad (2.16)$$

where  $T$  = solution temperature ( $40 \leq T \leq 350^\circ \text{F}$ ),

$T'$  = refrigerant temperature ( $0 \leq T' \leq 230^\circ \text{F}$ ),

$P$  = pressure (psia),

$$A = -2.00755 + 0.16976X - (3.133362E - 3)X^2 + (1.97668E - 5)X^3$$

$$B = 321.128 - 19.322X + 0.374382X^2 - (2.0637E - 3)X^3$$

$$C = 6.21147, D = -2886.373, \text{ and } E = -337269.46.$$

$$X = \text{percent LiBr } (45\% \leq X \leq 70\%),$$

In performing the first law analysis of an absorption system, the heat transfer within each heat exchange component is calculated from the change of enthalpy of the working fluids. The enthalpy of the lithium bromide/water solution is calculated as a function of solution temperature  $T$  and concentration  $X$ .

$$h = A + BT + CT^2 \quad (2.17)$$

$$A = -1015.07 + 79.5387X - 2.358016X^2 + 0.03031583X^3 - (1.40026E - 4)X^4$$

$$B = 4.6811 - 0.30378X + (8.4485E - 3)X^2 - (1.0477E - 4)X^3 + (4.8E - 7)X^4$$

$$C = -(4.9E - 3) + (3.83E - 4)X - (1.08E - 5)X^2 + (1.315E - 7)X^3 - (5.9E - 10)X^4$$

#### Entropy and exergy of LiBr/H<sub>2</sub>O solution

The entropy of LiBr/H<sub>2</sub>O solution was calculated theoretically by Gupta and Sharma (1976), Koehler et al. (1987), Anand and Kumar (1987), Cheng and Shih (1988), and by Aphornratana and Eames (1995). In this study, the procedure to calculate the entropy and exergy of LiBr/H<sub>2</sub>O solution is obtained from the method proposed by Aphornratana and Eames (1995) and is described in this section.

From the relations for the Gibbs' free energy and Helmholtz function for a binary system such as the lithium bromide/water solution, the specific entropy of the solution can be derived from

$$\begin{aligned} s_{T,X} - s_{T_{ref},X_{ref}} &= \int_{T_{ref}}^T \frac{1}{T} \left( \frac{\partial h}{\partial T} \right)_{P,X} dT - \int_{P_{ref}}^P \left( \frac{\partial v}{\partial T} \right)_{P,X} dP \\ &+ R \left\{ \int_{X_{ref}}^X \frac{\ln a_{water} - \ln a_{LiBr}}{M_{sol}} dX \right\} \end{aligned} \quad (2.18)$$

The first term on left hand side in Equation (2.18) is the entropy of the solution at a specified temperature and concentration. The second term is the reference entropy at a reference state. Here the reference state is selected to correspond to 25°C. Based on the assumptions made by Aphornratana and Eames (1995), only the temperature variation is

considered, thus the reference entropy is a function of the concentration. The first integral term on the right hand side in Equation (2.18) can be calculated by the data of the specific enthalpy of the lithium bromide/water solution available from McNeely (1979) mentioned earlier. The pressure effect on entropy for a liquid may be neglected, therefore, the second integral term dropped out. The last term on the right hand side is recognized as the difference between the entropy of mixing ( $\Delta s_{mix}$ ) at the reference temperature  $T_{ref}$  and at the temperature  $T$ . The procedure for evaluating it is outlined in Aphornratana and Eames (1995). The entropy change with temperature at constant concentration can be expressed as

$$s_T - s_{T_{ref}} = \int_{T_{ref}}^T \frac{1}{T} \left( \frac{\partial h}{\partial T} \right)_{P,X} dT + (\Delta s_T - \Delta s_{T_{ref}})_{mix} \quad (2.19)$$

and 
$$\Delta s_{mix} = - \frac{R}{M_{sol}} [\bar{X}_{LiBr} \ln(\bar{X}_{LiBr} \gamma) + \bar{X}_{water} \ln(P / P^*)] \quad (2.20)$$

where

$R$ : Universal gas constant,

$M_{sol}$ : Solution molecular weight,

$P$  and  $P^*$ : Pressure of water vapor of the solution and pure water

$\bar{X}$ : Mole fractions of LiBr and water,

$\gamma$ : Mean molar activity coefficient

The solution molecular weight  $M_{sol}$  is:  $18.015/(1-0.7926X)$ . The reference entropy of the lithium bromide/water solution at 25°C is

$$s_{sol} = \frac{h_{sol} - g_{sol}}{T_{ref}} \quad (2.21)$$

The Gibbs' free energy of the LiBr/H<sub>2</sub>O solution,  $g_{sol}$  is calculated from

$$g_{sol} = \frac{1-X}{M_{LiBr}} \mu_{LiBr} + \frac{X}{M_{water}} \mu_{water} \quad (2.22)$$

where  $X$  is the concentration,  $M$  is the molecular weight, and  $\mu$  is the chemical potential.

The chemical potential of water in the solution is

$$\mu_{water} = (\bar{h}_v - T_{ref} \bar{s}_v)_{water} \quad (2.23)$$

The enthalpy and entropy of the water vapor is obtained from steam tables at the reference temperature. And the chemical potential of LiBr in the solution is

$$\mu_{LiBr} = 2RT_{ref} \ln(m\gamma)_{LiBr} + \bar{K} T_{ref} + \mu_{LiBr}^* \quad (2.24)$$

where  $\bar{K} = -192.2$  kJ/kmol K,  $\gamma$  is the mean molar activity coefficient, and  $m$  is the LiBr molality

$$m_{LiBr} = \frac{\text{number of moles of solute (LiBr)}}{\text{number of moles of solvent (water)}} = \frac{X}{86.845(1-X)} \quad (2.25)$$

The chemical potential of pure LiBr is

$$\mu_{LiBr}^* = \bar{h}_{LiBr} - T_{ref} \bar{s}_{LiBr} \quad (2.26)$$

This chemical potential becomes zero as pure LiBr at 25°C has been assigned a zero enthalpy and a zero entropy. Then the entropy of the LiBr/H<sub>2</sub>O solution at 25°C can be calculated using Equations (2.21) to (2.26).

The mean molar activity coefficient  $\gamma$  in Equations (2.20) and (2.24) is now calculated as follows. For a single electrolyte solution at 25°C,

$$\Gamma^0 = [1 + B(1 + \frac{I}{10})^q - B]\Gamma^* \quad (2.27)$$

where  $\Gamma^0$  is the reduced activity coefficient of pure solution at 25°C;  $B = 0.75 - 0.065q$ ;  $q$  is Meissner's parameter ( $q=7.27$ ) (Zemaitis et al. 1986);

$$\ln \Gamma^* = (-0.5107\sqrt{I})/(1 + C\sqrt{I})$$

$$C = 1 + 0.055q \exp(-0.023I^3)$$

$I$  is the ionic strength ( $I = \frac{1}{2} \sum m_i Z_i^2 = m_{LiBr}$ );  $Z$  is the number of charges on the cation or anion ( $Z = 1$  for LiBr/H<sub>2</sub>O solution). Then the mean molar activity coefficient of the LiBr/H<sub>2</sub>O solution is calculated from the following relationship

$$\gamma = (\Gamma^0)^{Z_+ Z_-} = \Gamma^0 \quad (2.28)$$

For the solution at other temperatures, the reduced activity coefficient is

$$\ln \Gamma_T^0 = (1.125 - 0.005T) \ln(\Gamma_{25^\circ C}^0) - (0.125 - 0.005T) \ln(\Gamma_{ref}^0) \quad (2.29)$$

where  $\Gamma_{25^\circ C}^0$  is obtained from Equation (2.27),  $T$  is the temperature in °C; and

$$\ln(\Gamma_{ref}^0) = (-0.41\sqrt{I})/(1 + \sqrt{I}) + 0.039I^{0.92}$$

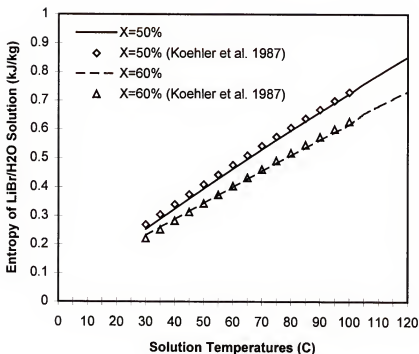


Figure 2-2. Comparison of the calculated entropy of LiBr/H<sub>2</sub>O solution with the data by Koehler et al. (1987)

And then the mean molar activity coefficient at a temperature  $T$  can be calculated by substituting the result of Equation (2.29) into Equation (2.28).

With the entropy  $s_T$  in Equation (2.19) and the enthalpy expression by McNeely (1979), the exergy of the LiBr/H<sub>2</sub>O solution in Equation (2.7d) can be calculated. The calculated entropy of the lithium bromide/water solution in this study is compared with the data reported by Koehler et al. (1987) as shown in Figure 2-2.

### 2.3.2 Thermal Properties of Water and Vapor

Irvine and Liley (1984) developed approximate equations from steam table data for saturated and superheated properties of water and steam. These property equations

including the relationships of temperature, pressure, enthalpy, and entropy of water and water vapor were employed in this study to replace the corresponding equations in the simulation model.

Saturation Temperature  $T(S)$ :

$$T(S) = A + \frac{B}{(\ln P(S)) + C} \quad (2.30)$$

where  $0.000611 \leq P(S) < 12.33$  MPA

$$273.16 \leq T(S) < 600 \text{ K}$$

The constants  $A$ ,  $B$ , and  $C$  in Equation (2.30) are listed in Table 2-1.

Saturation Pressure  $P(S)$ :

$$\ln P(S) = \sum_{N=0}^9 A(N)T(S)^N + \frac{A(10)}{T(S) - A(11)} \quad (2.31)$$

For calculation of enthalpy and entropy of saturated water and vapor, the following equations need to be calculated first. Then the calculated numbers are substituted into the individual equation of those saturation properties. The constants in Equation (2.32) for each saturation property are list in Table 2-1.

$$Y(S) = A + BT(C)^{1/3} + CT(C)^{5/6} + DT(C)^{7/8} + \sum_{N=1}^7 E(N)T(C)^N \quad (2.32)$$

$$T(C) = [T(CR) - T(S)]/T(CR) \quad T(CR) = 647.3 \text{ K}$$

Liquid saturation enthalpy:  $H(F) = Y(S)H(FCR)$

Vapor saturation enthalpy:  $H(G) = Y(S)H(GCR)$

Liquid saturation entropy:  $S(F) = Y(S)S(FCR)$

Vapor saturation entropy:  $S(G) = Y(S)S(GCR)$

The thermodynamic property equations for superheated water vapor are calculated as functions of pressure  $P$  and temperature  $T$  as follows.

Enthalpy  $H(PT)$ :

$$H(PT) = \sum_{N=0}^2 A(N)T^N - A(3)EXP\left(\frac{T(S) - T}{M}\right) \quad (2.33)$$

where  $A(0)=B(11)+B(12)P+B(13)P^2$



Table 2-1. Constants and Coefficients in Equations (2.30) to (2.34)

Equation (2.30)						
	A=0.426776E2	B=-0.38927E4	C=-0.948654E1			
Equation (2.31)						
	A(0)=0.104592E2	A(1)=-0.404897E-2	A(2)=-0.41752E-4	A(3)=-0.36851E-6	A(4)=-0.10152E-8	A(5)=0.86531E-12
	A(6)=0.903668E-5	A(7)=-0.19969E-17	A(8)=0.779287E-21	A(9)=0.191482E-24	A(10)=-0.39681E4	A(11)=-0.395735E2
Equation (2.32)						
	H(F)	H(F)	H(G)	S(F)	S(F)	S(G)
	273.2≤T(S)<300 K	300≤T(S)<600 K	273.2≤T(S)≤647K	273.2≤T(S)<300 K	300≤T(S)<600 K	273.2≤T(S)≤647K
A	0	8.83923E-01	1	0	9.12763E-01	1
B	0	0	4.57874E-01	0	0	3.77391E-01
C	0	0	5.08441288	0	0	-2.78368
D	0	0	-1.48513244	0	0	6.93135
E(1)	6.2469884E+02	-2.67172935	-4.81351884	-1.83693E+03	-1.75702956	-4.34839
E(2)	-2.3438537E+03	6.22640035	2.69411792	1.47066E+04	1.68754095	1.34672
E(3)	-9.5081210E+04	-1.317896E+01	-7.39064542	-4.31466E+04	5.82215341	1.75261
E(4)	7.1628793E+04	-1.913224E+00	1.04962E+01	4.86067E+04	-6.33355E+01	-6.22295
E(5)	-1.6353522E+05	6.879377E+01	-5.46840036	7.99751E+03	1.88077E+02	9.99004
E(6)	1.6653109E+05	-1.248199E+02	0	-5.83340E+04	-2.52345E+02	0
E(7)	-6.4785459E+04	7.214354E+01	0	3.31401E+04	1.28059E+02	0
	H(FCR)=2099.3	H(FCR)=2099.3	H(GCR)=2099.3	S(FCR)=4.4289	S(FCR)=4.4289	S(GCR)=4.4289
Equation (2.33)						
	B(11)= 2.04121E3	B(12)= -4.04002E1	B(13)= -4.8095E-1	B(21)= 1.610693	B(22)= 5.4721E-2	B(23)= 7.5175E-4
	B(31)= 3.38312E-4	B(32)= -1.9757E-5	B(33)= -2.8741E-7	B(41)= 1.70782E3	B(42)= -1.6994E1	B(43)= 6.2746E-2
	B(44)= -1.02843E-4	B(45)= 6.4561E-8	M = 45.			
Equation (2.34)						
	A(0)= 4.616291	A(1)= 1.03901E-2	A(2)= -9.87309E-6	A(3)= 5.43411E-9	A(4)= -1.171E-12	
	B(1)= -4.65031E-1	B(2)= 1.0E-3	M = 85.			
	C(0)= 1.777804	C(1)= -1.80247E-2	C(2)= 6.854459E-5	C(3)= -1.184424E-7	C(4)= 8.1422E-11	

$$A(1)=B(21)+B(22)P+B(23)P^2$$

$$A(2)=B(31)+B(32)P+B(33)P^2$$

$$A(3)=B(41)+B(42)T(S)+B(43)T(S)^2+B(44)T(S)^3+B(45)T(S)^4$$

Entropy  $S(PT)$ :

$$S(PT) = \sum_{N=0}^4 A(N)T^N + B(1)\ln(10P + B(2)) - \sum_{N=0}^4 C(N)T(S)^N \left[ \exp\left(\frac{T(S)-T}{M}\right) \right] \quad (2.34)$$

All constants and coefficients for the thermal properties of water and steam in Equations (2.30) to (2.34) are listed in Table 2-1. The uncertainty of using the above correlations for computing saturated properties is less than 0.15%. And the maximum errors for the superheated properties in Equations (2.33) and (2.34) are less than 1% (Irvine and Liley 1984).

## 2.4 Component Models

The standard components of an absorption heat pump system are the absorber, generator, condenser, evaporator, solution heat exchanger, throttling valve, mixer, splitter, and solution pump, as shown in Figure 2-3 with their respective state points (Grossman and Gomed 1987). Each component is treated as a control volume with its own inputs and outputs. According to the thermodynamic principles described above, the governing equations of each component of an absorption system can be derived.

### 2.4.1. Absorber

In an absorber system, a strong solution (State 1, high concentration of absorbent LiBr in the solution) from the generator absorbs the refrigerant (water) vapor (State 2) from the evaporator in the absorber and becomes a weak solution (State 5, low concentration of absorbent in the solution) and leaves the absorber. The entering strong

solution may be subcooled or superheated; it is therefore allowed to reach an equilibrium at State 6 by adiabatic absorption before the absorption process  $6 \rightarrow 5$  begins (Grossman 1982). For an absorption chiller, since the absorption process between the strong solution and refrigerant vapor is exothermic, an external cooling medium (State 3) is required to be introduced into the absorber to remove the absorption heat and keep the temperature and pressure in the absorber from increasing. However, this absorption heat is the useful energy output for an absorption heat transformer. The governing equations for the absorber are as follows:

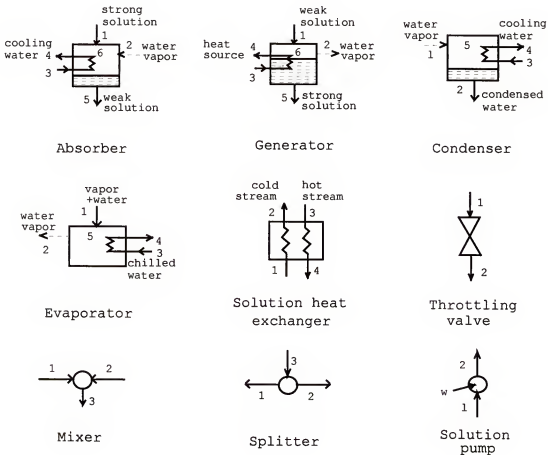


Figure 2-3. Schematic of components that form absorption systems

$$\text{Total mass balance: } m_5 - m_1 - m_2 = 0 \quad (2.35a)$$

$$\text{Absorbent mass balance: } m_5 X_5 - m_1 X_1 = 0 \quad (2.35b)$$

$$\text{Energy balance: } m_5 h_5 + m_4 h_4 - m_1 h_1 - m_2 h_2 - m_3 h_3 = 0 \quad (2.35c)$$

$$\text{Heat transfer: } Q_a = (UA)_a \frac{(T_6 - T_4) - (T_5 - T_3)}{\ln[(T_6 - T_4)/(T_5 - T_3)]} = m_3 (h_4 - h_3) \quad (2.35d)$$

$$\text{Entropy generation: } S_{gen,a} = m_5 s_5 + m_4 s_4 - m_1 s_1 - m_2 s_2 - m_3 s_3 \quad (2.35e)$$

$$\text{Exergy change: } \Delta E_a = m_5 \varepsilon_5 + m_4 \varepsilon_4 - m_1 \varepsilon_1 - m_2 \varepsilon_2 - m_3 \varepsilon_3 \quad (2.35f)$$

#### 2.4.2. Generator

In the generator, a heat source (State 3) is supplied to generate refrigerant (State 2) out of the weak solution (State 1) from the absorber. Then, the strong solution (State 5) leaves the generator. The entering weak solution may be subcooled or superheated; it is therefore allowed to reach an equilibrium at State 6 by adiabatic desorption before the desorption process  $6 \rightarrow 5$  begins (Grossman 1982). The governing equations of thermodynamic analysis for this component are listed as follows:

$$\text{Total mass balance: } m_5 + m_2 - m_1 = 0 \quad (2.36a)$$

$$\text{Absorbent mass balance: } m_5 X_5 - m_1 X_1 = 0 \quad (2.36b)$$

$$\text{Energy balance: } m_5 h_5 + m_4 h_4 + m_2 h_2 - m_1 h_1 - m_3 h_3 = 0 \quad (2.36c)$$

$$\text{Heat transfer: } Q_g = (UA)_g \frac{(T_4 - T_6) - (T_3 - T_5)}{\ln[(T_4 - T_6)/(T_3 - T_5)]} = m_3 (h_3 - h_4) \quad (2.36d)$$

$$\text{Entropy generation: } S_{gen,g} = m_5 s_5 + m_4 s_4 + m_2 s_2 - m_1 s_1 - m_3 s_3 \quad (2.36e)$$

$$\text{Exergy change: } \Delta E_g = m_5 \varepsilon_5 + m_4 \varepsilon_4 + m_2 \varepsilon_2 - m_1 \varepsilon_1 - m_3 \varepsilon_3 \quad (2.36f)$$

#### 2.4.3. Condenser

The function of the condenser is to condense the refrigerant vapor (State 1) from the generator by introducing an external cooling water loop (State 3) in the cooling and temperature boost applications. But when an absorption system operates for heating

purposes, the condenser heat becomes the useful output. The vapor entering the condenser is either superheated or saturated. If it is superheated, it first cools to the condensation temperature at State 5. The condensation process takes place between States 5 and 2. The governing equations for this component are:

$$\text{Total mass balance:} \quad m_2 - m_1 = 0 \quad (2.37a)$$

$$\text{Energy balance:} \quad m_4 h_4 + m_2 h_2 - m_1 h_1 - m_3 h_3 = 0 \quad (2.37b)$$

$$\text{Heat transfer:} \quad Q_c = (UA)_c \frac{(T_2 - T_3) - (T_5 - T_4)}{\ln[(T_2 - T_3)/(T_5 - T_4)]} = m_3 (h_4 - h_3) \quad (2.37c)$$

$$\text{Entropy generation:} \quad S_{gen,c} = m_4 s_4 + m_2 s_2 - m_1 s_1 - m_3 s_3 \quad (2.37d)$$

$$\text{Exergy change:} \quad \Delta E_c = m_4 \varepsilon_4 + m_2 \varepsilon_2 - m_1 \varepsilon_1 - m_3 \varepsilon_3 \quad (2.37e)$$

#### 2.4.4. Evaporator

In the evaporator, the condensed refrigerant (State 1) from the condenser vaporizes by extracting the heat from an external water loop (State 3) and leaves the evaporator at State 2. This external water loop becomes the useful cooling capacity of the absorption system in the cooling mode, or is the input heat source for the temperature boosting mode. The condensed refrigerant entering the evaporator is either subcooled or saturated. If it is subcooled, it first heats to the evaporation temperature at State 5. The evaporation process takes place between States 5 and 2. The governing equations for this component are:

$$\text{Total mass balance:} \quad m_2 - m_1 = 0 \quad (2.38a)$$

$$\text{Energy balance:} \quad m_4 h_4 + m_2 h_2 - m_1 h_1 - m_3 h_3 = 0 \quad (2.38b)$$

$$\text{Heat transfer:} \quad Q_e = (UA)_e \frac{(T_3 - T_2) - (T_4 - T_1)}{\ln[(T_3 - T_2)/(T_4 - T_1)]} = m_3 (h_3 - h_4) \quad (2.38c)$$

$$\text{Entropy generation:} \quad S_{gen,e} = m_4 s_4 + m_2 s_2 - m_1 s_1 - m_3 s_3 \quad (2.38d)$$

$$\text{Exergy change:} \quad \Delta E_e = m_4 \varepsilon_4 + m_2 \varepsilon_2 - m_1 \varepsilon_1 - m_3 \varepsilon_3 \quad (2.38e)$$

#### 2.4.5. Solution Heat Exchanger

The main function of the solution heat exchanger in absorption systems is to recover heat from a higher temperature solution stream to a lower temperature one. This component is not necessary for absorption systems completing their job. But it does reduce the heat duties of the required input heat source and the external cooling water, and thus increases the efficiency. The governing equations of this component are:

$$\text{Energy balance:} \quad m_4 h_4 + m_2 h_2 - m_1 h_1 - m_3 h_3 = 0 \quad (2.39a)$$

$$\text{Heat transfer:} \quad Q_{hx} = (UA)_{hx} \frac{(T_3 - T_2) - (T_4 - T_1)}{\ln[(T_3 - T_2)/(T_4 - T_1)]} = m_1 (h_2 - h_1) \quad (2.39b)$$

$$\text{Entropy generation:} \quad S_{gen,hx} = m_4 s_4 + m_2 s_2 - m_1 s_1 - m_3 s_3 \quad (2.39c)$$

$$\text{Exergy change:} \quad \Delta E_{hx} = m_4 \varepsilon_4 + m_2 \varepsilon_2 - m_1 \varepsilon_1 - m_3 \varepsilon_3 \quad (2.39d)$$

#### 2.4.6. Throttling Valve

The function of throttling valve is to reduce the refrigerant and solution pressure levels. Sometimes, this component may be used to control flow rates of the working fluids in absorption systems.

$$\text{Energy balance:} \quad m_2 h_2 - m_1 h_1 = 0 \quad (2.40a)$$

$$\text{Entropy generation:} \quad S_{gen,v} = m_2 s_2 - m_1 s_1 \quad (2.40b)$$

$$\text{Exergy change:} \quad \Delta E_v = m_2 \varepsilon_2 - m_1 \varepsilon_1 \quad (2.40c)$$

#### 2.4.7. Mixer

The mixer is a minor component in the piping of absorption heat pump systems. Two flow streams mix together and become one stream.

$$\text{Total mass balance:} \quad m_3 - m_2 - m_1 = 0 \quad (2.41a)$$

$$\text{Absorbent mass balance:} \quad m_3 X_3 - m_1 X_1 - m_2 X_2 = 0 \quad (2.41b)$$

$$\text{Energy balance:} \quad m_3 h_3 - m_1 h_1 - m_2 h_2 = 0 \quad (2.41c)$$

$$\text{Entropy generation:} \quad S_{gen,m} = m_3 s_3 - m_1 s_1 - m_2 s_2 \quad (2.41d)$$

$$\text{Exergy change:} \quad \Delta E_m = m_3 \varepsilon_3 - m_1 \varepsilon_1 - m_2 \varepsilon_2 \quad (2.41e)$$

#### 2.4.8. Splitter

Splitter is another minor component in the piping layout of absorption systems. It exists in the systems operating with parallel flow connections.

$$\text{Total mass balance:} \quad m_1 + m_2 - m_3 = 0 \quad (2.42)$$

#### 2.4.9. Solution Pump

$$\text{Energy balance:} \quad m_2 h_2 - m_1 h_1 - W = 0 \quad (2.43a)$$

$$\text{Exergy change:} \quad \Delta E_p = m \varepsilon_2 - m_1 \varepsilon_1 - W \quad (2.43b)$$

### 2.5 Methodology of Simulation and Assumptions

In this study, a computer code has been developed and used to investigate the first law performance for various configurations of absorption heat pump systems. Similar computer codes have been successfully used by other researchers and shown to be a good tool in the investigation of absorption systems (Grossman et al. 1994; ORNL 1995; Garimella et al. 1996). However, these codes were designed to analyze only the first law performance. In order to analyze the second law performance, many subroutines for thermal properties of the working fluid pair were added into the computer code developed by the author to calculate the entropy and exergy of the working fluid at each state point, as well as the exergy destruction for each of the components in the systems.

The procedure of simulation and analysis for the absorption systems in this study is illustrated in Figure 2-4. The simulation starts from drawing a candidate absorption cycle on Duhring (T-X-P) diagram of the working fluid. This will provide some

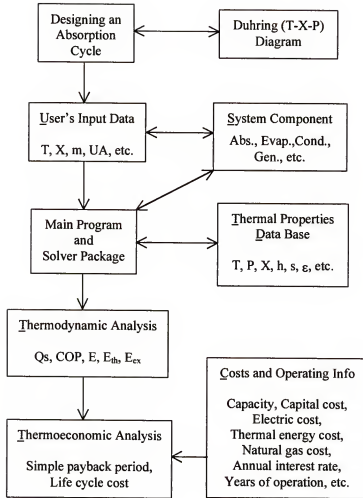


Figure 2-4 Procedure of simulation and analysis of absorption systems



information regarding the operating conditions and limits of the cycle selected. Then, configuration of the absorption system can be created by selecting its units from standard components such as absorber, generator, etc. The computer code requires a simple input by a user which contains given operating conditions and working fluid at each state point. The user also offers the code an image of the system by indicating the different components and their interconnections. A main program activates these unit subroutines from a user input for the cycle, calls these units, and links them to each other in an order corresponding to the user input. A property data base for the thermodynamic properties (temperature, pressure, enthalpy, etc.) of the working fluids is also addressed when each unit subroutine is activated. When all of the governing equations for the cycle have been generated by the computer code, a mathematical solver package then is employed to solve them simultaneously. Based on the input information, the computer code calculates temperature, mass flow rate, enthalpy, entropy, exergy, concentration, pressure, vapor fraction at each state point, and heat transfer rate and exergy change of each component in the system. Then, both the first and second law analyses for the absorption system can be conducted from the simulation results.

For purposes of simplifying the simulation and analysis, the following assumptions were made:

1. Heat losses and heat gains between the system and its environment are neglected;
2. Work inputs to solution and refrigerant circulation pumps are negligible as compared to the primary energy input to the systems;
3. Heat sources supplied to the generators of absorption chillers and heat pumps and to the generators and evaporators of absorption heat transformers are in the form of pressurized hot water;
4. Friction or pressure losses in components and pipes are ignored;

5. The product UA is used to represent the heat transfer model of the heat exchange components; and,
6. Solution in the generators and absorbers are in equilibrium with refrigerant vapors at the same temperatures and pressures.

Although, in the practical operation of absorption systems, heat transfer between the system and its surrounding (about 3 to 5% of heat input) and frictional losses inside the system will result in more energy and exergy losses and reduce the system efficiency and increase irreversibilities, these effects were not accounted for in this study. A large number of model runs have been performed and compared in order to investigate the interactions of different operating conditions on the performance for various configurations of absorption chillers, heat pumps, and heat transformers discussed in Chapters 3 and 4.

In addition to performing first and second law analyses for those absorption systems, results obtained are also used to evaluate the life cycle costs of absorption chillers and heat transformers in Chapter 5 by employing the applications of thermoeconomics. Both capital and operating costs of absorption systems are considered under different operating conditions. Evaluation of energy cost is based on the exergy the stream carries. The objective is to investigate the optimal selections for specific operating conditions on the basis of life cycle costs for each absorption system considered in this study.

### CHAPTER 3

#### ABSORPTION CHILLERS AND HEAT PUMPS

Heat pump systems have the ability to transfer heat from lower to higher temperature levels by employing external means, such as compression work or thermal energy. Absorption heat pump systems are one of several types of heat pump systems used in residential, commercial and industrial applications. Based on their operation and applications, absorption heat pump systems can be classified into three types: type I, operating as a chiller (ACH) or refrigerator for cooling purposes; type II, operating as a heat pump (AHP) for heating; and type III, operating as a heat transformer (AHT) for heat recovery and temperature boosting applications. The types I and II absorption heat pump systems are investigated and compared in this chapter while the type III will be discussed in Chapter 4.

In this chapter, various configurations of absorption chillers using a  $\text{LiBr}/\text{H}_2\text{O}$  solution as the working fluid are analyzed and compared on the basis of the first and second laws of thermodynamics. These absorption chillers include single-, double-, and triple-effect systems that are categorized by the number of times the primary heat input is used by the absorption machine, either directly or indirectly. The coefficient of performance, thermodynamic efficiency, and exergetic efficiency of the absorption chillers considered are investigated under a wide range of operating conditions including the heat source, cooling water, and supply chilled water temperatures. Similar approach is also applied to an absorption heat pump for heating applications on the basis of the first and second laws of thermodynamics. Thermodynamic performance of the absorption heat pump is evaluated for different operating conditions including the heat source, cooling water, and supply hot water temperatures.

### 3.1 Ideal Absorption Chiller and Heat Pump Cycles

The types I and II of absorption systems have the same operating model despite of having two different useful outputs. Each of them can be treated as a combination of a heat engine cycle (1) and a refrigeration cycle (2). The operating model and temperature-entropy (T-S) diagram of the two types are shown in Figure 3-1 (Takada 1982; Herold et al. 1996). The principal interactions between the absorption system and its surroundings are represented by the heat transfer quantities  $Q_a$ ,  $Q_c$ ,  $Q_e$ , and  $Q_g$  at the fixed four temperatures  $T_a$ ,  $T_c$ ,  $T_e$ , and  $T_g$ , respectively, where  $T_e < (T_c, T_a) < T_g$ . The subscripts  $a$ ,  $c$ ,  $e$ , and  $g$  symbolize absorber, condenser, evaporator, and generator; the primary components in an absorption system. The  $W$  in Figure 3-1 is an equivalent thermal work. In the operating model, the Carnot heat engine (1) produces the “work”  $W$  by applying the heat  $Q_g$  from a heat source at the higher temperature  $T_g$  and rejecting heat  $Q_a$  to a heat sink at an intermediate temperature  $T_a$ , and the refrigeration cycle (2) uses that work to extract the heat  $Q_c$  at the lower temperature  $T_e$  and releasing heat  $Q_e$  to another heat sink at another intermediate temperature  $T_c$ .

The energy balance equation of this combined cycle can be written as

$$Q_a + Q_c = Q_e + Q_g \quad (3.1)$$

The useful energy output of an absorption chiller is the cooling capacity  $Q_e$  in the evaporator and the energy input is the primary heat  $Q_g$  added into the generator. On the other hand, the useful energy output of an absorption heat pump is the heat from the absorber and condenser,  $Q_a + Q_c$ . Therefore, from Equation (2.4), the cooling and heating COP of the absorption chiller and heat pump can be expressed as follows:

$$COP_{ACH} = \frac{Q_e}{Q_g} \quad (3.2)$$

$$COP_{AHP} = \frac{Q_a + Q_c}{Q_g} \quad (3.3)$$

The total entropy generation equation of the combined cycle is written as

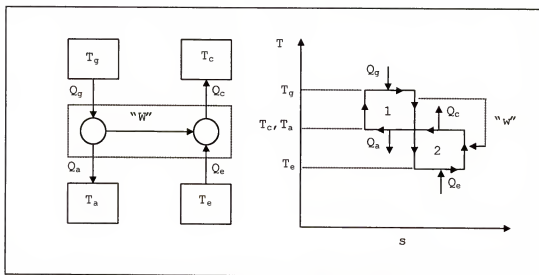


Figure 3-1. Schematic of an ideal absorption chiller and heat pump cycle and its T-S diagram

$$S_{gen} = \frac{Q_g}{T_g} + \frac{Q_e}{T_e} - \frac{Q_a}{T_a} - \frac{Q_c}{T_c} \quad (3.4)$$

In the ideal cycle, all of the processes are reversible; therefore, the total entropy generation  $S_{gen}$  in Equation (3.4) is equal to zero. Then by collecting Equations (3.1), (3.2) and (3.4), the Carnot COP of the ideal absorption chiller can be derived as follows

$$\begin{aligned} \frac{Q_g}{T_g} + \frac{Q_e}{T_e} - \frac{Q_g + Q_e - Q_c}{T_a} - \frac{Q_c}{T_c} &= 0 \\ Q_e \left( \frac{T_a - T_e}{T_e T_a} \right) &= Q_g \left( \frac{T_g - T_a}{T_a T_g} \right) + Q_c \left( \frac{T_a - T_c}{T_c T_a} \right) \\ COP_{ACH, Carnot} &= \frac{Q_e}{Q_g} = \left( \frac{T_g - T_a}{T_g} \right) \left( \frac{T_e}{T_a - T_e} \right) + \frac{Q_c}{Q_g} \left( \frac{T_a - T_c}{(T_a - T_e) T_c} \right) \end{aligned} \quad (3.5)$$

This COP is the maximum achievable by absorption chillers. Furthermore, if  $T_c$  and  $T_a$  are assumed equal, the second term on the right-hand side of Equation (3.5) drops out and the Carnot COP becomes a sole function of the operating temperatures of the cycle.

Similarly, the corresponding expression for the ideal heating COP for an AHP can be written by collecting Equations (2.4), (3.3) and (3.4).

$$COP_{AHP, Carnot} = \frac{Q_a + Q_c}{Q_g} = \left( \frac{T_g - T_e}{T_g} \right) \left( \frac{T_c}{T_c - T_e} \right) \quad (3.6)$$

These reversible Carnot COP in Equations (3.5) and (3.6) were calculated at different operating temperature levels, and compared with simulation results of various absorption chillers and heat pumps in this chapter.

### 3.2 Single-Effect Absorption Chillers

#### 3.2.1 Description of Single-Effect Absorption Chillers

The most basic absorption chiller using a LiBr/H<sub>2</sub>O solution as the working fluid pair is the single-effect system. It consists of an evaporator, a condenser, a generator, an absorber, a solution heat exchanger, a throttling valve, and a solution pump. The system

schematics and its cycle on the Duhring diagram are shown in Figure 3-2. There are two pressure levels,  $(P_c = P_g) > (P_a = P_e)$ , in this absorption system.

In Figure 3-2, a strong solution (State 11, high concentration of lithium bromide in the solution) leaving the generator (G) through the solution heat exchanger (HX) enters the absorber (A) to absorb the water vapor (State 3, refrigerant) from the evaporator (E) and becomes a weak solution (State 6). External cooling water (State 4) is introduced into the absorber to extract heat and keep the temperature from rising since the absorption process is exothermic. Then, the weak solution is delivered to the generator by the solution pump through the solution heat exchanger where this solution recovers some heat transferred from the strong solution. An external heat source at a high temperature (State 8) supplies heat into the generator to generate water vapor from the weak solution. The vaporized water (State 10) goes into the condenser (C) where it is condensed by means of an external cooling water loop (State 13). After this, the condensed water (State 15) passes through a throttling valve (V) and goes back to the evaporator where the water is evaporated at a low temperature by extracting heat from the chilled water (State 1) to create a cooling effect. Finally, this water vapor leaves the evaporator to the absorber and is absorbed by the strong solution, thus completing the cycle.

The solution heat exchanger in Figure 3-2 is not a necessary component for an absorption system to complete a job, but this component is important for performance improvement of the system. Because the solution heat exchanger can recover the heat from the strong solution and pass it on to the weak solution, this contributes to reducing the heat duty of the external heat source at the generator as well as the amount of cooling water required at absorber.

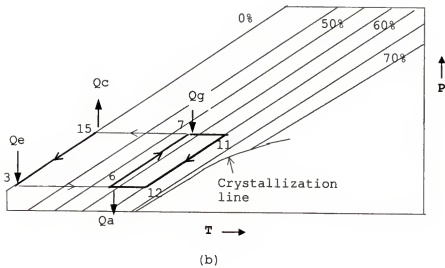
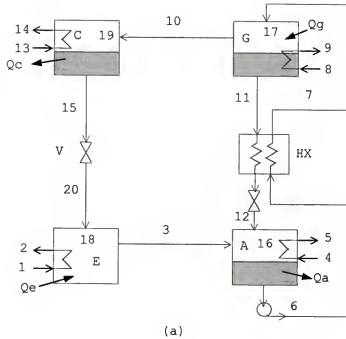


Figure 3-2. Single-effect absorption chiller: (a) Schematic of the system; (b) Duhring diagram of cycle



### 3.2.2 Thermodynamic Analysis of Single-Effect Absorption Chillers

Both the first and second laws of thermodynamics are employed to investigate the chiller's performance. For an absorption chiller, the primary input energy is supplied into the generator from an external heat source and the useful output energy is the cooling capacity obtained in the evaporator. Therefore, the COP of the single-effect absorption chiller shown in Figure 3-2 can be calculated by combining Equations (3.2), (2.36d) and (2.39b)

$$COP = \frac{Q_e}{Q_g} = \frac{m_3(h_3 - h_{20})}{m_{11}h_{11} + m_{10}h_{10} - m_7h_7} \quad (3.7)$$

The exergetic efficiency (Equation 2.13) of the single-effect absorption chiller can be expressed as the ratio of exergy change of the chilled water leaving the evaporator to that of the hot water (heat source) entering the generator

$$E_{ex} = \frac{m_1(\varepsilon_1 - \varepsilon_2)}{m_8(\varepsilon_8 - \varepsilon_9)} \quad (3.8)$$

The main parameters of the single-effect absorption chiller are listed in Table 3-1. This includes the heat transfer characteristics (UA) of the heat exchange component, mass flow rates and design point temperatures of the external water streams, and the weak solution circulation rate. The values of the heat transfer characteristics and mass flow rates were reported in the literature by Grossman and Gommend (1987). And the operating temperatures were selected on the basis of being typical values for purposes of evaluating the performance of absorption chillers (ARI 1992). A large number of model runs have been performed and compared in order to investigate the interactions of different operating conditions on the performance of single-effect absorption chillers. The effect of varying different operating conditions is evaluated and discussed. A sample output data of the simulation for the single-effect absorption chiller in Figure 3-2 is listed in Appendix A.

Table 3-1 Operating parameters of the single-effect absorption chiller

* Heat transfer characteristics (UA) *	
Absorber	6.06 kW/°C
Condenser	17.74 kW/°C
Evaporator	11.84 kW/°C
Generator	8.42 kW/°C
Solution heat exchanger	2.01 kW/°C
* Mass flow rates *	
Cooling water to absorber	2.93 kg/s
Cooling water to condenser	3.28 kg/s
Heat source to generator	3.62 kg/s
Chilled water from evaporator	2.25 kg/s
Weak solution from absorber	0.45 kg/s
* Operating temperatures *	
Cooling water inlet temperatures	29.4°C; 35.0°C
Chilled water outlet temperatures	7.2°C; 10.0°C
Heat source temperatures	71.1°C - 98.9°C

### 3.2.3 Discussion

#### Effect of heat source and cooling water temperatures

Figure 3-3 shows the variation of the coefficient of performance (COP) and exergetic efficiency ( $E_{ex}$ ) of the single-effect absorption chiller with two different cooling water temperatures (29.4 and 35.0°C) entering the absorber and the condenser versus the heat source temperature supplied to the generator. In Figure 3-3, it can be seen that the COP of the system is higher for the lower cooling water temperature as expected, and increasing the heat source temperature contributes to more improvement in the COP of the system with a higher cooling water temperature. It should be noted that, although the COP of the system increases with increasing the heat source temperature, the rate of

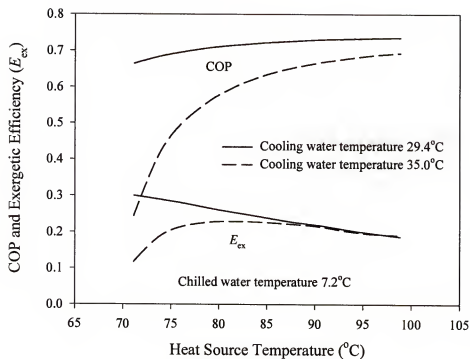


Figure 3-3. Variation of COP and exergetic efficiency of single-effect absorption chiller with different cooling water temperatures

increase of the COP becomes smaller as the former is increased. This behavior may be explained by the fact that although the high heat source temperature tends to increase the cooling COP, it also increases the average temperatures in the condenser and absorber, a trend that results in a decrease in the COP. This negative result trades off the beneficial effect of the high temperature of the heat source on the COP.

In the second law analysis of the system, a lower cooling water temperature gives the single-effect absorption chiller a higher exergetic efficiency as expected. The effect of the heat source temperature on the exergetic efficiency does not produce the same behavior as that of the COP for the absorption chiller within the operating range of the heat source temperature. As shown in Figure 3-3, the exergetic efficiency of the system with the lower cooling water temperature decreases monotonically when increasing the heat source temperature. But for the case with the high cooling water temperature, the exergetic efficiency increases first, levels off, and then decreases with a further increase in the heat source temperature. This decrease of the exergetic efficiency can be explained by the fact that even though a high temperature heat source increases the output cooling exergy, it also means that more input exergy is added to the system, and the net result leads to a smaller exergetic efficiency from a second law viewpoint.

#### Effect of leaving chilled water temperatures

The influence of different leaving chilled water temperatures on both the COP and exergetic efficiency of the single-effect absorption chiller considered when keeping the cooling water inlet temperature constant (29.4°C) is shown in Figure 3-4. As expected, the absorption system has a better cooling COP with a higher chilled water outlet temperature, since more cooling capacity can be produced from the evaporator under this operating condition. But it also shows that increasing the heat source temperature does not provide much improvement for the cooling COP of the absorption system. This can be explained by the same negative trade off due to the increase of the average

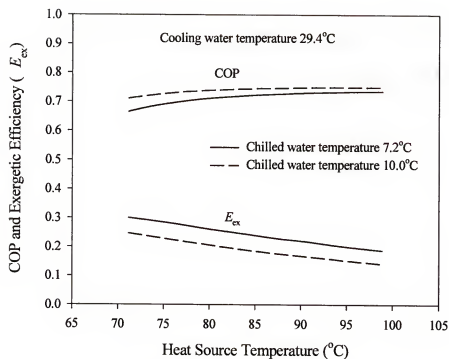


Figure 3-4. Variation of COP and exergetic efficiency of single-effect absorption chiller with different chilled water temperatures

temperatures in both the condenser and absorber when the heat source temperature increases as discussed earlier.

Unlike the result of the first law analysis that the higher chilled water outlet temperature leads to a higher COP, the single-effect absorption chiller has a higher exergetic efficiency when producing the chilled water at a lower temperature, even though less cooling capacity has been created as can be seen in Figure 3-4. This can be explained by the fact that chilled water at a lower temperature has a bigger potential to create a cooling effect at the same flow rate. This compensates for the decrease in the cooling capacity associated with the first law.

### 3.3 Double-Effect Absorption Chillers

#### 3.3.1 Description of Double-Effect Absorption Chillers

As discussed in the previous section, a higher temperature heat source does not promise a better system performance for the single-effect system. Thus, it may be necessary to develop advanced absorption chillers in order to apply the high temperature heat source that may be available from steam or waste heat of industrial processes. Double-effect systems represent a significant improvement in system performance over the single-effect systems and have been commercialized in the market worldwide by several US and Japanese manufactures.

The double-effect absorption chillers in this study form an extension of the single-effect system and have higher performance than the basic system. There are several types of cycles for double-effect absorption chillers. According to the manner with which the LiBr/H<sub>2</sub>O solution circulates, these absorption chillers can be categorized into three types: parallel-flow, series-flow, and dual-loop-flow types. Both the parallel and series flow types consist of two generators, two condensers, one absorber, one evaporator, and

two solution heat exchangers in their systems. Meanwhile the dual-loop flow type basically is a combination of two single-effect systems having heat transfer interactions with each other.

#### Parallel-flow type

Figure 3-5 shows schematically the parallel-flow, double-effect system and its cycle on the Duhring diagram. In this system, there are three pressure levels: high, medium, and low. The high-temperature generator (G1) and high-temperature condenser (C1) are at a high-pressure level, while the low-temperature generator (G2) and low-temperature condenser (C2) are at a medium pressure level, and the evaporator (E) and absorber (A) are at a low-pressure level. The weak solution leaving the absorber (State 5) is delivered to the high- and low-temperature generators in a parallel arrangement. This design can improve the energy efficiency of the system (Gommed and Grossman 1990) and reduce the risk of crystallization of the LiBr/H<sub>2</sub>O solution in the cycle. A higher-temperature heat source (State 15) adds heat into the high-temperature generator to generate water vapor (State 14) from the weak solution. The heat rejected from the high-temperature condenser is introduced into the low-temperature generator in order to generate additional water vapor (State 9) from the weak solution. Thereby, nearly 70% more water vapor is generated out of the solution in the system without extra heat input and this results in higher COP values than those of the single-effect system.

#### Series-flow types

Series-flow type, double-effect systems have the same component configuration and same circulation scheme for the refrigerant (water) as the parallel-flow type discussed above. High temperature heat source is supplied to the high-temperature generator, cooling water to the absorber and the low temperature condenser, while chilled water is obtained from the evaporator. The only difference between these two types is the manner with which the LiBr/H<sub>2</sub>O solution leaving the absorber to the generators circulates.

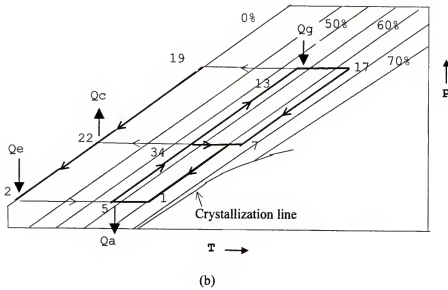
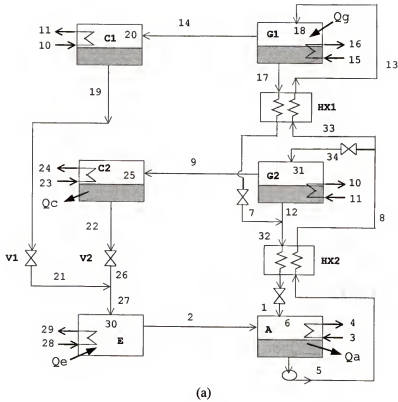


Figure 3-5. Double-effect absorption chiller: (a) Schematic of the system; (b) Duhring diagram of cycle



In the series-flow type, there are two possible circulation arrangements for the weak solution as illustrated in Figure 3-6. In one arrangement all of the weak solution is delivered to the high temperature generator first after leaving the absorber, and then is allowed to enter the low temperature generator to generate additional water vapor from the solution. The other arrangement is that all the weak solution enters the low temperature generator first and then enters the high temperature generator. Both of these two circulation schemes experience high risk of crystallization of the LiBr because of high concentration and low temperature before the strong solution returns to the absorber. Operating conditions of the systems should be carefully monitored to avoid crystallization.

#### Dual-loop flow type

Two individual single-effect absorption systems are cascaded and operate together as a dual-loop, double-effect chiller as shown in the Duhring diagram in Figure 3-7. One of the two systems is operated at relatively low pressure and temperature levels, and is labeled a low stage system or loop 1. The other is operated at high pressure and temperature levels and is designated a high stage system or loop 1. Each of the two systems operates independently like the single-effect system described in Figure 3-2, except that there are heat transfer interactions between the two systems.

In the dual-loop double-effect absorption chiller, a high temperature heat source is employed in the generator of the high stage loop (or cycle) to generate water vapor from the LiBr/H<sub>2</sub>O solution in the absorber. The heat rejected from the condenser of the high stage system is recovered and introduced into the generator of the low stage system to generate water vapor from the solution. Cooling water is distributed to the condenser and absorber of the low stage system as well as the absorber of the high stage system. If the operating conditions of the high stage system are carefully selected, both evaporators of the two systems have the potential to create cooling capacity simultaneously.

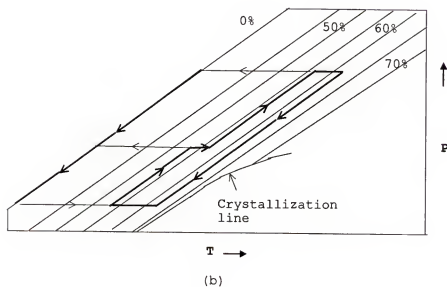
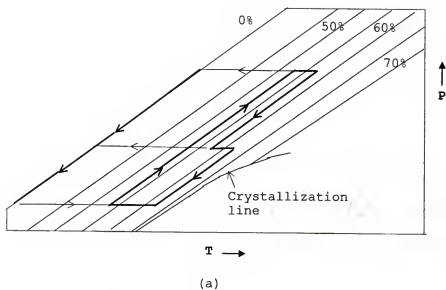
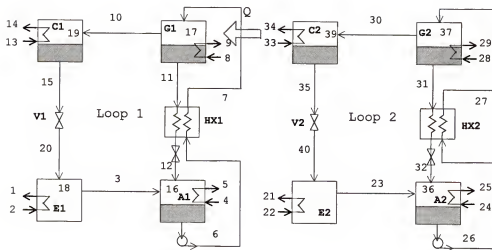
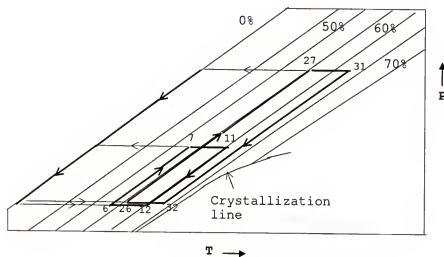


Figure 3-6. Duhring diagrams of two series flow types of double-effect absorption chillers: (a) Solution to high stage generator first; (b) Solution to low stage generator first.



(a)



(b)

Figure 3-7. Dual-loop type of double-effect absorption chiller:  
 (a) Schematic of the system; (b) Duhring diagram of cycle

The advantage of the dual-loop double-effect absorption system is that the system can employ different working fluid pairs for each loop or system since they are operated independently. System designers may select suitable working pairs for each loop of the dual-loop system. In this study, the LiBr/H<sub>2</sub>O solution is used in both the low and high stage systems.

### 3.3.2 Thermodynamic Analysis of Double-Effect Absorption Chillers

The four double-effect absorption chillers (Figures 3-5, 3-6, and 3-7) utilizing higher temperature heat sources were analyzed in the same process as discussed in Section 3.2. Except for heat source (hot water) temperatures, all other operating parameters have the same values as those listed in Table 3-1 for the single-effect chiller for comparison purposes. The design parameters of the double-effect systems are listed in Table 3-2. Again, the values of the heat transfer characteristics and mass flow rates were reported in the literature by Grossman and Gommend (1987). And the cooling and water temperatures were selected on the basis of being typical values for purposes of evaluating the performance of absorption chillers (ARI 1992).

First and second law analyses were performed for the four double-effect systems. In the parallel- and series-flow absorption chillers, the primary energy input is added into the high-temperature generator by an external water loop and the cooling capacity is delivered from the evaporator via another external water loop. Therefore the coefficient of performance can be calculated by combining Equations (3.2), (2.36d), and (2.39b) as follows:

$$COP = \frac{Q_e}{Q_g} = \frac{m_2(h_2 - h_{27})}{m_{17}h_{17} + m_{14}h_{14} - m_{13}h_{13}} \quad (3.9)$$

Since both the two evaporators of the dual-loop double-effect absorption chiller have the potential to create cooling capacity simultaneously, the COP of the dual-loop absorption chiller can be expressed as

Table 3-2 Operating parameters for double-effect absorption chillers

* Heat transfer characteristics (UA) *	
Absorber	6.06 kW/°C
Condensers 1 & 2	17.74 kW/°C
Evaporator	11.84 kW/°C
Generators 1 & 2	8.42 kW/°C
Solution heat exchangers 1 & 2	2.01 kW/°C
* Mass flow rates *	
Cooling water to absorber	3.62 kg/s
Cooling water to condenser 2	2.93 kg/s
Heat source to generator 1	3.12 kg/s
Chilled water from evaporator	2.25 kg/s
Weak solution from absorber	0.45 kg/s
* Operating temperatures *	
Cooling water inlet temperatures	29.4°C; 35.0°C
Chilled water outlet temperatures	7.2°C; 10.0°C
Heat source temperatures	93.3°C - 160°C

$$COP_{Dual-loop} = \frac{Q_{e,low} + Q_{e,high}}{Q_{g,high}} \quad (3.10)$$

The exergetic efficiencies of the double-effect absorption chillers can also be calculated as the ratio of the exergy change of the chilled water loop at the evaporator to that of the external hot water loop at the high temperature generator.

$$E_{ex} = \frac{\Delta E_{chilled\ water}}{\Delta E_{heat\ source}} = \frac{m_{28}(\varepsilon_{29} - \varepsilon_{28})}{m_{15}(\varepsilon_{15} - \varepsilon_{16})} \quad (3.11)$$

### 3.3.3 Discussion

#### Comparison of various double-effect absorption chillers

Figure 3-8 shows the variation of the coefficient of performance (COP) of the four double-effect absorption chillers against the heat source temperature. The COP curve of the single-effect absorption chiller was also plotted in Figure 3-8 for comparison purposes. The chilled water outlet temperature was set at 7.2°C and the cooling water inlet temperature at 29.4°C. It is obvious that all of the four double-effect absorption systems have a higher cooling COP compared with the single-effect one, but this is the case only if the temperature of the external heat source is high enough (approximately above 100°C in this study). As the supply temperature of the external heat source decreases, it is advisable to switch to the single-effect system if the temperature is below 100°C. In comparing the cooling COP of the four flow types of double-effect absorption chillers, Figure 3-8 shows that the parallel and dual-loop flow type systems outperform the two series flow types. This can be explained by the fact that since there is more LiBr/H<sub>2</sub>O solution delivered to the high stage generator in the series flow type systems, a larger amount of heat is required at the source to heat up the additional LiBr/H<sub>2</sub>O solution, which results in a lower COP. Thus, from the vantage point of the first law of thermodynamics, the parallel and dual-loop flow types are better choices to design double-effect absorption systems.

The ratio of the COP of the absorption system to the reversible Carnot COP (defined as the thermodynamic efficiency  $E_m$  in Equation (2.12)), can be calculated easily and is illustrated in Figure 3-9. This quantity only measures the relative value of the cycle COP to the Carnot COP. As can be seen, the single-effect system has a better thermodynamic efficiency than the four double-effect systems. This is because more irreversibility occurs in the double-effect systems due to the presence of more heat exchange components. In comparing the four double-effect systems, the parallel and dual-loop types have similar

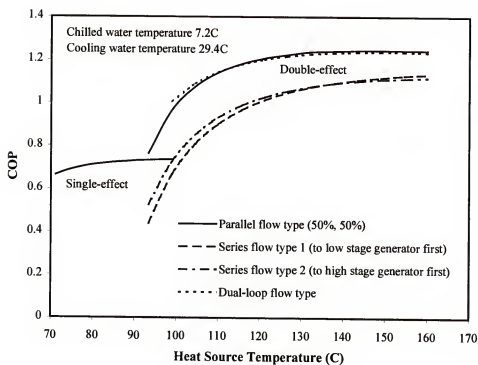


Figure 3-8. Comparison of COP of single-effect and four double-effect absorption chillers

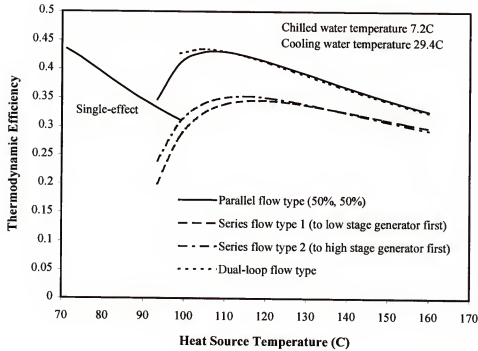


Figure 3-9. Comparison of thermodynamic efficiency of single-effect and four double-effect absorption chillers



thermodynamic efficiencies and are better than the series ones. Within their own heat source temperature domains, the thermodynamic efficiency of each double-effect absorption system increases significantly at first, and then declines continuously as the heat source temperature increases. This might be because the Carnot COP of the ideal cycle is a function of the operating temperatures only, and increases with increasing the heat source temperature. However, the advantage of employing a higher temperature heat source does not necessarily translate into a significant improvement in the COP for real systems. This may again be explained by the fact that a higher heat source temperature causes the average temperature in the condenser and absorber to increase, thus contributing negatively to the COP.

Figure 3-10 shows a comparison among the exergetic efficiencies of the different absorption chillers considered. Within their own heat source temperature domains, the exergetic efficiency of each double-effect absorption system increases significantly at first, and then declines continuously as the heat source temperature increases. The parallel flow type absorption chiller has a higher exergetic efficiency than other double-effect systems, but it loses to the dual-loop flow type as the heat source temperature increases further. It can also be seen in Figure 3-10 that the single-effect system has a relatively high exergetic efficiency within its low heat source temperature range when compared with the four double-effect systems. Thus, from the vantage point of the exergetic efficiency, the single-effect absorption system has better performance than the double-effect systems.

There exists an optimum in the exergetic efficiency for each of the absorption chillers considered with a constant cooling water temperature. This can be explained by the fact that although a higher heat source temperature can drive more water vapor from the  $\text{LiBr}/\text{H}_2\text{O}$  solution and more useful output exergy to create cooling, this also implies a much larger external input exergy to be supplied to the system. This means generating larger exergy losses in the generators, condensers, and absorber as their

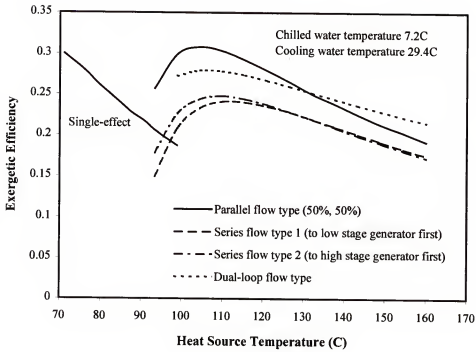


Figure 3-10. Comparison of exergetic efficiency of single-effect and four double-effect absorption chillers

average temperatures rise up as discussed earlier, which contributes negatively to the exergetic efficiency of the systems. Figure 3-11 shows how these effects manifest themselves for the parallel-flow double-effect absorption chiller with cooling water inlet temperature of 29.4°C and chilled water outlet temperature of 7.2°C.

#### Effect of split ratio for parallel flow type

Since the LiBr/H<sub>2</sub>O solution leaving the absorber is distributed to the high and low temperature generators simultaneously in the parallel flow type, the split ratio (ratio of mass flow rates of State 13 to State 5 in Figure 3-5) becomes an important parameter for the system. The effect of the split ratio of the LiBr/H<sub>2</sub>O solution on the cooling COP and the exergetic efficiency is shown in Figure 3-12 while keeping other parameters constant. It can be seen that there is a highest COP for the system when about 25% of the LiBr/H<sub>2</sub>O solution leaving the absorber is delivered to the high temperature generator. The COP drops slightly when the split ratio increases from 25% as more solution is distributed to the high stage generator. Figure 3-12 also shows that the exergetic efficiency decreases continuously with an increasing solution flow rate ratio for the high temperature generator. The decrease in the cooling COP and the exergetic efficiency can be explained by the fact that as more LiBr/H<sub>2</sub>O solution is delivered to the high stage generator, more heat duty of the external heat source is needed to heat the solution. This causes more irreversibilities to take place at the high stage generator and the high stage solution heat exchanger.

### 3.4 Triple-Effect Absorption Chillers

#### 3.4.1 Description of Triple-Effect Absorption Chillers

From the thermodynamic analysis of double-effect absorption chillers in Section 3.3, it can be concluded that increasing the heat source temperatures further does not

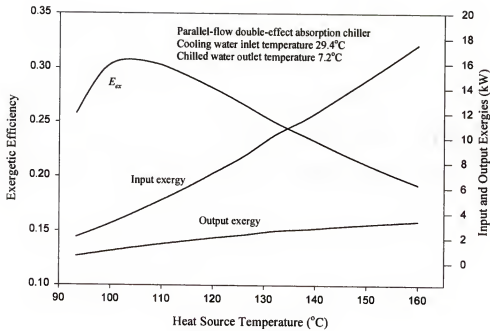


Figure 3-11. Variation of exergetic efficiency and input and output exergies of parallel-flow double-effect absorption chillers

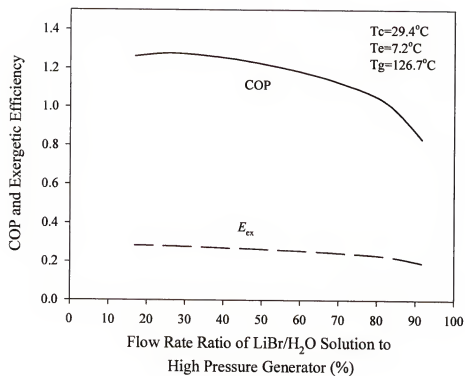


Figure 3-12. Variation of COP and exergetic efficiency of the parallel flow double-effect absorption chiller

necessarily promise a higher cooling COP or a higher exergetic efficiency. In order to further improve energy efficiency of absorption systems and utilization of high temperature heat sources available from natural gas, cogeneration systems, or other sources, many advanced triple-effect systems have been proposed and are shown to be capable of substantial performance improvement over single- and double-effect systems. The triple-effect absorption chiller in this study is the proposed double-condenser-coupled system (Miyoshi et al. 1985; DeVault and Biermann 1993; Grossman et al. 1994) comprised of three generators, three condensers, one absorber, one evaporator, and three solution heat exchangers (Figure 3-13). Four pressure levels exist in this system.

Since high temperature heat source (above 150°C) is necessary to drive the triple-effect absorption chillers, the risk of crystallization of LiBr becomes higher because of the higher concentration of the strong solution. The series flow type would not be a proper choice for this advanced absorption chiller any more. Therefore, in this study, the weak LiBr/H<sub>2</sub>O solution leaving the absorber is divided and pumped to the three (high-, medium-, and low-temperature) generators in a parallel arrangement.

Like the double-effect system, as the heat source (State 35) adds heat to the high-temperature generator (G1) to generate water vapor (State 38) from the weak solution, the triple-effect system recovers heat from each high-temperature condenser (C1 or C2) to the next lower temperature generator (G2 or G3) twice to generate additional water vapor from the weak solution. Thus, more water vapor can be generated from the weak solution in a triple-effect system than in single- or double-effect systems, which means more cooling capacity can be delivered. Cooling water (States 3 and 23) is supplied to the absorber (A) and the low-temperature condenser (C3), respectively, and a cooling effect is obtained from the evaporator at the lowest temperature of the cycle through the external chilled water loop (State 28).

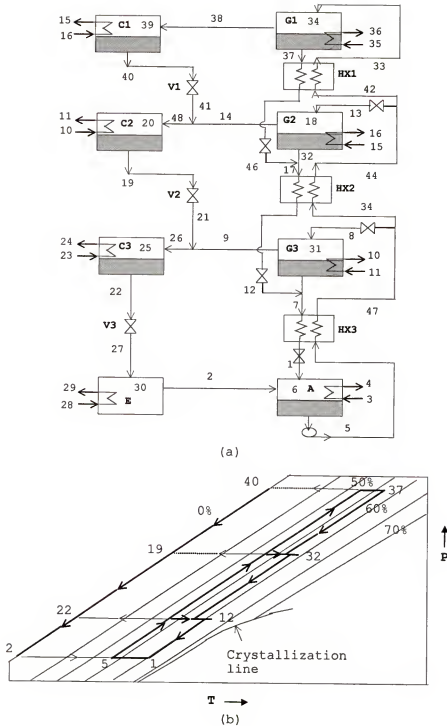


Figure 3-13. Triple-effect absorption chiller: (a) Schematic of the system; (b) Duhring diagram of cycle

### 3.4.2 Thermodynamic Analysis of Triple-Effect Absorption Chillers

In the triple-effect absorption chiller, external heat source (stream 35) is employed at the high temperature generator, and chilled water (stream 29) is delivered from the evaporator. From the definitions, the coefficient of performance of the triple-effect absorption chiller can be expressed as

$$COP = \frac{Q_e}{Q_g} = \frac{m_2(h_2 - h_{27})}{m_{37}h_{37} + m_{38}h_{38} - m_{33}h_{33}} \quad (3.12)$$

and the exergetic efficiency is

$$E_{ex} = \frac{\Delta E_{\text{chilled water}}}{\Delta E_{\text{heat source}}} = \frac{m_{28}(\varepsilon_{29} - \varepsilon_{28})}{m_{35}(\varepsilon_{35} - \varepsilon_{36})} \quad (3.13)$$

Thermodynamic first and second law analyses were performed for the triple-effect system over its operating conditions which are listed in Table 3-3. The values of the heat transfer characteristics and mass flow rates in Table 3-3 were referenced to the literature by Grossman and Gommend (1987). The cooling and chilled water temperatures were selected on the basis that it is typical values for evaluating the performance of absorption chillers.

### 3.4.3 Discussion

#### Effect of heat source and cooling water temperatures

Figure 3-14 shows the variation of the coefficient of performance (COP) of the single-, double-, and triple-effect absorption chillers versus the heat source temperature. Effects of different cooling water temperatures on the performance of the systems were also compared. The chilled water outlet temperature was set at 7.2°C. It is obvious that the triple-effect system has the highest cooling COP compared with the single- and double-effect ones, but this is the case only if the temperature of the external heat source is high enough (approximately above 155°C in this study). As the supply temperature of the external heat source decreases, it is advisable to switch to the double-effect system or



Table 3-3 Operating parameters for triple-effect absorption chiller

* Heat transfer characteristics (UA) *	
Absorber	6.06 kW/°C
Condensers 1, 2, & 3	17.74 kW/°C
Evaporator	11.84 kW/°C
Generators 1, 2, & 3	8.42 kW/°C
Solution heat exchangers 1, 2, & 3	2.01 kW/°C
* Mass flow rates *	
Cooling water to absorber	3.62 kg/s
Cooling water to condenser 3	2.93 kg/s
Heat source to generator 1	3.12 kg/s
Chilled water from evaporator	2.25 kg/s
Weak solution from absorber	0.45 kg/s
* Operating temperatures *	
Cooling water inlet temperatures	29.4°C; 35.0°C
Chilled water outlet temperatures	7.2°C; 10.0°C
Heat source temperatures	148.9°C - 198°C

even to the single-effect system if the temperature is below 100°C. Figure 3-14 also shows that the heat source temperature has a larger effect on the COP for each system when operating with a higher cooling water temperature.

It should be noted that the COP for all of the three systems increases at first with an increasing heat source temperature, then the COP curves become flat. The COP of the double-effect system even decreases slightly when the heat source temperature increases further. This behavior may be explained by observing that, although the high heat-source temperature causes the COP to increase, it also increases the average temperatures in the condenser and the absorber, which contributes to decreasing the COP. This negative result on the COP trades off the beneficial effect of a high heat source temperature. In Figure 3-14 it can be seen that a lower cooling water temperature (29.4°C) yields a higher

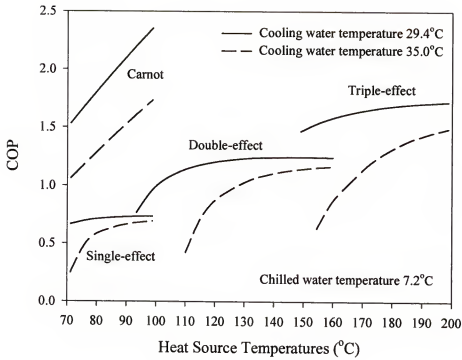


Figure 3-14. Comparison of COP of the three absorption chillers with different cooling water temperatures

cooling COP for all three systems. This is because the external cooling water at a lower temperature contributes to keeping the average temperatures in the condenser and the absorber from increasing, and hence decreases the likelihood of crystallization of the solution entering the absorber in addition to increasing the COP. And this positive effect of the lower cooling water temperature is more significant on the double-effect and triple-effect systems than on the single-effect system since it also results in a decrease in the operating temperatures at the middle stages of these systems. This is probably the reason why most absorption systems employ water instead of air as the cooling medium for its better heat transfer characteristics.

In addition, the reversible Carnot COP in Equation (3.6) of an ideal absorption chiller cycle varying with operating temperature levels were also plotted in Figure 3-14. As can be seen, the Carnot COP increases linearly with increasing the heat source temperature. It is obvious that the cooling COP of the three absorption systems differ from the reversible Carnot COP. This is because of irreversibilities in the real systems which are due to irreversible heat and mass transfer in the components, vapor absorption in the absorber, vapor generation in the generator, and mixing of two solutions at different temperatures.

A comparison of the thermodynamic efficiency of the three absorption chillers with different cooling water temperatures is illustrated in Figure 3-15. As can be seen, the single-effect system has a better thermodynamic efficiency than either the double-effect or the triple-effect systems. This is because more irreversibility occurs in the double-effect and triple-effect systems due to the presence of more heat exchange components. Also, the three systems experience better thermodynamic efficiencies at the high cooling water temperature than at the low one within some heat source temperature ranges as shown in Figure 3-15. This may seem to go against the expected and the well known trend that the efficiency increases with a decreasing cooling water temperature. While this is true, it still has the opposite trend for the thermodynamic efficiency. This quantity

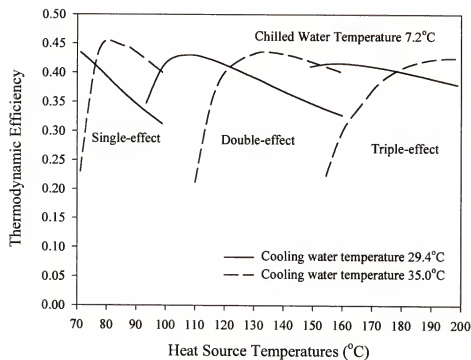


Figure 3-15. Comparison of thermodynamic efficiency of the three absorption chillers with different cooling water temperatures

only measures the relative value of the cycle COP to the Carnot COP. This might be because the Carnot COP of the ideal cycle is a function of the operating temperatures only, and increases with increasing the heat source temperature or decreasing the cooling water temperature. However, the advantage of employing a higher temperature heat source or a lower cooling water temperature does not necessarily translate into a significant improvement in the COP for real systems even at a lower cooling water temperature. This may again be explained by the fact that a higher heat source temperature causes the average temperature in the condenser and absorber to increase, thus contributing negatively to the COP.

Figure 3-16 shows a comparison among the exergetic efficiencies of the three absorption chillers considered. Unlike the thermodynamic efficiency results discussed above, the three systems have better exergetic efficiencies when operating with a low cooling water temperature as expected. Within their own heat source temperature domains, the exergetic efficiency of each absorption system increases significantly at first, and then declines continuously as the heat source temperature increases. This is because a higher heat source temperature means more external input exergy supplied to the system even though the latter can drive more water vapor from the  $\text{LiBr}/\text{H}_2\text{O}$  solution to create cooling. And it also generates more exergy losses in the generators, condensers, and absorber as their average temperatures rise up as discussed earlier. This contributes negatively to the exergetic efficiency of the three absorption systems. It can also be seen that the single-effect system has a relatively high exergetic efficiency within its low heat source temperature range when compared with the other two advanced systems. Thus, from the vantage point of the exergetic efficiency, the single-effect absorption chiller has better performance than either the double-effect or the triple-effect chillers.

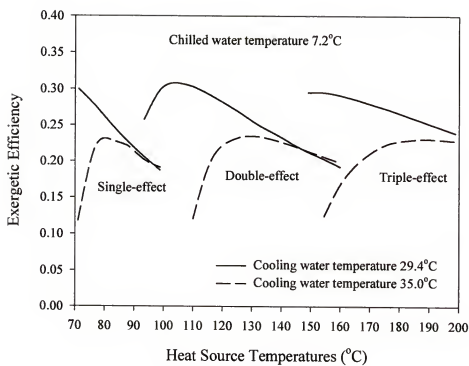


Figure 3-16. Comparison of exergetic efficiency of the three absorption chillers with different cooling water temperatures

### Effect of leaving chilled water temperatures

The influence of different leaving chilled water temperatures on the cooling COPs of the three absorption chillers considered when keeping the cooling water inlet temperature constant (29.4°C) is shown in Figure 3-17. As expected, all three systems experience better cooling COPs with a higher chilled water outlet temperature, since more cooling capacity can be produced from the evaporator under this operating condition. But it also shows that increasing the heat source temperature does not provide much improvement for the COPs of the three absorption chillers. All COP curves for the three chillers with the higher chilled water outlet temperature even decline slightly as the heat source temperature increases further. And this can be explained by the same negative trade off due to the increase of average temperature in the condenser and absorber as the heat source temperature increases as discussed earlier in Figure 3-14. The curves for the reversible Carnot COP were also plotted in the figure for comparison. The thermodynamic efficiency of the three systems was calculated for two chilled water outlet temperatures (7.2°C and 10°C) and is plotted against the external heat source temperature in Figure 3-18. As can be seen, the three absorption chillers have similar thermodynamic efficiency values within their own operating domain. Unlike the result of first law analysis that the higher chilled water outlet temperature leads to a better COP, the lower chilled water outlet temperature provides the three systems with a higher thermodynamic efficiency within most of their own heat source operating temperature range. This is because higher heat source temperatures do not provide the real systems with the same increase in COP as they do the ideal system when producing chilled water at a high temperature. Thus the thermodynamic efficiency of the three chillers with the high chilled water temperature is lower than that with a low chilled water temperature.

Figure 3-19 shows a comparison among the exergetic efficiencies for the three absorption chillers operating with different chilled water outlet and external heat source temperatures. The trends of the exergetic efficiency curves in Figure 3-19 are

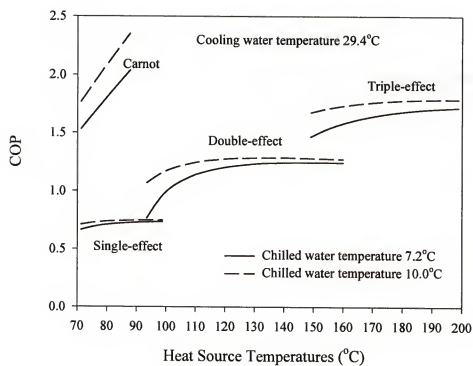


Figure 3-17. Comparison of COP of the three absorption chillers with different chilled water temperatures



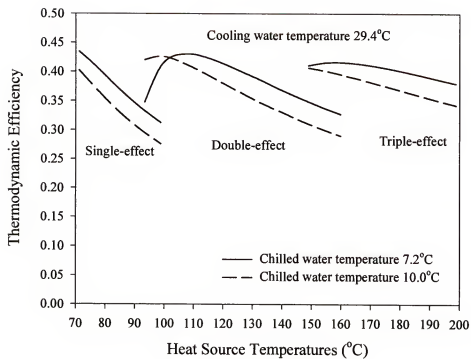


Figure 3-18. Comparison of thermodynamic efficiency of the three absorption chillers with different chilled water temperatures

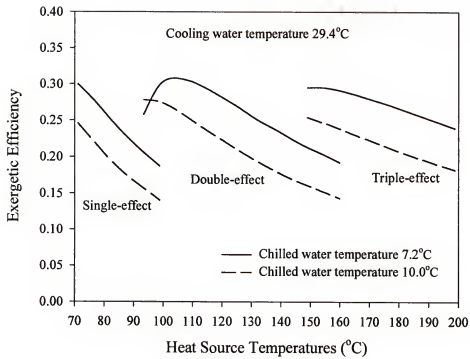


Figure 3-19. Comparison of exergetic efficiency of the three absorption chillers with different chilled water temperatures

qualitatively similar to those of the thermodynamic efficiency curves in Figure 3-18, but are quantitatively different. As can be seen, like the results of Figure 3-18, all three absorption systems have a higher exergetic efficiency when producing the chilled water at a lower temperature, even though less cooling capacity has been created as mentioned in discussions pertaining to Figure 3-17. This can be explained by the fact that chilled water at a low temperature has a higher potential to create a cooling effect than at a high temperature at the same flow rate. This compensates for the decrease in the cooling capacity associated with the first law. Still, the single-effect system has a better performance than the multi-effect systems from the standpoint of the second law.

It is important to note that the quantitative discrepancy between the thermodynamic and exergetic efficiencies has been addressed by Tozer and James (1994, 1997a) by adopting a different definition for the Carnot COP. Tozer and James adopt a two-temperature definition (as opposed to the four-temperature definition adopted here) which causes the driving and cooling cycles not to be independent of each other. The two-temperature definition seems to explain some of the discrepancies observed here between the two efficiencies in question. The reader is advised to consult the works of Tozer and James (1994, 1997a) to further understand this behavior as this is a bit outside the scope of the present study.

### 3.5 Absorption Heat Pumps for Heating

#### 3.5.1 Description of Absorption Heat Pumps for Heating

A basic absorption heat pump for heating purposes has exactly the same components and configuration as the single-effect absorption chiller shown in Figure 3-2. The difference of operation between the two applications is the useful output energy and the operating temperature and pressure levels in the system. The useful output energy of

the system for heating is the heating capacity obtained from the absorber and condenser, while the input energy is supplied to the generator. Furthermore, the evaporator extracts heat from the environment employing an external water loop. Therefore the absorption system is operated at higher temperature and pressure levels in the condenser and generator, and a higher temperature level in the absorber. The schematics of the absorption heat pump and Duhring diagram of its cycle are illustrated in Figure 3-20.

In the absorption heating system, the LiBr/H<sub>2</sub>O solution and water travel in the same manner as described in the single-effect absorption chiller. The external heat source adds heat to the generator (G) to generate water from the weak solution and the evaporator (E) extracts heat from its cold environment by an external water loop. At the same time, useful heat output (hot water) is obtained at the absorber (A) and the condenser (C) via an external hot water loop that passes through them. In this study, the supply hot water is preheated in the absorber first and then is heated to the desirable temperature at the condenser in order to keep the operating cycle away from the crystallization line of LiBr/H<sub>2</sub>O solution.

### 3.5.2 Thermodynamic Analysis of Absorption Heat Pumps for Heating

The coefficient of performance of the absorption heat pump is defined as the ratio of useful heat output at the condenser and absorber to the heat input to the generator, and can be expressed from Equations (3.3), (2.35c), (2.36c), and (2.37b) as

$$\begin{aligned} COP &= \frac{Q_c + Q_a}{Q_g} = \frac{m_{10}(h_{10} - h_{15}) + (m_{12}h_{12} + m_3h_3 - m_6h_6)}{m_{11}h_{11} + m_{10}h_{10} - m_7h_7} \\ &= \frac{m_4(h_5 - h_4) + m_{13}(h_{14} - h_{13})}{m_8(h_8 - h_9)} \end{aligned} \quad (3.13)$$

The thermodynamic efficiency of the absorption heat pump can be calculated by the COP of the real system and the Carnot COP of the ideal cycle in Equations (2.12), (3.13), and (3.6). And the exergetic efficiency (Equation 2.13) of this system can be

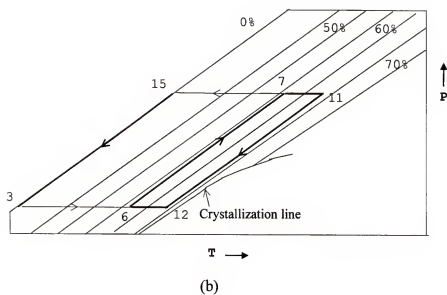
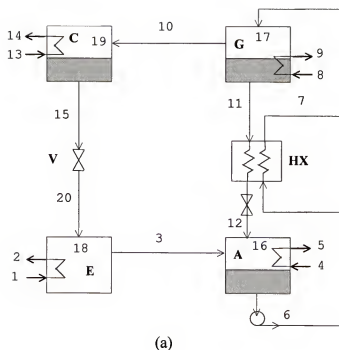


Figure 3-20. Absorption heat pump for heating: (a) Schematic of the system; (b) Dühring diagram of cycle

expressed as the ratio of exergy change of the hot water loops at the condenser and the absorber to that of the heat source water loop at the generator.

$$E_{ex} = \frac{m_{13}(\varepsilon_{14} - \varepsilon_{13}) + m_4(\varepsilon_5 - \varepsilon_4)}{m_8(\varepsilon_8 - \varepsilon_9)} \quad (3.14)$$

Thermodynamic performance of the absorption heat pump for heating is evaluated under different operating conditions. These operating conditions include the heat source, supply hot water, and cold side water temperatures. ARI Standard (ARI 1992) recommends the supply hot water temperature at 60°C for the evaluation of performance of absorption chillers. In this study, another supply hot water temperature at 54.4°C is also investigated. The operating parameters of the absorption heat pump are listed in Table 3-4.

Table 3-4 Operating parameters for absorption heat pump

* Heat transfer characteristics (UA) *	
Absorber	12.37 KW/°C
Condenser	11.49 KW/°C
Evaporator	11.88 KW/°C
Generator	11.02 KW/°C
Solution heat exchanger	3.16 KW/°C
* Mass flow rates *	
Heat source to generator	3.12 Kg/s
Cold water to evaporator	2.25 Kg/s
Weak solution from absorber	1.12 Kg/s
* Operating temperatures *	
Supply hot water temperatures	54.4°C; 60.0°C
Return hot water temperatures	48.9°C
Cold water inlet temperatures	7.2°C; 10.0°C
Heat source temperatures	113°C - 130°C

### 3.5.3 Discussion

#### Effect of heat source and supply hot water temperatures for heating applications

Figure 3-21 shows both the heating COP and exergetic efficiency of the absorption system for heating applications with different supply hot water temperatures versus the heat source temperature. The cold side water temperature at the evaporator is set at 10.0°C. It can be seen that the heating COP of the system increases with the heat source temperature as expected. However, increasing the heat source temperature leads to a high risk of crystallization for the strong solution before it enters the absorber. It is also found that the system providing a higher supply hot water temperature (60°C) experiences a lower heating COP and has a smaller operating range due to the crystallization problem when compared with the one providing a low supply hot temperature (54.4°C).

Like the heating COP, the exergetic efficiency increases with increasing the heat source temperature, but the rate of increase of the exergetic efficiency becomes smaller as the heat source temperature further increases. This can be explained by the fact that although the system with the heat source at high temperature can provide more supply hot water, it also means more input exergy is supplied to the system and more exergy losses can occur in the generator during the heat transfer process. The exergetic efficiency even tends to decline if the heat source temperature increases beyond a certain value. This is not shown in the figure, however, because crystallization of the LiBr was predicted to happen under those conditions.

#### Effect of cold side water temperatures for heating applications

In addition to employing energy from the heat source at the generator, the absorption system also extracts some heat from its cold environment by the evaporator. The effect of the temperatures of cold water entering the evaporator on the heating COP is shown in Figure 3-22 along with the exergetic efficiency. The supply hot water temperature from the condenser was set at 54.4°C. As can be seen, the absorption system

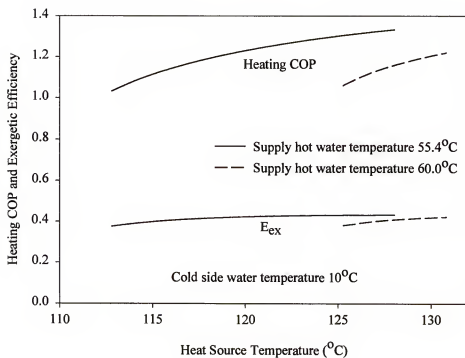


Figure 3-21. Comparison of heating COP and exergetic efficiency of the absorption heat pump with different supply hot water temperatures



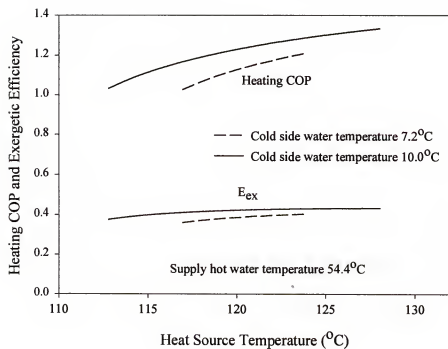


Figure 3-22. Comparison of heating COP and exergetic efficiency of the absorption heat pump with different cold side water temperatures

extracting heat from the cold side water at a higher temperature experiences a better heating COP and a better exergetic efficiency than the one with low cold side water temperature. This is because it is more difficult for the absorption system to utilize energy from the cold side water loop at lower temperatures. In such a situation of a low environmental temperature, the system needs a heat source at a higher temperature to obtain a high heating COP. But this would result in increasing the likelihood of crystallization. Therefore, the LiBr/H<sub>2</sub>O absorption system would not have a good thermal performance, and the system may not even operate normally when the environmental temperature is very low. In this case, however, the LiBr/H<sub>2</sub>O system can switch to an operating mode that supplies the heat source stream directly to the space to be heated without having to operate the system.

### 3.6 Conclusions

Performance simulations have been carried out for single-effect, double-effect, and triple-effect absorption chillers and absorption heat pumps using LiBr/H<sub>2</sub>O solution as their working fluids. Both the first and second law efficiencies of these absorption systems have been investigated and compared over a host of operating conditions. In the parametric analysis of the absorption chillers with varying operating conditions, it is clear that a low cooling water temperature yields a higher cooling COP and a higher exergetic efficiency for all of the absorption chillers as expected. Results also shows that, although the chillers operating with high chilled water temperature have better cooling COP, these systems experience smaller exergetic efficiency than those having a low chilled water temperature. Increasing heat source temperature can improve the cooling COP of the absorption chillers, but as the heat source temperature further increases furthermore, the COP of the systems levels off and even decreases. This negative effect of increasing the

heat source temperature is more dominant on the exergetic efficiency of the systems considered.

Comparing both first-law and second-law efficiencies of the four double-effect absorption chillers with different solution flow types, results show that the parallel flow and dual-loop flow types are better a choice for the multi-effect systems. In the comparison of performance of various absorption chillers, it can be concluded that the triple-effect system has a superior cooling COP over the single-effect or the double-effect systems. Thus, if high temperature heat source is available, it is better to operate an absorption chiller in a triple-effect mode. From a second law standpoint, however, all three chillers have similar exergetic efficiency within their own operating temperature ranges. The single-effect system still is a good choice since it uses lower grade heat sources and costs less.

In the parametric analysis of the absorption system for heating, it is clear that increasing the heat source temperature will increase both the heating COP and the exergetic efficiency. However, increasing the heat source temperature could result in a high risk of crystallization for the LiBr/H<sub>2</sub>O solution. The system also has a small operating range and a high crystallization risk when the system needs to provide the supply hot water at a higher temperature. In the situation of low environmental temperature, the LiBr/H<sub>2</sub>O absorption system does not have good thermodynamic performance for heating, and may not even be able to operate normally because of the freezing problem of refrigerant (water). When such a situation arises, the heat source stream should probably be supplied to the heating spaces directly without operating the absorption system.

## CHAPTER 4

### ABSORPTION HEAT TRANSFORMERS

Very large quantities of waste heat at low temperatures are rejected to the environment from power plants and industrial processes everyday around the world. These energy losses not only result in low efficiencies but also cause thermal pollution to the global environment. Industrial heat pumps have the ability to recover low-temperature heat and upgrade it to a higher temperature for process use, thus saving energy and reducing emissions of gases like  $\text{CO}_2$ ,  $\text{SO}_x$ , and  $\text{NO}_x$  that cause air pollution and global warming from the combustion of oil, natural gas, and other fuels. Industrial heat pumps can also provide a number of process-related benefits that include increasing capacity of existing process heating systems and improving product quality. There are many different kinds of systems applied for heat recovery or recuperation purposes. Absorption heat transformers are one of the more favorable systems for such temperature boost applications, because the absorption systems have the advantage of using a part of the waste heat to power the systems themselves while upgrading the temperature and only consuming little electric power.

In this chapter, single-, double-, and triple-stage absorption heat transformers (AHTs) using a lithium bromide/water ( $\text{LiBr}/\text{H}_2\text{O}$ ) solution as the working fluid will be evaluated and compared on the basis of both the first and second laws of thermodynamics. The coefficient of performance, thermodynamic efficiency, and the exergetic efficiency of the three systems are investigated under different operating conditions including the waste heat and cooling water temperatures and the magnitude of the temperature boost. Results obtained here should provide some theoretical bases for the optimal operation and design of real AHT systems.

#### 4.1 Ideal Absorption Heat Transformer Cycle

Like the types I and II of absorption systems discussed earlier in Chapter 3, an ideal type III absorption system can also be treated as a combination of a Carnot heat engine cycle (1) and a heat pump cycle (2). A type III operating model and its temperature-entropy ( $T$ - $S$ ) diagram are shown in Figure 4-1. This model is just like the types I and II in Figure 3-1 operated in a reversed mode (Herold et al. 1996). Again, the principal interactions between the absorption heat transformer and its surroundings are represented by the heat transfer quantities  $Q_a$ ,  $Q_c$ ,  $Q_e$ , and  $Q_g$  at the fixed four temperatures  $T_a$ ,  $T_e$ ,  $T_c$ , and  $T_g$ , respectively, where  $T_a > (T_e, T_g) > T_c$ . In the operating model, the Carnot heat engine cycle (1) produces the "work"  $W$  by applying the heat  $Q_e$  from a heat source at the medium temperature  $T_e$  and rejecting heat  $Q_c$  to a heat sink at the lower temperature  $T_c$ , and the heat pump cycle (2) uses that work to extract the heat  $Q_g$  from another heat source at the temperature  $T_g$  and supply useful heat  $Q_a$  at the higher temperature  $T_a$ . The  $W$  in here is still an equivalent thermal work.

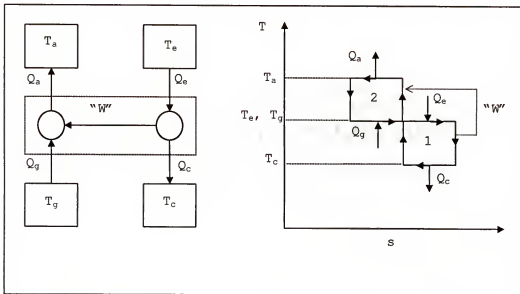


Figure 4-1. Schematic of ideal absorption heat transformer and its  $T$ - $S$  diagram

The energy balance for the absorption heat transformer can be written as

$$Q_a + Q_c = Q_g + Q_e \quad (4.1)$$

and the coefficient of performance COP for an AHT is defined as the ratio of the useful heat output  $Q_a$  to the input energy  $Q_g$  and  $Q_e$ .

$$COP_{AHT} = \frac{Q_a}{Q_g + Q_e} \quad (4.2)$$

From the second law of thermodynamics, the total entropy generation for a system is equal to the summation of entropy changes of all processes. Thus, for an absorption system, it can be written as

$$S_{gen} = -\frac{Q_g}{T_g} - \frac{Q_e}{T_e} + \frac{Q_a}{T_a} + \frac{Q_c}{T_c} \quad (4.3)$$

And, in an ideal cycle, all of the processes are reversible; therefore, the total entropy generation of the ideal absorption cycle becomes zero.

$$S_{gen} = -\frac{Q_g}{T_g} - \frac{Q_e}{T_e} + \frac{Q_a}{T_a} + \frac{Q_c}{T_c} = 0 \quad (4.4)$$

Generally, it is assumed that  $T_g = T_e$  for an absorption heat transformer cycle since the generator and evaporator of the system employ energy from the same heat source. By collecting Equations (4.1), (4.2), and (4.4), a maximum COP for the absorption heat transformer can be obtained from the following:

$$\begin{aligned} \frac{Q_g + Q_e}{T_e} &= \frac{Q_a}{T_a} - \frac{Q_a - (Q_g + Q_e)}{T_c} \\ (Q_g + Q_e) \left( \frac{1}{T_e} - \frac{1}{T_c} \right) &= Q_a \left( \frac{1}{T_a} - \frac{1}{T_c} \right) \\ COP_{AHT, Carnot} &= \frac{Q_a}{Q_g + Q_e} = \left( \frac{T_e - T_c}{T_e} \right) \left( \frac{T_a}{T_a - T_c} \right) \end{aligned} \quad (4.5)$$

As expressed by Equation (4.5), the maximum COP is a simple function of the operating temperature levels. It should be noted that, when a very large temperature boosting is required, the term in the second bracket is almost equal to 1 and then the reversible Carnot COP of the ideal AHT system is equal to the thermal efficiency of the Carnot heat

engine operating between  $T_e$  and  $T_c$ . This Carnot COP was calculated at different temperature levels for comparison with the simulation results of absorption heat transformers discussed in the following sections.

## 4.2 Single-Stage Absorption Heat Transformers

### 4.2.1 Description of the Single-Stage Absorption Heat Transformer

The system schematic of the single-stage absorption heat transformer (AHT) and its operating cycle on the Duhring diagram are shown in Figure 4-2. This basic heat transformer consists of a generator, a condenser, an evaporator, an absorber, and a solution heat exchanger. The high pressure level of the single-stage AHT system exists inside the evaporator and absorber while the lower pressure level exists on the condenser and generator side. Therefore, the pressure and temperature levels in an AHT are that  $(P_a=P_e) > (P_g=P_c)$  and  $T_a > (T_g, T_c) > T_e$ .

In Figure 4-2, a heat source such as waste heat from industrial processes at an intermediate temperature is introduced to the generator (G) to generate water vapor from the weak LiBr/H<sub>2</sub>O solution. Then the generated water vapor leaves the generator and is condensed in the condenser (C) employing an external cooling water loop. The condensed water is delivered to the evaporator (E) and in there the water is evaporated again by employing waste heat from the same heat source as supplied to the generator. The strong LiBr/H<sub>2</sub>O solution leaving the generator is pumped through the solution heat exchanger (HX) to the absorber (A), where the strong solution absorbs the water vapor from the evaporator and becomes a weak solution. Then this weak solution passes through the solution heat exchanger and returns to the generator and completes the cycle. Since the absorption process between the water vapor and the lithium bromide/water solution in the absorber is exothermic, absorption heat at the highest temperature of the

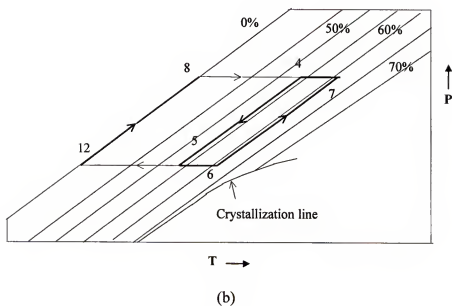
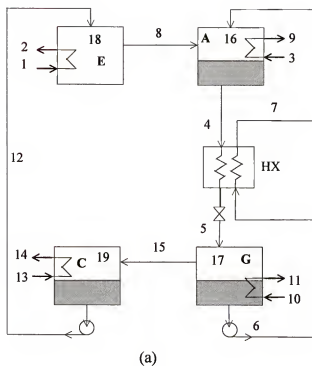


Figure 4-2. Single-stage absorption heat transformer: (a) schematic of the system, (b) Durhing diagram of the cycle



system is utilized in the absorber employing a portion of the waste heat stream. The waste heat stream is thus upgraded to a higher temperature and becomes the useful energy output. The temperature difference between the inlet and outlet streams of the waste heat source at the absorber is usually defined as the temperature boost or lift.

#### 4.2.2 Thermodynamic Analysis of Single-Stage Absorption Heat Transformers

From the Carnot coefficient of performance of the ideal absorption heat transformer in Equation (4.5), it is evident that the operating temperatures of the system are important. These operating temperatures include the available heat source and cooling medium temperatures, and, of course, the desired temperature boosting. These operating temperatures not only constrain the operating models of an AHT, but are also major factors in choosing the proper working fluids. Therefore, thermodynamic investigations of these operating parameters of a single-stage absorption heat transformer are conducted in detail in this study.

As described earlier, the single-stage absorption heat transformer applies waste heat at a medium temperature as heat source to the evaporator and generator, and supplies an upgraded heat at a higher temperature from the absorber. Thus, the coefficient of performance of an absorption heat transformer is defined as the ratio of useful heat from the absorber to the input heat to the generator and evaporator, and can be expressed from Equations (4.2), (2.35c), (2.36c), and (2.38b) as follows:

$$COP = \frac{Q_a}{Q_g + Q_e} = \frac{m_7 h_7 + m_8 h_8 - m_4 h_4}{(m_{15} h_{15} + m_6 h_6 - m_5 h_5) + m_8 (h_8 - h_{12})} \quad (4.6)$$

Then, the thermodynamic efficiency,  $E_{th}$ , defined as the ratio of the COP of the real cycle to the corresponding Carnot COP of the ideal cycle of the absorption heat transformer, can be calculated from Equations (2.12), (4.5), and (4.6). And the exergetic efficiency (Equation (2.13)) of the system can be expressed as the ratio of exergy change of the

heated water loop at the absorber to that of the hot water loops at the evaporator and generator.

$$E_{ex} = \frac{\Delta E_a}{\Delta E_e + \Delta E_g} = \frac{m_3(\varepsilon_9 - \varepsilon_3)}{m_1(\varepsilon_1 - \varepsilon_2) + m_{10}(\varepsilon_{10} - \varepsilon_{11})} \quad (4.7)$$

A large number of model runs have been performed and compared to simulate and investigate the thermodynamic performance of the single-stage absorption heat transformer with different heat source and cooling water temperatures and temperature boosts. The operating parameters for this system are listed in Table 4-1. This includes heat transfer characteristics UA (overall heat transfer coefficient times area) values, which represent the heat transfer performance of heat exchange components; the external heat source (hot water), cooling water, and the strong solution (leaving the generator) mass flow rates; and temperatures of the external flow streams. The values of the heat transfer characteristics (UA) and mass flow rates were referenced to the literature by Grossman (1985). The cooling temperatures were selected on the basis that it is typical values for evaluating the performance of absorption heat transformers. And the heat source temperatures were selected on the basis of average waste heat temperatures from industrial processes and power plants.

#### 4.3 Multi-Stage Absorption Heat Transformers

According to the performance of the single-stage absorption heat transformer investigated in the previous section, high temperature boosting is difficult to achieve by single-stage AHTs unless the original waste heat sources are at high temperature levels. Therefore, in order to reach a higher temperature boosting value, multi-stage absorption heat transformers that have the potential to produce higher temperature lifts should be employed. There are many possible configurations of multi-stage absorption heat transformers (Alefeld and Radermacher 1994). In this study, a parallel flow, double-stage

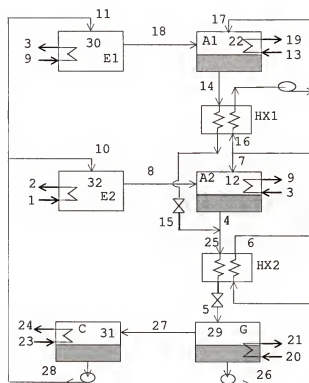
Table 4-1. Operating parameters of the single-stage absorption heat transformer

* Heat transfer characteristics (UA) *	
Absorber	3.35 kW/°C
Condenser	12.52 kW/°C
Evaporator	6.31 kW/°C
Generator	27.65 kW/°C
Solution heat exchanger	2.03 kW/°C
* Mass flow rates *	
Cooling water entering condenser	1.87 kg/s
Heat source entering generator	2.52 kg/s
Heat source entering evaporator	2.88 kg/s
Strong solution from generator	0.45 kg/s
* Operating temperatures *	
Cooling water inlet temperatures	29.4°C; 35.0°C
Heat source temperatures	60°, 71.1°, 82.2°C
Temperature boosting	10°C - 55°C

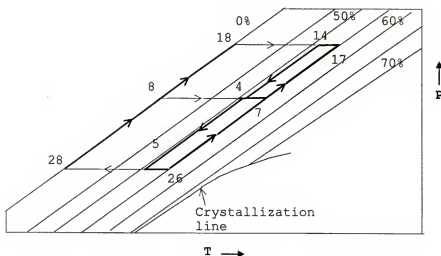
and a parallel-flow, triple-stage absorption heat transformer systems are analyzed under different operating conditions.

#### 4.3.1 Description of Double- and Triple-Stage Absorption Heat Transformers

The double-stage absorption heat transformer considered in this study consists of two absorbers, two evaporators, two solution heat exchangers, one generator, and one condenser. This double-stage absorption heat transformer is an extension of the single-stage system as described earlier. The configuration and cycle on the Duhring diagram of the double-stage absorption heat transformer are illustrated in Figure 4-3. Since one more set of evaporator, absorber, and solution heat exchanger has been added on the top of single-stage system, the double-stage AHT system has three operating pressure levels:



(a)



(b)

Figure 4-3. Double-stage absorption heat transformer: (a) schematic of the system; (b) Duhring diagram of the cycle

high pressure for the high-temperature absorber and high-temperature evaporator, medium pressure for the low-temperature absorber and low-temperature evaporator, and low pressure for the generator and condenser.

A waste heat source is supplied to the generator (G) to generate water vapor from weak LiBr/H<sub>2</sub>O solution. The water vapor then travels to the condenser (C) in there it is condensed by an external cooling water loop. The strong LiBr/H<sub>2</sub>O solution leaving the generator is pumped through the solution heat exchanger (HX2) to the low-temperature absorber (A2) and the high-temperature absorber (A1) in a parallel arrangement, and also the condensed water in the condenser is delivered to the two evaporators by another parallel connection. A heat stream from the same heat source as it supplied to the generator is employed at the low-temperature evaporator (E2) to evaporate the condensed water from the condenser. This water vapor travels to the low-temperature absorber (A2) and is absorbed by the strong solution from the generator. The heat generated from this absorption process inside the low-temperature absorber is recovered and applied to the high-temperature evaporator (E1) via an internal water loop to evaporate the water from condenser mentioned earlier. After that, the water vapor enters the high-temperature absorber (A1), and in there the vapor is combined with the strong solution from the generator through the two solution heat exchangers (HX1 and HX2). Thus, a much higher temperature boosting value can be obtained by introducing a portion of the waste heat stream into the high-temperature absorber to carry out the heat of the absorption process at a higher temperature level than in the low-temperature absorber. The two weak solution streams from the two absorbers then return to the generator through solution heat exchangers, thus completing the cycle.

When a further higher temperature lift is desired, advanced triple-stage absorption heat transformers would be needed for this application. The triple-stage AHT in this study consists of three evaporators, three absorbers, three solution heat exchangers, a condenser, and a generator. The schematic of the system is illustrated in Figure 4-4 along

with its cycle on the Duhring diagram. The basic operation of the advanced triple-stage AHT is similar to that of the single- or double-stage AHTs. Still the waste heat source stream is supplied to the generator (G) and low-stage evaporator (E3) and the cooling water is introduced to the condenser (C) in the triple-stage AHT. The difference for the triple-stage AHT is that, as the strong LiBr/H<sub>2</sub>O solution is delivered from the generator to the three absorbers, the medium- and high-stage evaporators (E2 and E1) utilize the absorption heat from the low- and medium-stage absorbers (A3 and A2) via internal flow streams, respectively. Thus the temperature of the waste heat source is upgraded three times by this advanced system, and the useful output stream at a much higher temperature level can be produced from the high-stage absorber (A1) where the highest temperature level of the entire system occurs.

#### 4.3.2 Thermodynamic Analysis of Double-and Triple-Stage Absorption Heat Transformers

Two heat streams from the same waste heat source are supplied to the generator and low-temperature evaporator in the double-stage absorption heat transformer as input energy, while a useful upgraded heat stream is obtained from the high-temperature absorber. Therefore, from the definition in Equation (4.2), the coefficient of performance of the double- and triple-stage absorption heat transformers can be expressed in Equations (4.8a) and (4.8b)

$$COP = \frac{Q_{a1}}{Q_g + Q_{e2}} = \frac{m_{17}h_{17} + m_{18}h_{18} - m_{14}h_{14}}{(m_{26}h_{26} + m_{27}h_{27} - m_5h_5) + m_8(h_8 - h_{10})} \quad (4.8a)$$

$$COP = \frac{Q_{a1}}{Q_g + Q_{e3}} = \frac{m_{39}h_{39} + m_{35}h_{35} - m_{42}h_{42}}{(m_{26}h_{26} + m_{27}h_{27} - m_5h_5) + m_8(h_8 - h_{10})} \quad (4.8b)$$

Then the thermodynamic efficiency of the double- and triple-stage AHTs can be obtained from the ratio of the real COP in Equations (4.8a) and (4.8b) and the Carnot COP in Equation (4.5). And the exergetic efficiency of the double- and triple-stage absorption

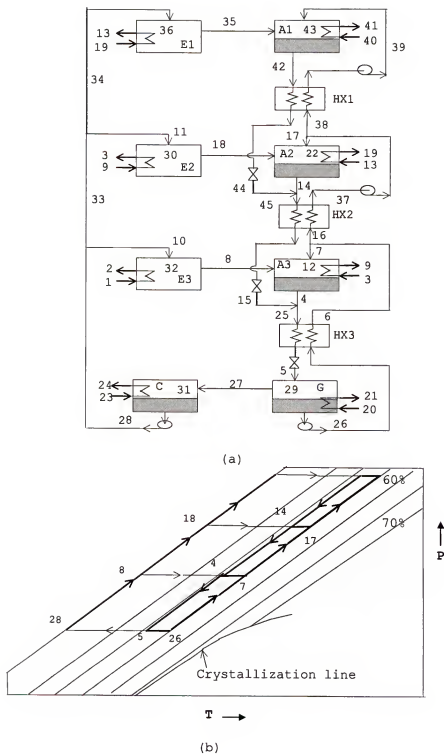


Figure 4-4. Triple-stage absorption heat transformer: (a) schematic of the system; (b) Duhring diagram of the cycle

Table 4-2. Operating parameters of the double- and triple-stage absorption heat transformers

Heat Transfer Characteristics (UA)		Mass Flow Rates		Operating Temperatures	
Absorber	3.35 kW/°C	Cooling water to condenser	1.87 kg/s	Cooling water inlet temperatures	29.4°C; 35.0°C
Condenser	12.5 kW/°C	Heat source to generator	2.52 kg/s	Heat source temperatures	60.0°C; 71.1°C
Evaporator	6.31 kW/°C	Heat source to evaporator	2.88 kg/s	Temperature boost	30°C - 105°C
Generator	27.6 kW/°C	Strong solution from generator	0.45 kg/s		
Solution heat exchanger	2.03 kW/°C				

heat transformers can also be calculated from its definition as mentioned earlier, and expressed as

$$E_{ex} = \frac{\Delta E_{a1}}{\Delta E_{e2} + \Delta E_g} = \frac{m_{13}(\varepsilon_{19} - \varepsilon_{13})}{m_1(\varepsilon_1 - \varepsilon_2) + m_{20}(\varepsilon_{20} - \varepsilon_{21})} \quad (4.9a)$$

$$E_{ex} = \frac{\Delta E_{a1}}{\Delta E_{e3} + \Delta E_g} = \frac{m_{40}(\varepsilon_{41} - \varepsilon_{40})}{m_1(\varepsilon_1 - \varepsilon_2) + m_{20}(\varepsilon_{20} - \varepsilon_{21})} \quad (4.9b)$$

A large number of model runs have been performed and compared in order to investigate the interactions of different operating conditions on the performance of the two multi-stage absorption heat transformers mentioned above. The main parameters of the two absorption heat transformers required for input in the computer code are listed in Table 4-2. This includes the heat transfer characteristics of the heat exchange components, mass flow rates and design point temperatures of the external streams, and the weak solution circulation rate. Again, the values of the heat transfer characteristics (UA) and mass flow rates were referenced to the literature by Grossman (1985). The cooling temperatures were selected on the basis that it is typical values for evaluating the performance of absorption heat transformers. And the heat source temperatures were selected on the basis of average waste heat temperatures from industrial processes and



power plants. The simulation results of the double-stage and triple-stage absorption heat transformers will be compared with that of the single-stage AHT.

#### 4.4 Results and Discussion

##### 4.4.1 Effect of Waste Heat Source Temperatures and Temperature Boost on AHTs

Figure 4-5 shows the variation of the coefficient of performance (COP) of the single-, double-, and triple-stage absorption heat transformers (AHTs) against the temperature boost values. Effects of different waste heat source temperatures (60°C and 71.1°C) on the performance of the three AHTs were conducted. The cooling water inlet temperature was set at 29.4°C. It is obvious that, with the waste heat source at the same temperature, the triple-stage absorption heat transformers can achieve higher temperature boost values than the single- and double-stage systems although the COP of the former is less than that of the latter within their own operating ranges. This is because the waste heat source stream is not just being upgraded once or twice but three times in the triple-stage AHT, therefore higher temperature streams can be obtained from the high-temperature absorber. But, of course, some output flow rate of this upgraded stream has been sacrificed for the purpose of achieving a high temperature boost in the triple-stage absorption heat transformer. As can be seen, the COP of the three AHT systems decreases slightly at first and then declines dramatically as the temperature boost values continue to increase. Results also show that there are temperature boost limits for all the AHT systems. Also the three AHT systems experience better COPs at the higher waste heat source temperature than at the lower waste heat source temperature while they upgrade the other waste heat source stream to a higher temperature level. This is because the heat source stream at the higher temperature has more potential energy stored in it and that means more energy can be utilized and converted to higher grade without further

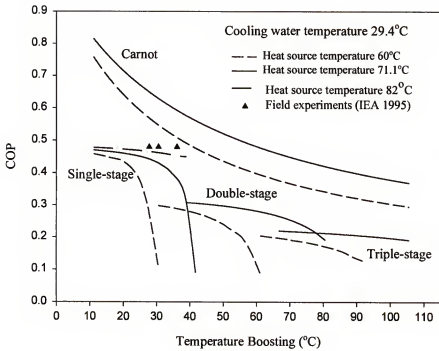


Figure 4-5. Comparison of the COP of single-, double-, and triple-stage absorption heat transformers with different heat source temperatures

sacrificing the COP. With waste heat at 71.1°C, the single-, double-, and triple-stage AHTs are generally capable of upgrading approximately 46, 30, and 20% of the energy of the waste heat source to a higher temperature, respectively. From the standpoint of the first law, the knee point of each COP curve in Figure 4-5 may represent the optimal operating condition for the AHT with a specific heat source. For example, the optimal operating condition for the single-stage AHT with a heat source at 71.1°C and cooling water at 29.4°C is to deliver a temperature boost of about 37.5°C. The reversible Carnot COP of the ideal AHT cycle in Equation (4.5) was calculated at the corresponding temperatures and combined in Figure 4-5 for comparison purposes. It is clear that the COP of real AHT systems is smaller than the reversible Carnot COP because of irreversibilities in the systems.

The COP of the single-stage AHT with a heat source of 82°C is also plotted in Figure 4-5 in order to compare with existing AHT plants. As can be seen, the predicted COP varies between 0.45 and 0.48 for a temperature boost range between 10°C and 40°C at this waste heat temperature. When comparing this data with the actual data reported for absorption heat transformers installed in Japan, Germany, and the Netherlands that have COPs varying between 0.47 and 0.49 under similar operating conditions (IEA 1995), one can conclude that the simulation results agree very favorably with the data from field experiments (see Figure 4-5).

Figure 4-6 shows the thermodynamic efficiency,  $E_{th}$ , of the three AHT systems with different waste heat source temperatures against the temperature boost values. The thermodynamic efficiency of the three AHT systems increases at first as the desired temperature boost increases, and then it levels off and drops sharply as the temperature boost becomes higher. And it also should be noticed that, within a low temperature boost domain, the three AHT systems with the higher waste heat source temperature have a smaller thermodynamic efficiency than those with the lower temperature. This may seem counter intuitive that the efficiency increases with an increasing heat source temperature.

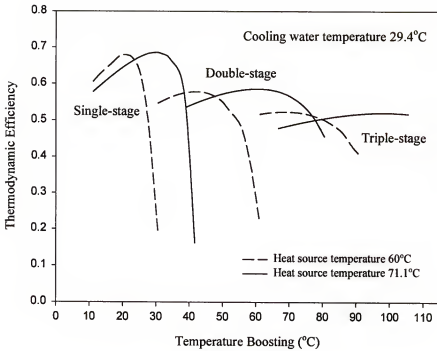


Figure 4-6. Comparison of the thermodynamic efficiency of single-, double- and triple-stage absorption heat transformers with different heat source temperatures

While this is true, it still produces the opposite trend for the thermodynamic efficiency. The latter quantity only measures the relative value of the cycle COP to the Carnot COP. Thus, one explanation may be attributed to the fact that the Carnot COP of the ideal cycle is a function of the operating temperatures only, and increases with increasing the waste heat source temperature. However, the advantage of employing a higher temperature heat source does not necessarily translate into a significant improvement in the COP for real systems.

Effect of the waste heat source temperatures on the exergetic efficiency of the three AHT systems considered against the temperature boost is illustrated in Figure 4-7. The figure shows that the double- and triple-stage AHTs can provide higher temperature boost while the single-stage AHT has better exergetic efficiency with a low temperature boost. Unlike the COP of the three systems which decreases first as shown in Figure 4-5, the exergetic efficiency of the three systems increases slightly at first. This can be explained by the fact that although the systems produce less mass flow rate for the output stream as the achievable temperature increases, this upgraded high temperature output stream also contains more exergy on the same mass basis and results in a net increase in exergetic efficiency. However, as the desired temperature increases further, the exergetic efficiency of the three AHT systems levels off and then declines dramatically as the COP does in Figure 4-5. Also, in Figure 4-7, it is clear that the three AHT systems with a higher heat source temperature have the potential to provide higher temperature boost values and higher exergetic efficiencies than with a lower heat source temperature as may be expected. With waste heat at 71.1°C, the single-, double-, and triple-stage AHTs are generally capable of upgrading approximately 55, 43, and 36% of the exergy of the waste heat source to a higher temperature, respectively. But it should be noted that the single-stage AHT system employing a high temperature heat source experiences less exergetic efficiency than the one employing a low temperature heat source within its own low temperature boost range. This may be because of more irreversibilities occurring due to

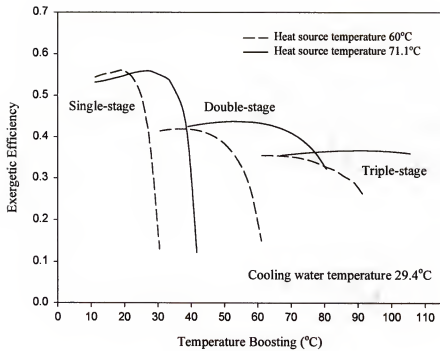


Figure 4-7. Comparison of the exergetic efficiency of single-, double-, and triple-stage absorption heat transformers with different heat source temperatures

the higher temperature difference in the heat transfer processes taking place in the evaporator and generator when the system employs a high temperature heat source but only provides a low temperature lift. Also from the point of view of the second law, the knee of each exergetic efficiency curve for the three absorption heat transformers represents an optimal operating condition. For example, the optimal operating condition for the double-stage AHT with a heat source at 71.2°C and external cooling water at 29.4°C is to create a temperature boost at about 78°C.

It should be noted that, although the triple-stage LiBr/H<sub>2</sub>O AHT can produce a higher temperature boost than the single- or double-stage ones, the system is operating at extremely high temperature levels for its working fluids. The corrosion problems inside this system might become more serious due to the characteristics of the LiBr/H<sub>2</sub>O solutions and novel corrosion inhibitor (Verma et al. 1999) would be necessary.

#### 4.4.2 Effect of Cooling Water Temperatures on AHTs

The effect of different cooling water temperatures employed in the condenser of the absorption heat transformers was also investigated. Figure 4-8 shows a comparison of the COP of the single-, double- and triple-stage AHT systems with two different cooling water inlet temperatures (29.4° C and 35° C), with the waste heat source temperature set at 71.1° C. As can be seen, all three systems with a low cooling water temperature experience higher COPs and a higher reachable temperature boost as may be expected. This can be explained by the fact that cooling water at a lower temperature can help keep the temperature and pressure inside the condenser from rising, thus making the generation of water vapor from the LiBr/H<sub>2</sub>O solution in the generator easier and more water will be circulated in the AHT systems. Therefore in the double-stage AHT for example, more water can be delivered from the condenser to the evaporators, and then to the low-temperature or the high-temperature absorbers. Thus, more absorption heat in the low-

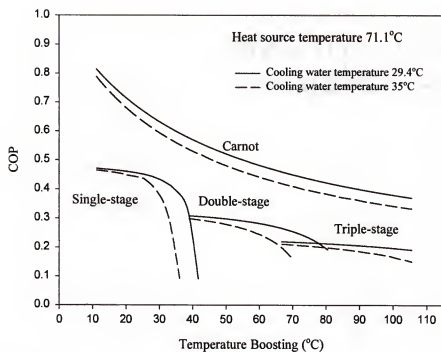


Figure 4-8. Comparison of the COP of single-, double-, and triple-stage absorption heat transformers with different cooling water temperatures



temperature absorber can be recovered by the high-temperature evaporator and, in the end, more heat can be provided from the high-temperature absorber as the useful output. The reversible Carnot COP of the ideal cycle with the different operating temperatures were also added in Figure 4-8 for comparison purposes.

The thermodynamic efficiencies of the three AHTs are illustrated in Figure 4-9. It may also be noticed that, within their own low temperature boost domains, all three AHT systems with the low cooling water temperature experience a smaller thermodynamic efficiency than with the high one. Again this might be because the Carnot COP of the ideal cycle is a function of the operating temperatures only, and increases with decreasing the cooling water temperature. However, the advantage of employing a low temperature cooling water does not necessarily translate into a significant improvement in the COP for real systems. Figure 4-10 illustrates the effect of cooling water temperature on the exergetic efficiency of the three AHT systems. Unlike the thermodynamic efficiency in Figure 4-9, the exergetic efficiency of the three AHT systems employing cooling water at the lower temperature is higher than that at the higher temperature within most of the systems' own temperature boost range. This can be explained by the same reasoning discussed earlier for the variation of the COP of AHT systems versus the cooling water temperatures in Figure 4-8. The exergetic efficiency is a better measure of second law performance because it reveals the relationship between the input and output exergies.

#### 4.5 Conclusions

Performance comparison for single-, double-, and triple-stage LiBr/H<sub>2</sub>O absorption heat transformers (AHT) has been conducted on the basis of the first and second laws of thermodynamics. In the parametric analysis of the three AHT systems with different operating conditions, it was shown that the COP of the three systems decrease slightly at first as the desirable temperature boost increases, and then declines

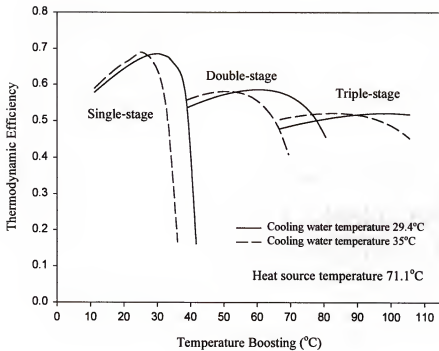


Figure 4-9. Comparison of the thermodynamic efficiency of single-, double-, and triple-stage absorption heat transformers with different cooling water temperatures

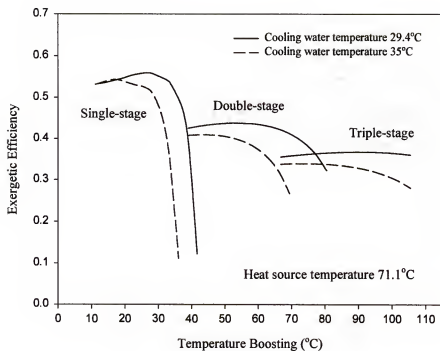


Figure 4-10. Comparison of the exergetic efficiency of single-, double-, and triple-stage absorption heat transformers with different cooling water temperatures

dramatically when the temperature boost increases further. On the other hand, the exergetic efficiency increases slightly at first, and then declines sharply as the temperature boost increases. Results also show that there is a limitation of the achievable temperature boost for absorption heat transformers employing waste heat and an external cooling water loop. It is also evident that increasing the heat source temperature or decreasing the cooling water temperature provides the AHT systems a better COP and a better exergetic efficiency in the higher temperature boost range.

In the comparison of the three absorption heat transformers, it became obvious that, at the same waste heat source and cooling water temperatures, the double- and triple-stage AHTs can reach higher temperature boost values than the single-stage one. And the multi-stage AHT can maintain both a high COP and a high exergetic efficiency within the high temperature boost range. But results also show that there is still a potential limit of achievable temperature boost for the double-stage AHT. Also the high temperature level of the triple-stage AHT may cause serious corrosion problems by the LiBr/H<sub>2</sub>O solution. New suitable working fluids or novel corrosion inhibitors for the higher temperature boost applications are thus necessary.

## CHAPTER 5 THERMOECONOMIC ANALYSIS OF ABSORPTION CHILLERS AND HEAT TRANSFORMERS

### 5.1 Concepts of Thermoeconomics

Chapters 3 and 4 have investigated the thermal efficiencies for various configurations and different operating conditions of absorption chillers and heat transformers based on the first and second laws of thermodynamics. However, a combination of improving thermal efficiency and investigating optimization of thermal systems is not purely a technique issue. There are several factors involved in designing thermal systems for which energy resources are utilized. Many of these factors are basically economic issues and the decision-making process is usually dominated by cost considerations. Total ownership costs of a thermal system must include both initial and operating costs. Usually the initial costs refer to the capital cost of purchases for the thermal system and auxiliary components. The operating costs include the driving energy sources costs of the thermal system and the maintenance costs over its lifetime. Thus, energy resource utilization is only one of many contributors to the total costs of a thermal system. A design engineer also needs to consider the capital, maintenance, and other costs of the system. Therefore, the purpose of this study is to provide life cycle cost guidelines for the absorption systems considered by employing the principles of thermoeconomics.

Thermoeconomics (or exergoeconomics) as reported in Tsatsaronis (1993) combines the principles of thermodynamic analysis and economic optimization for the purpose of rational decision-making in the development, design, and operation of complex thermal systems such as power plants and heat pump systems. Thermodynamic

analysis of a thermal system is usually biased to purely thermodynamic measures like energy efficiency, entropy generation, irreversibilities, exergy destruction, and exergetic efficiency. Meanwhile, economic considerations require a proper balance between appropriate thermodynamic measures and capital expenditures in order to achieve either a minimum unit product cost or a maximum product capacity for the thermal system. The development of thermoeconomics was first presented by Tribus and Evans in 1962 for sea water desalination processes. Since then, many investigators such as Valero et al. (1994) have successfully applied this to power plants and cogeneration systems and found that thermoeconomics is a good tool for optimization studies of thermal systems. Tozer and James (1995, 1997b) used thermoeconomics to determine life cycle costs of single- and double-effect absorption chillers applied to combined heat and power (CHP) systems with various forms of energy sources.

Moran (1989) indicated that thermoeconomics has an advantage in that the balance mentioned above is an economic feature which applies to the whole complicated thermal system and to each of its components. When thermoeconomic analysis is conducted on the basis of exergy, the formulation in many cases is more concise and easily understood. Moran explained that this is because exergy considers both the quantity and quality of energy in the analysis and also offers an explicit and consistent measure of both exergy losses and destructions.

For a complete thermoeconomic analysis of a thermal system, Tsatsaronis (1993) included the following necessary topics:

1. a detailed exergy analysis of the thermal system;
2. an economic analysis of each component in the system;
3. an exergy costing for any input or output energy; and
4. an exergoeconomic evaluation of each component.

The first topic has been addressed for various absorption chillers and heat transformers under different operating conditions in Chapters 3 and 4, respectively. The other topics will be investigated for these absorption systems in the following sections.

## 5.2 Thermoeconomic Optimization

Although a thermal system operating with a high energy efficiency means less operating costs, this does not necessarily imply that it is the optimal choice since the system may require a bigger initial investment in order to achieve that efficiency. On the other hand, lower initial costs of a thermal system sometimes would result in larger operating costs. Thus, there exists a balance point between the initial and operating costs for thermal systems. The optimal objectives of thermal systems need to be specified.

In thermoeconomic optimization, the objective is either to minimize the unit product cost of the thermal system for a fixed output product or to maximize the product output amount for a fixed total cost of the system over its life cycle. The objective function is composed of additive functions that evaluate energy source, equipment, and other associated costs in terms of money. A relationship between product cost and total cost of a thermal system can be written as

$$C_t = \sum_o c_o \varepsilon_o = \sum_i c_i \varepsilon_i + \sum_n Z_n \quad (5.1)$$

The general form of the function (El-Sayed and Evans 1970) can be expressed as

$$\min_{(x)} c_o = \frac{C_t}{\sum_o \varepsilon_o} = \frac{\sum_i c_i \varepsilon_i + \sum_n Z_n}{\sum_o \varepsilon_o} \quad (5.2)$$

where

$c_o$  = unit product exergy cost,

$C_t$  = total annual cost,

$\varepsilon_o$  = annual exergy rate for output products,

- $c_i$  = unit cost of external exergy inputs,  
 $\varepsilon_i$  = annual exergy input from external sources,  
 $Z_n$  = annual zone cost of capital expenditure and other  
 associated cost (in zone n), and  
 $\{x\}$  = a set of decision variables.

For a system like most of the absorption systems with a single output product such as chilled water for cooling applications, Equation (5.2) becomes

$$\min_{\{x\}} c_o = \frac{C_i}{E_p} = \frac{\sum_i c_i \varepsilon_i + \sum_n Z_n}{E_p} \quad (5.3)$$

where  $E_p$  is the exergy rate of the output product (e.g., chilled water of an absorption chiller) and  $c_o$  is the unit product cost.

### 5.3 Applications of Thermoeconomics to Absorption Chillers

In this section, applications of thermoeconomics are directed to lithium bromide/water (LiBr/H<sub>2</sub>O) single-, double-, and triple-effect absorption systems for cooling applications to evaluate the capital and operating costs of the systems and their auxiliary equipment over a wide range of heat source temperatures. The objective is to investigate the optimal selections for specific operating conditions of absorption chillers on the basis of life cycle costs. The life cycle cost of an electric-powered vapor-compression chiller is also evaluated for comparison purposes. Results are shown to provide guidelines for designing and selecting cost-efficient absorption chillers.

#### 5.3.1 Energy and Cost Evaluation of Absorption Chillers

Configuration and operations of the heat-driven single-, double-, and triple-effect absorption chillers are described in detail in Chapter 3. Performance comparison of the three absorption chillers is also evaluated theoretically in this study over various



Table 5-1. Operating conditions\* of the three absorption chillers and the vapor-compression chiller

Chiller Type	Primary Energy	Temperature Range
Single-effect absorption chiller	Hot water	60°C – 100°C
Double-effect absorption chiller	Hot water	90°C – 160°C
Triple-effect absorption chiller	Hot water	140°C – 230°C
Vapor-compression chiller	Electricity	N/A

\*Cooling capacity 500 ton, supply chilled water 7.2°C, and supply cooling water 29.4°C

operating conditions, including different heat source, cooling water, and chilled water temperatures. In the study, the primary energy supplied to the heat-driven absorption chillers is hot water at different temperature ranges for different systems. The supply cooling water temperature is set at 29.4°C and the chilled water outlet temperature is set at 7.2°C. Table 5-1 lists the operating conditions for both the absorption and vapor-compression chillers considered. Cooling capacities of absorption chillers have a wide range varying from 3 tons for small packages to more than 1500 tons for commercial buildings (Trane 1989). In this study, the cooling capacity of the chillers was picked at 500 tons as a representative mid-range size.

Figure 5-1 shows a comparison of the coefficient of performance (COP) of the three absorption chillers versus the heat source temperature. The COP is defined as the ratio of the cooling capacity to the primary energy input of the chillers:

$$COP = \frac{\text{cooling capacity } (Q_c)}{\text{primary energy input } (Q_g \text{ or } W_c)} \quad (5.4)$$

The cooling capacity ( $Q_c$ ) in Equation (5.4) is produced at the evaporator. And the primary energy input is the heat supplied to the generator ( $Q_g$ ) for the absorption chillers or the electrical energy to the compressor ( $W_c$ ) for the vapor-compression chiller. It can be seen that the COP of the single-effect absorption chiller is between 0.4 to 0.73, 0.73 to 1.24 for the double-effect chiller, and 1.25 to 1.7 for the triple-effect chiller, each within

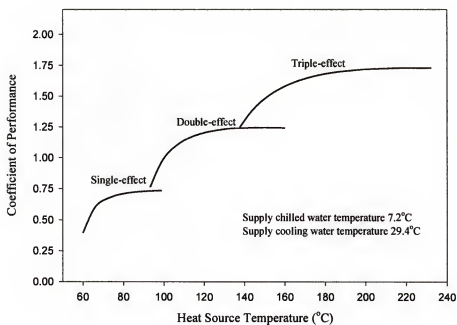


Figure 5-1. Comparison of the COP of the three absorption chillers

their respective heat source temperature range. Generally, the COP of vapor-compression chillers is between 4.5 and 5.2. Some vapor-compression chillers with high efficiency centrifugal compressors have COP around 5.5. In this study, the COP of the vapor-compression chiller was selected at 5.0 as a representative average value.

Thermodynamic analysis is based on exergy in thermoeconomics. If a large reference environment is at a temperature  $T_0$ , then the exergy associated with the transfer by heat interaction becomes

$$E_q = (1 - T_0 / T)Q \quad (5.5)$$

where  $(1 - T_0 / T)$  is the Carnot factor (Tozer and James 1997b). And the interaction of mechanical work and electrical energy is directly transferred into exergy:  $E_w = W$ .

In addition to the primary energy input, there are secondary energy inputs required for both the absorption and vapor-compression chillers and their auxiliary equipment. These secondary energy inputs are basically from water pump motors, fan motor of the cooling tower, and electrical equipment of the chillers. The heat of the condenser and absorber (for absorption chillers only) is removed from the chillers through the cooling water of the cooling tower. This rejected heat is equal to the sum of the cooling capacity and primary energy input and can be expressed in Equations (5.6a) and (5.6b) for the absorption and vapor-compression chillers, respectively, as follows:

$$Q_{cw} = Q_e + Q_g \quad (5.6a)$$

$$Q_{cw} = Q_e + W_c \quad (5.6b)$$

The mass flow rate of the cooling water depends on the rejected heat in Equations (5.6a) or (5.6b), the specific heat, and the temperature difference of the cooling water and can be calculated as

$$m_{cw} = Q_{cw} / (c_p \Delta T_{cw}) \quad (5.7)$$

And the cooling water pump power is expressed in terms of the mass flow rate and pressure drop of the cooling water, and the water pump and motor efficiencies.

$$W_{cwp} = m_{cw} \Delta P_{cw} / (\eta_{cwp} \eta_m) \quad (5.8)$$

Equations (5.7) and (5.8) can also be applied to the calculation of the mass flow rate of the supply hot water,  $m_{hw}$ , and the required power of the hot water pump,  $W_{hwp}$ , for absorption chillers.

The electrical energy of the cooling tower fans  $W_{ctf}$  can be approximately evaluated in terms of cooling capacity, ratio of rejected heat of the chiller to that of a selected base case, and fan efficiency

$$W_{ctf} = K_1 Q_e (Q_{cw} / Q_{cw, \text{base case}}) / \eta_{ctf} \quad (5.9)$$

where the variable  $K_1$  is 0.0255kW per kW of cooling capacity and the single-effect absorption chiller with heat source at 98°C is selected as the base case (Dorgan et al. 1995).

Electrical demand of an absorption chiller results from solution and refrigerant pumps and can be estimated as  $W_{ac} = K_2 Q_e$ , where the variable  $K_2$  is equal to 0.015, 0.017, and 0.02kW/ton for the single-, double- and triple-effect absorption chillers, respectively (Dorgan et al. 1995). Thus the total electrical energy supplied to the absorption chillers can be summarized as follows:

$$W = W_{cwp} + W_{hwp} + W_{ctf} + W_{ac} \quad (5.10)$$

Operating data of both the absorption and vapor-compression chillers and their auxiliary equipment are provided in Table 5-2. This includes the COP, cooling capacity, primary energy input, and electrical power for various chiller types.

Since both the absorption and vapor-compression chillers considered deliver the chilled water at the same temperature, the total exergy of the output product  $E_p$  can be replaced by the cooling capacity  $Q_e$  in Equation (5.3). Thus the objective function becomes

Table 5-2 Operating data of input energy for absorption and vapor-compression chillers

	Single	Single	Single	Single	Double	Double	Double	Double	Triple	Triple	Triple	V-C
Heat source (°C)	71.1	82.2	93.3	98.9	110	126.7	143.3	160	176.7	193.3	210	N/A
Cooling capacity $Q_c$ (kW)	1750	1750	1750	1750	1750	1750	1750	1750	1750	1750	1750	1750
Coefficient of performance (COP)	0.664	0.716	0.732	0.735	1.14	1.224	1.244	1.243	1.581	1.671	1.71	1.726
Primary energy Input $Q_c$ or $W_c$ (kW)	2636	2444	2391	2381	1535	1430	1407	1408	1107	1047	1023	1014
Carnot Factor (=1-T <sub>0</sub> /T)	0.134	0.161	0.186	0.199	0.222	0.254	0.284	0.312	0.337	0.361	0.383	1
Primary Exergy Input (kW)	353	394	446	473	341	364	400	439	345	353	369	388
Thermal energy input $Q_c$ (kW)	2636	2444	2391	2381	1535	1430	1407	1408	1107	1047	1023	1014
Hot water temperature difference (°C)	7	7	7	7	7	7	7	7	7	7	7	N/A
Hot water flow rate (kg/s)	89.6	83.1	81.3	81	52.2	48.6	47.8	47.9	37.6	34.8	34.5	N/A
Hot water pressure drop (kPa)	20	20	20	20	20	20	20	20	20	20	20	N/A
Hot water pump power (kW)	2.5	2.3	2.3	2.3	1.5	1.4	1.3	1.3	1.1	1	1	N/A
Condenser and absorber heat (kW)	4386	4194	4141	4131	3285	3180	3157	3158	2857	2797	2773	2100
Cooling water temperature difference (°C)	7	7	7	7	7	7	7	7	7	7	7	7
Cooling water flow rate (kg/s)	149.2	142.7	140.8	140.5	111.7	108.2	107.4	107.4	97.2	95.1	94.3	94
Cooling water pressure drop (kPa)	150	150	150	150	150	150	150	150	150	150	150	150
Cooling water pump power (kW)	31.4	30	29.7	29.6	23.5	22.8	22.6	22.6	20.5	20	19.9	15
Cooling tower fan power (kW)	49.9	47.7	47.1	47	37.4	36.2	35.9	35.9	32.5	31.8	31.5	23.9
Absorption chiller electrical energy (kW)	7.5	7.5	7.5	7.5	9	9	9	9	10	10	10	10
Total thermal exergy for ACH (kW)	353	394	446	473	341	364	400	439	345	353	369	388
Total electrical power (kW)	91.3	87.6	86.5	86.3	71.3	69.3	68.8	68.9	64	62.8	62.4	389

Water pump efficiency 75%; motor efficiency 95%

$$\min_{\{x\}} c_o = C_i / Q_e = (\sum_i c_i \varepsilon_i + \sum_n Z_n) / Q_e \quad (5.11)$$

where  $c_o$  is the unit cost of the output product (cooling capacity). The decision variables  $\{x\}$  in the above equations can be the various operating temperatures for the absorption chillers such as the driving heat source, supply cooling water, and supply chilled water temperatures. In this study, only the influence of the heat source temperature is evaluated while keeping the other two temperatures constant.

Operating energy costs of the absorption chillers and auxiliary equipment include the costs of the primary thermal and electrical energies. Figure 5-2 illustrates the interactions of the external energy input (primary heat and electric power) and the output product (cooling capacity) of the completed system. In thermoeconomic analysis, since all the operating energy costs in Equation (5.3) are based on exergy, it can be assumed that both the primary thermal and electrical energies for absorption chillers are produced by a cogeneration system and have the same unit cost of exergy,  $c_e = c_{th}$ . Thus the cost of the primary thermal and electrical energies for absorption chillers can be expressed as follows, respectively:

$$C_{th} = c_{th} E_g \cdot (\text{EFLH}) = c_{th} (1 - T_o / T) Q_g \cdot (\text{EFLH}) \quad (5.12)$$

$$C_w = c_e W \cdot (\text{EFLH}) \quad (5.13)$$

Where  $E_g$  is the exergy of the primary thermal energy,  $W$  is the total electrical power, and EFLH is the equivalent full load hours per year for the absorption chillers. From a comparison of the total electric demand for the absorption and vapor-compression chillers in Table 5-2, it can be seen that the electric demand for all absorption chillers is much smaller than that for the vapor-compression chiller and will result in savings on the operating costs for absorption chillers. The savings on the electric demand  $S$  can be calculated employing the product of unit cost of the electric demand by the local utility company, difference of electric demand of chillers, and the time period. Thus the total operating cost of the absorption chillers becomes

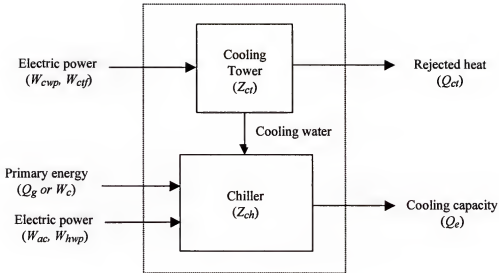


Figure 5-2. Interactions of the external energy input and product output of the completed system

$$C_{total} = C_{th} + C_W - S \quad (5.14)$$

In Equation (5.3) the capital cost of a cooling system includes initial investments on the chillers and cooling towers,  $Z_{ch}$  and  $Z_{ct}$ . The costs of absorption chillers generally depend on manufacturer's prices. Dorgan et al. (1995) summarize the costs of single- and double-effect absorption chillers by machine size, and the average of the costs listed in the reference is used for initial estimation purposes in this study.

The capital cost of the cooling tower depends on the quantity of the rejected heat. The equipment cost for the cooling tower is estimated by the following relationship (Bejan et al. 1996):

$$Z_{ct,Y} = Z_{ct,X} (Q_Y / Q_X)^\alpha \quad (5.15)$$

Equation (5.15) allows the initial investment of the cooling tower ( $Z_{ct,Y}$ ) at a given rejected heat capacity ( $Q_Y$ ) to be calculated when the initial cost of the same cooling tower ( $Z_{ct,X}$ ) at a different capacity ( $Q_X$ ) is known. The variable  $\alpha$  is a cost-estimating parameter and is equal to 0.93 for cooling towers. The  $Z_{ct,X}$  in this study is selected as the capital cost of the cooling tower for the vapor-compression chiller and is based on \$7/kW of the rejected heat (Tozer and James 1997b). It should be mentioned that the cost of the cooling water pump and piping is included in the costs of the cooling towers. Therefore the total capital costs of the systems can be calculated as

$$Z = Z_{ch} + Z_{ct} \quad (5.16)$$

For thermal systems such as absorption chillers with initial investment costs and operating cost over their lifetime, it is better to evaluate the life cycle cost of the system or the levelized cost of the final product. In engineering economy, the unit of time intervals for such purpose is usually taken as the year. The capital-recovery factor (CRF) is used to determine the equal amounts of  $n$  money transactions for an initial investment cost (Bejan et al. 1996), and can be expressed as



$$CRF = A / P = i(1+i)^n / [(1+i)^n - 1] \quad (5.17)$$

Where  $A$  is called annuity, a series of equal-amount money transactions,  $P$  is the present value of initial cost,  $i$  is the annual interest rate, and  $n$  is the number of time intervals or the number of years of chiller operation in this study. Thus the life cycle cost of both the absorption and vapor-compression chillers can be evaluated from Equations (5.14), (5.16) and (5.17) on a yearly basis

$$C_{LCC} = (CRF)Z + C_{total} \quad (5.18)$$

And the specific life cycle cost with respect to the cooling capacity (the final product) becomes

$$c_{SLCC} = C_{LCC} / [Q_e \cdot (EFLH)] \quad (5.19)$$

Chillers with a lower specific life cycle cost represent a better choice for cooling applications. Thus the specific life cycle cost,  $c_{SLCC}$ , in Equation (5.19) is the objective to be minimized in this study.

### 5.3.2 Results and Discussion

Table 5-3 lists calculation results of the total operating costs as well as capital costs for the three absorption chillers considered with varying primary heat source temperatures along with the cost of the vapor-compression chiller. It is assumed that the supply chilled and cooling water temperatures are 7.2°C and 29.4°C, respectively, that the annual interest rate is 8%, that the number of years of chiller operation is 15 years, and that the equivalent full load hour is 3000 hours per year. These values were selected on the basis that they are typical values for the evaluation of life cycle costs of chillers. The capital costs of the single-, double-, and triple-effect absorption chillers are set at \$355, \$450, and \$550 per ton, respectively, while that of the vapor-compression chiller is \$250/ton (Dogan et al 1995). It can be seen that the percentage of the capital cost in the

Table 5-3. Comparison of specific life cycle costs of the absorption and vapor-compression chillers

	Single	Single	Single	Single	Double	Double	Double	Double	Double	Triple	Triple	Triple	V-C
Heat source (°C)	71.1	82.2	93.3	98.9	110	126.7	143.3	160	160	176.7	193.3	210	N/A
Chiller cost (\$)	177500	177500	177500	177500	225000	225000	225000	225000	225000	275000	275000	275000	125000
Cooling tower cost (\$)	29156	27971	27640	27579	22287	21621	21476	21483	19572	19192	19039	18979	14700
Total capital costs (\$)	206656	205471	205140	205079	247287	246621	246476	246483	294572	294192	294039	293979	139700
Equivalent full load hours (hr)	3000	3000	3000	3000	3000	3000	3000	3000	3000	3000	3000	3000	3000
Years of chiller operation (yr)	15	15	15	15	15	15	15	15	15	15	15	15	15
Annual interest rate	0.08	0.08	0.08	0.08	0.08	0.08	0.08	0.08	0.08	0.08	0.08	0.08	0.08
Capital-recovery factor (CRF)	0.11683	0.11683	0.11683	0.11683	0.11683	0.11683	0.11683	0.11683	0.11683	0.11683	0.11683	0.11683	0.1168
Unit cost of electrical energy (\$/kWh)	0.04	0.04	0.04	0.04	0.04	0.04	0.04	0.04	0.04	0.04	0.04	0.04	0.04
Unit cost of thermal energy (\$/kWh)	0.04	0.04	0.04	0.04	0.04	0.04	0.04	0.04	0.04	0.04	0.04	0.04	0.04
Total electrical energy cost (\$/yr)	10955	10507	10382	10359	8561	8315	8261	8264	7680	7541	7485	7463	46670
Total thermal energy cost (\$/yr)	42361	47227	53492	56744	40866	43627	47963	52655	41398	42374	44316	46587	N/A
Total input energy cost (\$/yr)	53316	57734	63874	67104	49428	51942	56224	60919	49078	49914	51800	54050	46670
Electric demand cost saving* (\$/yr)	17858	18081	18144	18155	19054	19178	19204	19203	19495	19565	19593	19604	0
Total operating cost per year (\$/yr)	35458	39652	45730	48948	30373	32765	37020	41716	29583	30350	32208	34446	46670
Capital cost per year (\$/yr)	24144	24005	23966	23959	28890	28813	28796	28796	34415	34370	34352	34345	16321
Simple payback period (yr)	5.97	9.37	69.61	-28.7	6.6	7.69	11.06	21.36	9.06	9.47	10.67	12.62	N/A
Life cycle cost of chillers (\$/yr)	59602	63657	69696	72908	59264	61577	65816	70513	63998	64720	66560	68792	62991
% of capital cost in life cycle cost	40.5	37.7	34.4	32.9	48.7	46.8	43.8	40.8	53.8	53.1	51.6	49.9	25.9
Specific life cycle cost (\$/kWh)	0.0114	0.0121	0.0133	0.0139	0.0113	0.0117	0.0125	0.0134	0.0122	0.0123	0.0127	0.0131	0.0120

\*Electric demand cost: \$5/kWh per month.

life cycle cost of an absorption chiller is much larger than that of a vapor-compression chiller.

Figure 5-3 shows a comparison among the specific life cycle costs of the three absorption chillers considered versus the heat source temperature. The specific life cycle cost of a vapor-compression chiller is also plotted for comparison purposes. As can be seen, within the respective heat source temperature ranges, the specific life cycle cost of each absorption chiller declines significantly at first and then increases consistently as the heat source temperature increases. This is because a higher heat source temperature means more primary input thermal exergy supplied to the absorption chillers, which results in a higher exergy cost even though the chillers only require less input energy from the standpoint of the first law of thermodynamics. It can also be seen that the single-effect and double-effect absorption chillers have smaller specific life cycle costs than the vapor-compression chiller at various heat source temperature ranges. These operating conditions indicate that the single-effect and double-effect absorption chillers outperform the vapor-compression chiller and are better choices from a thermoeconomics vantage point.

Effect of the number of years of operation on the specific life cycle costs for the three absorption chillers and the vapor-compression chiller is illustrated in Figure 5-4. As expected, a long term operation can bring the specific life cycle cost of all chillers considered to a lower value. Figure 5-4 also shows that the single-effect absorption chiller has a lower specific life cycle cost than the vapor-compression chiller when the number of years of operation is approximately over 8 years. The double-effect absorption chiller will outperform the vapor-compression one if the chiller is to be operated longer than 10 years, and becomes a better choice than the single-effect system if it operated longer than 15 years. And the triple-effect absorption chiller would be a better option than its vapor-compression counterpart only if the chiller operates for more than 20 years. This is because a long term operation will reduce the negative effects of the high capital

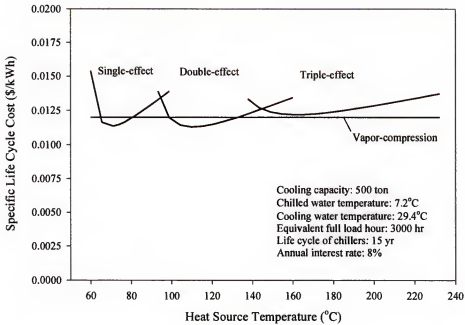


Figure 5-3. Comparison of specific life cycle costs of various absorption chillers and a vapor-compression chiller

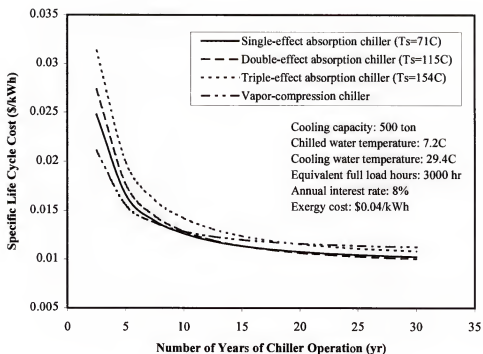


Figure 5-4. Comparison of specific life cycle cost of absorption and vapor-compression chillers versus number of years of operation

costs of absorption chillers vis-à-vis their specific life cycle costs and make the systems more market competitive.

Figure 5-5 shows a comparison of the specific life cycle costs of the chillers considered versus the equivalent full load hours. Equivalent full load hours represent the number of hours of operation per year for a chiller operating near 100% capacity. In practical applications, the number of equivalent full load hours is typically based on the geographic area the chiller is located in. The number of years of chiller operation is selected at 15 years. As can be seen, the single-effect absorption chiller has the lowest specific life cycle cost when the chiller is operating less than 3000 hours per year. This is primarily due to a lower operating cost than that of a vapor-compression chiller and a lower capital cost than multi-effect absorption chillers. When the equivalent full load hours is larger than 3000 hours, the double-effect absorption chiller becomes the best option. It should be noted that the specific life cycle cost of the vapor-compression chiller matches that of the double-effect absorption chiller at approximately 6000 hours per year. This is because larger operating hours will reduce the positive effect of the savings on the required electrical demand for the absorption chillers in Equation (5.14) since the total energy cost becomes higher.

In addition, initial capital costs of absorption chillers have a significant effect on their success in the air-conditioning market. Figure 5-6 shows a comparison of the specific life cycle costs of absorption chillers versus the capital cost ratio of absorption chillers to the vapor-compression chiller. As can be seen, if absorption chillers have the same capital cost as the vapor-compression chiller (i.e. cost ratio equals to 1), the triple-effect absorption chiller would be the best choice. However, the capital costs of the absorption chillers are higher than their vapor-compression counterparts due to more heat exchange components and surfaces. As illustrated in Figure 5-6, the single-effect absorption chiller has a smaller specific life cycle cost than the vapor-compression chiller if its capital cost is less than 1.65 times that of the latter. And the double-effect and

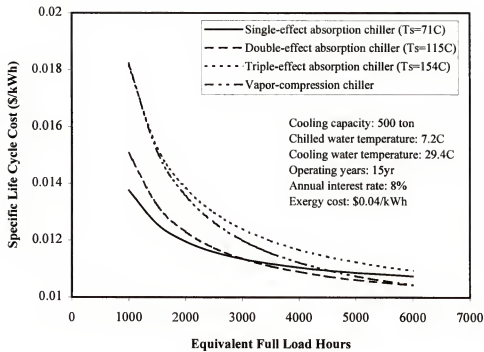


Figure 5-5. Comparison of specific life cycle cost of absorption and vapor-compression chillers versus equivalent full load hours

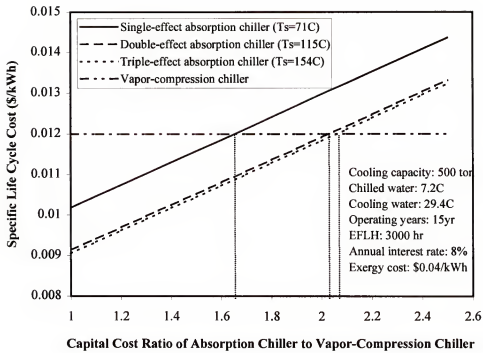


Figure 5-6. Comparison of specific life cycle cost of absorption and vapor-compression chillers versus capital cost ratio



triple-effect systems will have smaller life cycle costs and become more competitive if their capital costs can be kept under 2.02 and 2.08 times that of the vapor-compression chiller, respectively.

Prices of the thermal and electrical energies influence the total energy costs of absorption and vapor-compression chillers and, of course, their life cycle costs. Effect of the exergy unit costs of the primary thermal and electrical energies on the specific life cycle costs of the chillers considered is shown Figure 5-7. The number of years of operation is set at 15 years and the equivalent full load hours is set at 3000 hours per year. As can be seen, when the exergy cost ratio of the primary thermal energy to the electrical energy decreases, all three absorption chillers will have a lower specific life cycle cost than the vapor-compression chiller. If a free waste heat source is available (i.e. exergy cost ratio is equal to zero), it is strongly recommended that absorption chillers for cooling applications be employed.

It should be noted that there is an apparent controversy pertaining to the specific life cycle costs of the three absorption chillers when comparing the results of Figures 5-6 and 5-7. This apparent controversy has to do with the fact that the single-effect absorption chiller appears to have a higher specific life cycle cost than the double- and triple-effect systems based on Figure 5-6, but seems to have a lower *SLCC* based on Figure 5-7. This may be explained by the fact that, in Figure 5-6, when comparing the three absorption chillers on a capital cost ratio basis, the three systems have the same capital costs. However, since the single-effect system has a higher operating cost than the two multi-effect systems due to its lower efficiency, this causes the *SLCC* of the single-effect system to be higher than that of the double- and triple-effect systems. But, in Figure 5-7, the comparison of the *SLCC* of the absorption chillers is based on the actual capital costs listed in Table 5-3. The single-effect absorption chiller has the lowest capital cost. And the benefit of this lowest capital cost helps the single-effect absorption

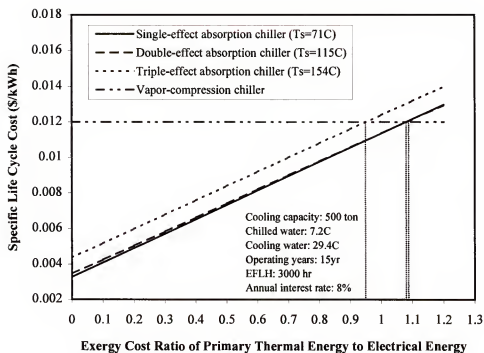


Figure 5-7. Comparison of specific life cycle cost of absorption and vapor-compression chillers versus exergy cost ratio

chiller to have a lower SLCC than the double- and triple-effect systems even though it has a higher operating cost.

#### 5.4 Applications of Thermoeconomics to Absorption Heat Transformers

Application of thermoeconomics is directed to single-, double-, and triple-stage lithium bromide/water absorption heat transformers in order to investigate life cycle costs of the systems. The objective of thermoeconomics here is to minimize the product cost of a thermal system for a given output capacity (upgraded heat). Life cycle costing includes all cost factors (e.g., capital costs, operation, and estimated energy use) and can be used to evaluate the total costs of the systems over a period of years. Electric-powered vapor-compression heat transformers are also evaluated for comparison purposes. The results provide guidelines for designing and selecting cost-efficient absorption heat transformers for industrial waste heat recuperation.

##### 5.4.1 Energy and Cost Evaluation of Absorption Heat Transformers

Figure 5-8 illustrates the schematics of the basic single-stage absorption and one-stage vapor-compression heat transformers. Configuration and operations of the heat-driven single-, double-, and triple-stage absorption heat transformers are described in detail in Chapter 4. Performance comparison of the three absorption heat transformers is also carried out theoretically over a host of operating conditions, including different waste heat source and cooling water temperatures, and achievable temperature boosts. In the section, the primary driving energy (waste heat) supplied to the three absorption heat transformers is hot water at 71°C and the supply cooling water temperature is set at 29.4°C. The vapor-compression systems use electricity as the primary energy to drive the compressors and employ some waste heat in the evaporators while boosting the waste heat to a higher temperature in the condensers as shown in Figure 5-8. Table 5-4 lists the

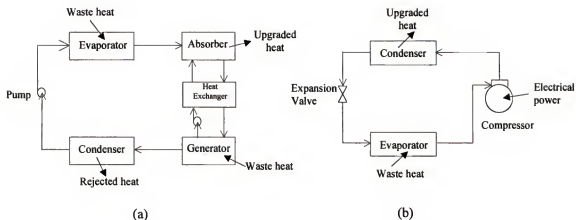


Figure 5-8. Schematics of a single-stage absorption heat transformer (a) and a one-stage vapor-compression heat transformer (b)

Table 5-4. Operating conditions\* of the three absorption and vapor-compression heat transformers

Heat Transformer Type	Primary Energy	Temperature Boost Range
Single-stage absorption heat transformer	Waste heat (hot water)	11°C – 42°C
Double-stage absorption heat transformer	Waste heat (hot water)	39°C – 83°C
Triple-stage absorption heat transformer	Waste heat (hot water)	66°C – 105°C
One-stage R-134a vapor-compression heat transformer	Electricity	11°C – 25°C
One-stage R-113 vapor-compression heat transformer	Electricity	11°C – 105°C
One-stage R-114 vapor-compression heat transformer	Electricity	11°C – 64°C
Two-stage R-113 vapor-compression heat transformer	Electricity	39°C – 105°C

\*Heat recovery capacity 1000kW, waste heat temperature 71°C, and supply cooling water 29.4°C

primary energy and operating conditions for both the absorption and vapor-compression heat transformers considered.

Figure 5-9 shows a comparison of the coefficient of performance (COP) of the three absorption heat transformers along with the vapor-compression heat transformers versus the magnitude of the temperature boost. The temperature boost (or temperature lift) is the temperature difference between the waste heat and upgraded useful heat. The COP is defined as the ratio of the heat recovery capacity to the primary energy input of the heat transformers:

$$COP = \frac{\text{heat recovery capacity } (Q_r)}{\text{primary energy input } (Q_e + Q_g \text{ or } W_c)} \quad (5.20)$$

The heat recovery capacity ( $Q_r$ ) in Equation (5.20) is produced at the absorbers for the absorption systems and at the condensers for the vapor-compression systems. And the primary energy input is the waste heat supplied to the evaporator and generator ( $Q_e + Q_g$ ) for the absorption heat transformers or the electrical energy to the compressor ( $W_c$ ) for the vapor-compression heat transformers. The actual electrical power needed to drive the compressor has to consider the isentropic efficiency of the compressor,  $\eta_{isen}$ ,

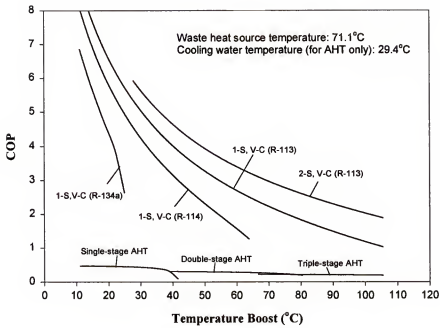


Figure 5-9. Comparison of the COP of absorption and vapor-compression heat transformers

and the efficiency of the driving motor,  $\eta_m$ . Thus, the electric power input for vapor-compression systems becomes:  $W_c / (\eta_{isen} \eta_m)$ . The isentropic efficiency of compressors and motor efficiencies are dependent on their sizes and operating conditions. In this study, the isentropic and motor efficiencies are set at the maximum values of 82 and 95%, respectively, as reported in the literature (IEA 1995). In Figure 5-9, the COP is between 0.09 and 0.47 for the single-stage absorption heat transformer, 0.19 and 0.31 for the double-stage heat transformer, and 0.19 and 0.22 for the triple-stage heat transformer, each within their respective temperature boost range. It is obvious that the COP of absorption heat transformers is much smaller when compared with the COP of the electric-powered vapor-compression systems. However, it should be noted that, despite their lower first-law efficiency (COP), absorption heat transformers use low-grade energy (waste heat) as their primary energy input while electric-powered vapor-compression systems utilize high-grade energy (electrical). The difference of the performance measure between these two systems can become smaller by introducing some sort of a second-law efficiency, such as the exergetic efficiency, which is defined as the ratio of the exergy of upgraded heat stream to that of the primary heat or electric power input. Comparison of the exergetic efficiency of the absorption and vapor-compression heat transformers versus the temperature boost is shown in Figure 5-10. As can be seen, absorption heat transformers outperform electric-powered vapor-compression systems within some temperature boost ranges based on the second law efficiency.

In addition to the primary energy input, there are secondary energy inputs required for both the absorption and vapor-compression heat transformers and their auxiliary equipment. These secondary energy inputs are basically from hot and cooling water pumps, cooling tower fans, and electrical equipment of the heat transformers. The heat of the condenser (for absorption heat transformers only) is removed from the heat transformers through the cooling water of the cooling tower. This rejected heat is equal

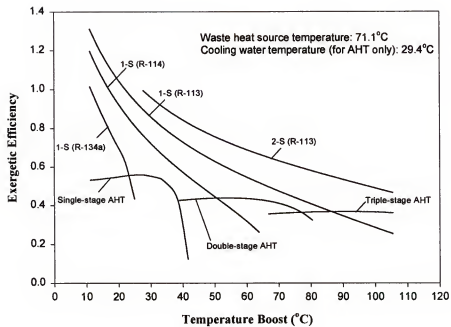


Figure 5-10. Comparison of the exergetic efficiency of absorption and vapor-compression heat transformers



to the difference of the heat recovery capacity and the primary energy input and can be expressed as

$$Q_{cw} = Q_e + Q_g - Q_r \quad (5.21)$$

The mass flow rates of the cooling water and hot water (waste heat) and the relative water pump powers ( $W_{cwp}$ ,  $W_{hwp}$ ) can be calculated as functions of the rejected or absorbed heat, the specific heat, the temperature difference of the water, and the water pump efficiency by using Equations (5.7) and (5.8). The electrical energy for the cooling tower fans  $W_{ctf}$  is approximately evaluated in terms of the dissipated heat of the absorption heat transformers and fan efficiency

$$W_{ctf} = K_1 Q_{cw} / \eta_{ctf} \quad (5.22)$$

where the variable  $K_1$  is 0.0108kW per kW of dissipated heat. Electrical demand of an absorption heat transformer results from solution and refrigerant pumps and other electrical equipment. It is assumed that the electrical power for the AHT machine itself is about 0.5% of the primary energy input and can be computed as  $W_{ahf} = 0.005(Q_e + Q_g)$ . Thus the total electrical energy supplied to the absorption heat transformers can be summarized as follows:

$$W = W_{cwp} + W_{hwp} + W_{ctf} + W_{ahf} \quad (5.23)$$

Operating data of both the absorption and vapor-compression heat transformers and their auxiliary equipment are provided in Table 5-5. This includes the temperature boost, COP, heat recovery capacity, primary thermal or electrical energy input, and secondary electrical power input for various heat transformer types.

For a system like the heat transformers with a single output product (the upgraded heat), Equation (5.3) becomes

$$\min_{\{x\}} c_o = C_i / E_r = (\sum_i c_i \varepsilon_i + \sum_n Z_n) / E_r \quad (5.24)$$

where  $E_r$  is the exergy of the upgraded heat at a specific temperature and can be calculated from Equation (5.5). The decision variables  $\{x\}$  in the above equation can be

Table 5-5 Operating data\* of input energy for absorption and vapor-compression heat transformers

System	Absorption Heat Transformers					Vapor-Compression Heat Transformers				
Type	1-S	1-S	2-S	2-S	3-S	(R134a)	(R113)	(R113)	(R114)	2(R113)
Temperature Boost (C)	11.1	25.0	38.9	55.6	83.3	11.1	11.1	16.7	11.1	36.1
Heat recovery capacity $Q_r$ (kW)	1000	1000	1000	1000	1000	1000	1000	1000	1000	1000
Coefficient of performance (COP)	0.4708	0.4510	0.3083	0.2900	0.2110	6.8543	8.8572	7.3133	8.0837	4.9982
Primary energy input: $Q_g+Q_e$ or $W_e$ (kW)	2124	2217	3244	3448	4739	146	113	137	124	200
Carnot Factor for input energy ( $=1-T_o/T$ )	0.1339	0.1339	0.1339	0.1339	0.1339	1	1	1	1	1
Primary Energy Input (kW)	284.4	296.9	434.4	461.8	634.7	145.9	112.9	136.7	123.7	200.1
Upgraded heat temperature (C)	82.2	96.1	110.0	126.7	154.4	82.2	82.2	87.8	82.2	107.2
Carnot Factor for upgraded heat ( $=1-T_o/T$ )	0.1610	0.1926	0.2218	0.2543	0.3027	0.1610	0.1610	0.1739	0.1610	0.2161
Exergy of upgraded heat (kW)	161	193	222	254	303	161	161	174	161	216
Thermal energy input (kW)	2124	2217	3244	3448	4739	854	887	863	876	800
Hot water temperature difference (C)	7	7	7	7	7	7	7	7	7	7
Hot water flow rate (kg/s)	72.2	75.4	110.3	117.3	161.2	29.1	30.2	29.4	29.8	27.2
Hot water pressure drop (kPa)	30.0	32.3	52.4	58.4	81.5	6.1	6.5	6.2	6.4	5.4
Hot water pump power (kW)	3.04	3.42	8.12	9.61	18.43	0.25	0.28	0.26	0.27	0.21
Condenser rejected heat (AHTs only) (kW)	1124	1217	2244	2448	3739	N/A	N/A	N/A	N/A	N/A
Cooling water temperature difference (C)	7	7	7	7	7	N/A	N/A	N/A	N/A	N/A
Cooling water flow rate (kg/s)	38.2	41.4	76.3	83.3	127.2	N/A	N/A	N/A	N/A	N/A
Cooling water pressure drop (kPa)	50.0	57.5	134.1	156.2	245.8	N/A	N/A	N/A	N/A	N/A
Cooling water pump power (kW)	2.68	3.34	14.36	18.26	43.88	N/A	N/A	N/A	N/A	N/A
Cooling tower fan power (kW)	12.78	13.84	25.51	27.83	42.51	N/A	N/A	N/A	N/A	N/A
Electrical energy for solution pumps (kW)	10.62	11.09	16.22	17.24	23.70	N/A	N/A	N/A	N/A	N/A
Total thermal energy for AHTs (kW)	2124	2217	3244	3448	4739	854	887	863	876	800
Total input electrical power (kW)	29.1	31.7	64.2	72.9	128.5	146.1	113.2	137.0	124.0	200.3

\*Waste heat temperature 71.1°C; Supply cooling water temperature (for AHT only) 29.4°C

Hot and cooling water pump efficiency 75%; compressor isentropic efficiency 82%; motor efficiency 95%

the various operating temperatures for the heat transformers such as the magnitude of temperature boost and the driving heat source and supply cooling water temperatures. In this study, only the influence of the temperature boost is evaluated while the other two temperatures will remain constant.

Operating energy costs of the absorption heat transformers and auxiliary equipment include the costs of the primary thermal and electrical energies. Figure 5-11 illustrates the interactions of the external energy input (primary heat and electric power) and the output product (heat recovery capacity) of the completed system. However, since the primary energy input ( $Q_e + Q_g$ ) for the absorption heat transformers is the “free” waste heat, therefore the cost of this primary energy input is zero. Only the costs of the minor electric energy for absorption heat transformers and auxiliary equipment are considered in the calculation of the total energy costs. Thus the cost of the total energy for absorption heat transformers can be expressed as:

$$C_W = c_{electric} W \cdot (AOH) \quad (5.25)$$

where  $c_{electric}$  is the unit cost of electrical energy,  $W$  is the electrical power obtained from Equation (5-23), and AOH is the annual operating hours for the heat transformers. And the total energy cost for the vapor-compression heat transformers becomes

$$C_W = c_{electric} [W_c / (\eta_{isen} \eta_m) + W_{hvp}] \cdot (AOH) \quad (5.26)$$

In addition to the energy cost, the total operating costs of heat transformers also include the costs of maintenance and electric demand after the operation of the heat transformers. The reported maintenance cost for absorption heat transformers is between 0.5% and 1.5% of the total investment cost (IEA 1995). In this study, the annual maintenance cost is set at 1% of the total investment cost for absorption heat transformers and at 2% for vapor-compression ones. Generally, utility companies have different rate schedules for industrial and commercial users. A simple schedule usually involves only electric consumption (kWh) charges and, therefore, the unit charge of electricity is higher. Another schedule involves not only electric consumption charges but also demand (kW)

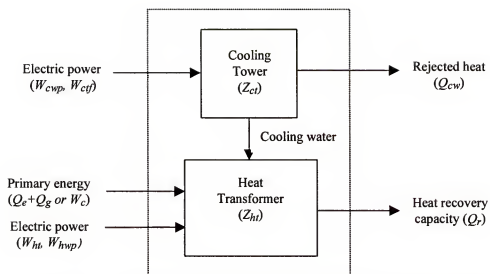


Figure 5-11. Interactions of the external energy input and product output of the completed system

charges, and usually the unit cost of electricity of this schedule is cheaper. A local utility company was consulted for the rate schedules. The cost of the electric demand  $C_{demand}$  is calculated employing the product of unit cost of the electric demand in the local utility company and the time period. Thus the total operating cost of the heat transformers becomes

$$C_{total} = C_W + C_{maintenance} + C_{demand} \quad (5.27)$$

The costs associated with a heat transformer installation for a heat recovery process can be divided into three parts: the heat transformer itself, auxiliary equipment such as cooling towers, and piping to and from the heat transformer (Franck 1996). The first two costs generally depend on manufacturer's prices. The last one, however, is always very site-specific and is not discussed here. The capital costs of the heat transformers,  $Z_{ht}$ , and cooling towers,  $Z_{ct}$  are included in the calculation of the life cycle costs of the heat recovery systems. However, determining the costs of heat transformers and auxiliary equipment can be a complex task. In this study, the initial estimation for each of the heat transformers considered is based on several surveys and actual data reported in literature (Dorgan, et al. 1995; IEA 1995; Cane and Clemes 1996). Furthermore, the original costs obtained from the references are corrected to the same reference year with the aid of an appropriate cost index ( $CI$ ). The cost index is an inflation indicator used to correct the cost of equipment to the date of the estimate and is defined as follows (Bejan et al. 1996):

$$\text{Cost at the reference year} = \text{original cost} \times (CI_{\text{reference year}} / CI_{\text{original year}}) \quad (5.28)$$

For example, the cost index is 326 for the year 1992 and is 378 for the year 1998.

The capital cost of the cooling tower depends on the quantity of the rejected heat from the absorption heat transformers. The equipment cost for the cooling tower is estimated by the relationship in Equation (5.15). The  $Z_{ct,x}$  for the AHTs considered is selected as the capital cost of the cooling tower for the single-stage absorption heat

transformer with temperature boost at 11°C and is based on \$7/kW of the rejected heat. It should be mentioned that the cost of the cooling water pump and piping are included in the costs for the cooling towers. Therefore the total capital costs of the systems can be calculated as

$$Z = Z_{ht} + Z_{ct} \quad (5.29)$$

One the most commonly used cost analysis methods is the simple payback period analysis. The simple payback period (*SPP*) determines the number of years required to recover the initial investment for the heat transformers and is calculated from the total capital costs of the systems with respect to the operating cost savings from reduction of fuel consumption.

$$SPP = Z / (C_{fuel} - C_{total}) \quad (5.30)$$

The fuel cost,  $C_{fuel}$ , in Equation (5.30) can be written in terms of the unit cost of natural gas, upgraded heat capacity, natural gas appliance (or heater) efficiency, and annual operating hours as follows:

$$C_{fuel} = c_{ng} Q_r \cdot (AOH) / \eta_{heater} \quad (5.31)$$

The advantage of the simple payback period is its simplicity and that it does provide a rough measure of the worth of a project. The disadvantage is that it does not consider the time value of money. For thermal systems such as absorption heat transformers with initial investment and operating costs over their lifetime, it is better to evaluate the life cycle cost of the system or the levelized cost of the final product. In engineering economy, the unit of time intervals for such purposes is usually taken as the year. The capital-recovery factor (*CRF*) in Equation (5.17) is used to levelize the capital cost of the heat transformer systems. Thus the life cycle cost of both the absorption and vapor-compression heat transformers can be evaluated from Equations (5.17), (5.27), and (5.29) on a yearly basis

$$C_{LCC} = (CRF)Z + C_{total} \quad (5.32)$$

And the specific life cycle cost with respect to the exergy of the upgraded heat (the final product) becomes

$$c_{SLCC} = C_{LCC} / [E_r \cdot (AOH)] \quad (5.33)$$

Heat transformers with a lower specific life cycle cost represent a better choice for heat recovery applications. Thus the specific life cycle cost,  $c_{SLCC}$ , in Equation (5.33) is the objective to be minimized in this study.

#### 5.4.2 Results and Discussion

Life cycle costing for the various heat transformers considered were calculated over a wide range of temperature boost values. As mentioned earlier, utility companies usually have different electricity rate programs to the customers. Therefore, a local utility company was consulted for the unit costs of both electric energy and natural gas. The utility company offers two different electricity rates for commercial purposes: (1) a higher rate with no monthly demand charge and (2) a lower rate with monthly demand charge. Table 5-6 lists part of calculation results of the total operating costs as well as capital costs for the three absorption heat transformers considered for a host of values for the temperature boost along with respective results for electric-powered vapor-compression heat transformers. The first of the two electricity rates of the local utility company, \$0.0555/kWh, is used in the calculation of the energy costs as listed in Table 5-6. The unit cost of natural gas is \$0.0068/kWh. It is assumed that the waste heat and supply cooling water temperatures are 71.1°C and 29.4°C, respectively, that the annual interest rate is 8%, that the number of years of heat transformer operation is 20 years, and that the annual operating hour is 8000 hours per year. Based on the data reported in the references and the cost index of the current year, the capital costs of the single-, double-, and triple-stage absorption heat transformers are set at \$140000, \$196000, and \$252000, respectively. These estimated costs for the AHT are based on the

Table 5-6. Comparison of specific life cycle costs of the absorption and vapor-compression heat transformers

System	Absorption Heat Transformers					Vapor-Compression Heat Transformers				
Type	1-S	1-S	2-S	2-S	3-S	(R134a)	(R113)	(R113)	(R114)	2S-R113
Temperature Boost (C)	11.1	25.0	38.9	55.6	83.3	11.1	11.1	16.7	11.1	36.1
Heat transformer cost (\$)	140000	140000	196000	196000	252000	80000	80000	80000	80000	100000
Cooling tower cost (\$/7/kW reject heat)	7868	8474	14963	16229	24063	N/A	N/A	N/A	N/A	N/A
Total capital costs (\$)	147868	148474	210963	212229	276063	80000	80000	80000	80000	100000
Annual operation hours (hr/yr)	8000	8000	8000	8000	8000	8000	8000	8000	8000	8000
Years of operation of heat transformers (yr)	20	20	20	20	20	20	20	20	20	20
Annual interest rate	0.08	0.08	0.08	0.08	0.08	0.08	0.08	0.08	0.08	0.08
Capital recovery factor (CRF)	0.10185	0.10185	0.10185	0.10185	0.10185	0.10185	0.10185	0.10185	0.10185	0.10185
Unit cost of natural gas (\$/kWh)	0.00684	0.00684	0.00684	0.00684	0.00684	0.00684	0.00684	0.00684	0.00684	0.00684
Unit cost of electrical energy (\$/kWh)	0.0555	0.0555	0.0555	0.0555	0.0555	0.0555	0.0555	0.0555	0.0555	0.0555
Unit cost of thermal energy (\$/kWh)	0	0	0	0	0	0	0	0	0	0
Total electrical energy cost (\$/yr)	12931	14070	28507	32385	57064	64887	50251	60825	55044	88924
Total thermal energy cost (\$/yr)	0	0	0	0	0	0	0	0	0	0
Total energy cost (\$/yr)	12931	14070	28507	32385	57064	64887	50251	60825	55044	88924
Maintenance cost (\$/yr)	1479	1485	2110	2122	2761	1600	1600	1600	1600	2000
Total operating cost (\$/yr)	14410	15555	30617	34508	59825	66487	51851	62425	56644	90924
Electric demand cost (\$/yr)	0	0	0	0	0	0	0	0	0	0
Total operating cost per year (\$/yr)	14410	15555	30617	34508	59825	66487	51851	62425	56644	90924
Heating appliance efficiency (%)	80	80	78	78	76	80	80	80	80	78
Cost of natural gas w/o heat recovery (\$/yr)	68400	68400	70154	70154	72000	68400	68400	68400	68400	70154
Savings from waste heat recovery (\$/yr)	53990	52845	39537	35646	12175	1913	16549	5975	11756	-20770
Simple payback period (yr)	2.74	2.81	5.34	5.95	22.67	41.83	4.83	13.39	6.80	-4.81
Life cycle cost of heat transformers (\$/yr)	29470	30677	52104	56124	87943	74636	59999	70573	64792	101109
Percentage of capital cost in life cycle cost	51.1	49.3	41.2	38.5	32.0	10.9	13.6	11.5	12.6	10.1
Specific life cycle cost of exergy (\$/kWh)	0.02288	0.01991	0.02936	0.02759	0.03632	0.05795	0.04659	0.05072	0.05031	0.05847
SLCC of exergy from burning NG (\$/kWh)	0.05311	0.04440	0.03953	0.03449	0.02973	0.05311	0.05311	0.04916	0.05311	0.04057



data reported in the literature (Dorgan et al. 1995; IEA 1995; Cane and Clemes 1996) after being adjusted for inflation. The initial investments for the one-stage vapor-compression heat transformers are set at \$80000 and \$90000 for temperature lifting between 11°C and 41°C, and between 41°C and 83°C, respectively, for their operating pressure ratio difference, and \$100000 for the two-stage compression ones.

As can be seen, the single-stage absorption heat transformer has the shorter simple payback period (about 2.7 to 3 years). It can also be seen that the percentage of the capital cost in the life cycle cost of an absorption heat transformer is much larger than that of a vapor-compression heat transformer. This means that the initial capital costs of absorption heat transformers are the key that leads to success in heat recovery and upgrading applications, while the operating costs are the more significant costs of a vapor-compression system.

Figure 5-12 shows a comparison of the simple payback period of the absorption and vapor-compression heat transformers versus the temperature boost. It can be seen that, the single-stage absorption heat transformer has the shortest simple payback period (about 2.7 to 4.22 years) vis-à-vis the vapor-compression ones within most of their operating domain. It is clear that vapor-compression systems do not have a favorable payback period due to their high operating costs. The simple payback period (*SPP*) of a double-stage AHT is about 5 to 10 years within a higher temperature boost range and may be still acceptable for industrial applications. And the triple-stage AHT has a payback period over 15 years at the operating conditions shown in Figure 5-12, and that may mean that triple-stage AHTs may not have enough economic potential as of yet.

Figure 5-13 shows a comparison of the specific life cycle costs (*SLCC*) of the exergy of the upgraded output heat as a function of the temperature boost. The *SLCC* of the upgraded heat obtained from employing a natural gas heater (curve 8) without an installation of any heat transformer is also plotted for comparison purposes. For those heat transformers with a *SLCC* located below the *SLCC* curve of the natural gas heater,

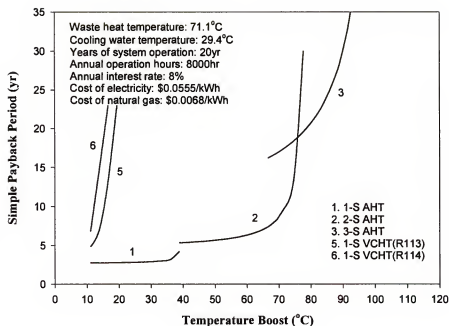


Figure 5-12. Comparison of simple payback period of various absorption and vapor-compression heat transformers at a higher electricity rate schedule with no monthly demand charges

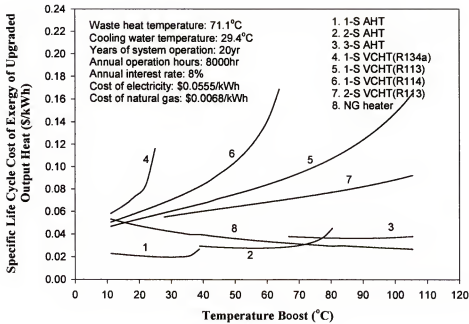


Figure 5-13. Comparison of specific life cycle costs of various absorption and vapor-compression heat transformers at a higher electricity rate schedule with no monthly demand charges

the system has the potential to conserve energy and also decrease air and water pollution to the regional and global environment by reducing fuel consumption. As can be seen, within the respective temperature boost range, the *SLCC* of each absorption heat transformer declines slightly at first and then increases significantly as the temperature boost increases. This is because a higher heat source temperature means more primary input thermal exergy supplied to the absorption heat transformers, and that results in a higher exergy cost even though the heat transformers only require less input energy from a first law vantage point. But, the specific life cycle costs of the compression systems increase monotonically as the systems deliver a higher temperature boost. It can also be seen that the single- and double-stage absorption heat transformers have smaller specific life cycle costs than the natural gas heater in their temperature boost ranges. This indicates that the single- and double-stage absorption heat transformers outperform both the vapor-compression heat transformer and the simple natural gas heater and are better choices for industrial heat recuperation and temperature lifting applications from a thermoeconomics vantage point.

Effect of the unit cost of electricity on the payback periods and life cycle costs of the heat transformers is also investigated. Figures 5-14 and 5-15 show comparisons of the simple payback period and specific life cycle cost among the absorption and vapor-compression heat transformers operating with a lower unit cost of electricity from the local utility company. The electricity rate is \$0.034/kWh and the monthly electric demand charge is \$4.66/kW from a local utility company. As can be seen, the simple payback periods of all the heat transformers considered applying this rate schedule become shorter when compared with those of the same systems employing the other schedule shown in Figure 5-12. The single-stage AHT has a simple payback period between 2.58 and 2.88 years for a temperature boost between 11°C and 36°C. And the payback period for the double-stage AHT is about 4.5 to 5 years with a temperature boost

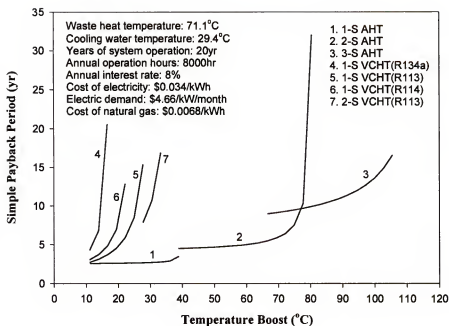


Figure 5-14. Comparison of simple payback period of absorption and vapor-compression heat transformers at a lower electricity rate schedule with monthly demand charges

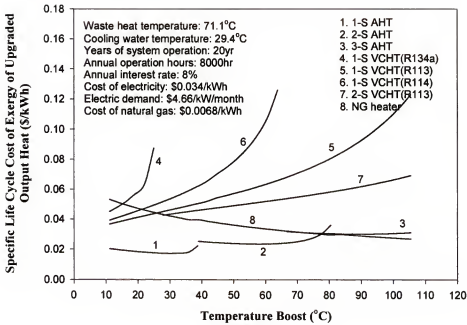


Figure 5-15. Comparison of specific life cycle cost of absorption and vapor-compression heat transformers at a lower electricity rate schedule with monthly demand charges

of 39 to 61°C. Even the triple-stage AHT has payback periods about 9 to 10 years with 64 to 90°C temperature boost values.

The effect of the electric rate on the specific life cycle cost of the heat transformers is shown in Figure 5-15. The *SLCC* of the natural gas water heater is also evaluated and plotted in Figure 5-15 for comparison purposes. As can be seen, both the single- and double-stage AHT have a lower *SLCC* than both the vapor-compression systems and natural gas water heater. The *SLCC* of the triple-stage AHT is also slightly lower than systems with no heat recovery machines within temperature boosting range between 64°C and 72°C. It can also be seen that operation of the one-stage vapor-compression heat transformers using R-134a, R-113, and R-114 results in lower *SLCC* within the low temperature boost range (< 25°C). However, neither the one-stage or two-stage vapor-compression heat transformers can recover and upgrade the waste heat to a higher temperature level in an economic way. This may be because of the thermal characteristics of the different refrigerants as well as the operating temperatures of the systems.

Figures 5-16 and 5-17 show a comparison of the simple payback periods and specific life cycle costs of the heat transformers as functions of the temperature boost with the price of the natural gas even lower (\$0.005/kWh). As can be seen, only the single-stage AHT has a favorable payback time (between 4.3 and 5 years) for a temperature boost between 11°C and 36°C (Figure 5-16). Furthermore, the single-stage AHT has a lower *SLCC* vis-à-vis natural gas based appliances (Figure 5-17). All other systems considered for industrial waste heat recuperation applications have failed in recovering the waste heat economically at relatively high electric rates and low natural gas cost.

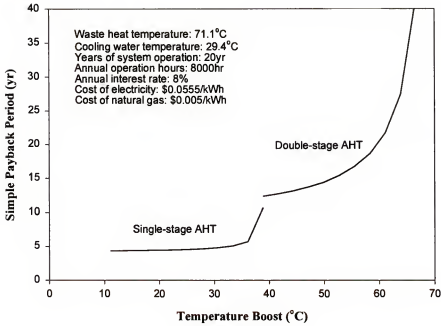


Figure 5-16. Comparison of simple payback periods of absorption and vapor-compression heat transformers with a lower natural gas cost



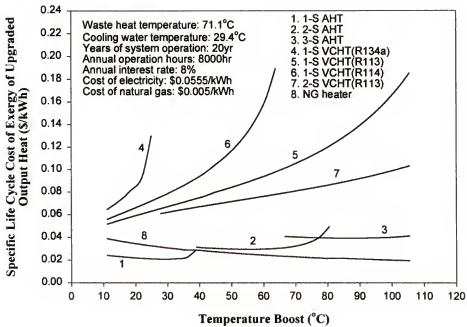


Figure 5-17. Comparison of specific life cycle cost of absorption and vapor-compression heat transformers with a lower natural gas cost

### 5.5 Conclusions

Application of thermoeconomics is directed to the study of single-, double-, and triple-effect absorption chillers with a given cooling capacity as well as single-, double-, and triple-stage absorption heat transformers with a given heat recovery capacity to evaluate the simple payback time and specific life cycle costs of the systems and their auxiliary equipment. Both initial capital and operating costs are considered based on exergy costing. The relative electric-driven vapor-compression chiller and heat transformers are also evaluated for comparison purposes.

For cooling applications, results show that both single- and double-effect absorption chillers in certain heat source temperature ranges can outperform the vapor-compression chiller. Long term operation can make the absorption chillers more competitive than their vapor-compression counterparts. Also reducing the initial capital costs of absorption chillers or applying lower cost thermal energy (such as waste heat) will make absorption chillers more attractive.

Results also show that, for heat recovery applications, both single- and double-stage absorption heat transformers in certain temperature boost ranges provide favorable simple payback periods (between 2.58 and 2.88 years and between 4.5 and 5.0 years, respectively), and also outperform the vapor-compression heat transformers and natural gas appliances based on the specific life cycle costs. Furthermore, the triple-stage absorption heat transformer can produce high temperature boost values between 64°C and 90°C with payback periods of 9 to 10 years. Lower electricity rate schedule and higher natural gas prices from utility companies can make the single- and double-stage absorption heat transformers more attractive in the applications of waste heat recovery for industrial processes and plants. Also reducing the initial capital costs of absorption heat

transformers will make them more attractive because the initial investment of the systems contributes to about 50, 40, and 33% of the specific life cycle costs for single-, double-, and triple-stage AHTs, respectively.

## CHAPTER 6 CONCLUSIONS AND RECOMMENDATIONS

### 6.1 Conclusions

Performance simulations have been carried out for various absorption systems using a LiBr/H<sub>2</sub>O solution as the working fluid. These systems include single-, double-, and triple-effect absorption chillers for cooling, absorption heat pumps for heating, and single-, double-, and triple-stage absorption heat transformers for waste heat temperature boosting applications. Both the first and second law efficiencies of these absorption systems have been investigated and compared over a host of operating conditions. Several conclusions can be drawn from the results presented in this study. In the parametric analysis of absorption chillers with varying operating conditions, it is clear that a low cooling water temperature yields a higher cooling COP and a higher exergetic efficiency for all of the absorption chillers. Results also show that, although the chillers operating with a high chilled water temperature have better cooling COP, these systems have a smaller exergetic efficiency than those having a low chilled water temperature. Increasing the heat source temperature can improve the cooling COP of absorption chillers, but as the heat source temperature increases further, the COP of the systems levels off and even decreases. This negative effect of increasing the heat source temperature is more dominant relative to the exergetic efficiency of the systems considered.

Comparing four double-effect absorption chillers with different solution flow types, results show that the parallel and dual-loop flow types are a better choice for the multi-effect systems. In the comparison of performance of various absorption chillers, it

can be concluded that the triple-effect system has a superior cooling COP over the single-effect or the double-effect systems. Thus, if a high temperature heat source is available, it is better to operate an absorption chiller in a triple-effect mode. From a second law vantage point, however, all three systems have similar exergetic efficiencies within their own operating temperature ranges. The single-effect system still is a good choice since it uses lower grade heat sources and costs less.

In the parametric analysis of the absorption system for heating, it is clear that increasing the heat source temperature will increase both the heating COP and the exergetic efficiency. However, increasing the heat source temperature could result in a high risk of crystallization for the LiBr/H<sub>2</sub>O solution. The system also has a small operating range and a high crystallization risk when the system needs to provide the supply hot water at a higher temperature. Furthermore, low environmental temperatures and freezing problems of the refrigerant (water) cause the LiBr/H<sub>2</sub>O absorption system to have a low heating efficiency and may not even be able to operate normally. When such a situation arises, the heat source stream should probably be supplied to the heating spaces directly without operating the absorption system.

From the performance comparison of single-, double-, and triple-stage LiBr/H<sub>2</sub>O absorption heat transformers (AHTs), it is shown that the COP of the three systems decreases slightly at first as the desirable temperature boost increases, and then declines dramatically when the temperature boost increases further. On the other hand, the exergetic efficiency increases slightly at first, and then declines sharply as the temperature boost increases. Results also show that there is a limitation of the achievable temperature boost for absorption heat transformers employing waste heat and an external cooling water loop. It is also evident that increasing the heat source temperature or decreasing the cooling water temperature provides the AHT systems a better COP and a better exergetic efficiency in the higher temperature boost range.

In the comparison of the three absorption heat transformers, it became obvious that, at the same waste heat source and cooling water temperatures, the double- and triple-stage AHTs can reach higher temperature boost values than the single-stage one. And the multi-stage AHT can maintain both a high COP and a high exergetic efficiency within the high temperature boost range. But results also show that there is still a potential limit of achievable temperature boost for the double-stage AHT. Also the high temperature level of the triple-stage AHT may cause serious corrosion problems by the LiBr/H<sub>2</sub>O solution. New suitable working fluids or novel corrosion inhibitors for the higher temperature boost applications are thus necessary.

In addition to performance comparisons, applications of thermoeconomics is also directed to the absorption chillers and heat transformers to evaluate specific life cycle costs of the systems and their auxiliary equipment over a wide range of heat source temperatures and temperature boost values. Both initial capital and operating costs are considered based on exergy costing. The relative electric-powered vapor-compression chiller and heat transformers are also evaluated for comparison purposes. For cooling applications, results show that both single- and double-effect absorption chillers in certain heat source temperature ranges can outperform the vapor-compression chiller. Although a tripe-effect absorption chiller has the highest COP, the specific life cycle cost of this system is much higher than the other two absorption and vapor-compression chillers due to its expensive investment. Long term operation can make the absorption chillers more competitive than their vapor-compression counterparts. Also reducing the initial capital costs of absorption chillers or applying lower cost thermal energy (such as waste heat) will make absorption chillers more attractive.

Results also show that, for heat recovery applications, both single- and double-stage AHTs in certain temperature boost ranges provide favorable simple payback periods (between 2.58 and 2.88 years and between 4.5 and 5.0 years, respectively), and also outperform the vapor-compression heat transformers and natural gas appliances based on

the specific life cycle costs. Furthermore, the triple-stage AHT can produce high temperature boost values between 64°C and 90°C with payback periods of 9 to 10 years. Lower electricity rate schedule and higher natural gas prices from utility companies can make the single- and double-stage AHTs more attractive in the applications of waste heat recovery for industrial processes and plants. Also reducing the initial capital costs of absorption heat transformers will make them more attractive because the initial investment of the systems contributes to about 50, 40, and 33% of the specific life cycle costs for single-, double-, and triple-stage AHTs, respectively.

## 6.2 Recommendations

The present investigation provides valuable insight into the design and comparison of various lithium bromide/water absorption chillers and heat transformers. Important operating parameters on thermodynamic performance have been brought forward, and the estimated specific life cycle costs of the absorption systems on the basis of exergy can be valuable as a reference for future system design and selection. Based on the results from the performance analysis, physical characteristics of working fluids and operating parameters of absorption systems were found to have a significant impact on the performance, operating limits, and system selection. Potential corrosion, freezing, and crystallization problems of lithium bromide/water solution may constrain the operating conditions and types of absorption systems for either cooling or temperature boosting applications. Thus, search for new working pairs and proper corrosion inhibitors is necessary.

Size allocations of heat exchange components of absorption systems is also of interest as they will determine constructing material costs and influence system performance. An optimization of a combination of those heat exchange components inside an absorption machine based on capital cost and energy efficiency would be

valuable. With further research it should be possible to develop energy efficient and cost competitive absorption chillers and heat transformers. Nonetheless, absorption systems have the advantage of saving energy by using low-grade heat to produce chilled and hot water for cooling and heating and to recover waste heat for temperature boosting applications when and where any possible heat source is available.



# APPENDIX A SAMPLE OUTPUT DATA OF SINGLE-EFFECT ABSORPTION CHILLER

Operating condition for every state point in the system

s.p.	T (°C)	h (kJ/kg)	m (kg/s)	X (%)	P (kPa)	V. F.	s (kJ/kg K)	ε (kJ/kg)
1	10.32	42.4	2.250	0.0	0.000	0.0000	0.151	1.445
2	7.22	29.6	2.250	0.0	0.000	0.0000	0.106	2.187
3	6.02	2512	0.012	0.0	0.936	1.0000	8.999	-167.9
4	29.44	122.7	2.933	0.0	0.000	0.0000	0.427	0.063
5	32.73	136.6	2.933	0.0	0.000	0.0000	0.472	0.348
6	36.10	86.3	0.450	55.2	0.936	0.0000	0.275	17.385
7	58.44	132.4	0.450	55.2	4.901	0.0000	0.412	22.677
8	73.89	310.1	3.623	0.0	0.000	0.0000	1.004	15.153
9	71.12	298.5	3.623	0.0	0.000	0.0000	0.971	13.559
10	69.33	2630	0.012	0.0	4.901	1.0000	6.938	565.2
11	69.33	159.5	0.438	56.7	4.901	0.0000	0.466	33.607
12	45.90	112.0	0.438	56.7	0.936	0.0000	0.329	26.989
13	29.44	122.7	3.285	0.0	0.000	0.0000	0.427	0.063
14	31.62	131.9	3.285	0.0	0.000	0.0000	0.457	0.236
15	32.46	135.5	0.012	0.0	4.901	0.0000	0.469	0.320
16	39.51	100.3	0.436	57.0	0.936	0.0000	0.290	26.793
17	65.64	146.4	0.453	54.9	4.901	0.0000	0.457	23.140
18	6.02	135.5	0.012	0.0	0.936	0.0446	0.485	-5.076
19	32.46	2561	0.012	0.0	4.901	1.0000	8.404	58.578
20	6.02	135.5	0.012	0.0	0.936	0.0446	0.485	-5.076

Heat transfer quantities for every component

NO.	TYPE	UA (kW/°C)	EFF (%)	LMTD (°C)	Q (kW)	ΔE (kW)
1	Evaporator	11.84	71.968	2.43	28.81	0.303
2	SHX	2.01	70.494	10.33	20.77	0.517
3	Generator	8.42	44.654	5.01	42.12	5.586
4	Condenser	17.74	72.158	1.70	30.23	6.277
5	Absorber	6.06	33.912	6.71	40.69	1.124
6	Valve	N/A	N/A	N/A	N/A	0.065

System performance

COP	$E_{ex}$
0.648	0.289

## REFERENCES

- Abrahamsson, K., Jernqvist, A., and Aly, G., 1994. "Thermodynamic Analysis of Absorption Heat Cycles," *Proc. of the International Absorption Heat Pump Conference*, New Orleans, LA, AES-Vol. 31, ASME, pp. 375-383.
- Ahern, J. E., 1980. *The Exergy Method of Energy Systems Analysis*, Wiley, New York.
- Alefeld, G., 1985. "Multi-Stage Apparatus Having Working-Fluid and Absorption Cycles, and Method of Operation Theorem," U.S. Patent No. 4,531,374.
- Alefeld, G., 1989. "Second Law Analysis for an Absorption Chiller," *Newsletter of the IEA Heat Pump Center*, Vol. 7, No. 2, June, pp. 54-57.
- Alefeld, G. and Radermacher, R., 1994. *Heat Conversion Systems*, CRC Press, Boca Raton, FL.
- Alefeld, G. and Ziegler, F., 1985a. "Advanced Heat Pump and Air-Conditioning Cycle for Working Pair  $H_2O/LiBr$ : Domestic and Commercial Applications," *ASHRAE Transactions*, Vol. 91, Pt. 2, pp. 86-95.
- Alefeld, G. and Ziegler, F., 1985b. "Advanced Heat Pump and Air-Conditioning Cycle for Working Pair  $H_2O/LiBr$ : Industrial Applications," *ASHRAE Transactions*, Vol. 91, Pt. 2, pp. 96-104.
- Ally, M. R., 1987. "Thermodynamic Properties of Aqueous Ternary Solutions Relevant to Chemical Heat Pumps," ORNL/TM-10258, Oak Ridge, TN.
- Amrane, K. and Radermacher, R., 1994. "Second-Law Analysis of Vapor Compression Heat Pump with Solution Circuit," *Journal of Engineering for Gas Turbines and Power*, Vol. 116, July, pp. 453-461.
- Anand, D. K. and Kumar, B., 1987. "Absorption Machine Irreversibility Using New Entropy Calculations," *Solar Energy*, Vol.39, No. 3, pp. 243-256.
- Anand, D. K., Lindler, K. W., Schweitzer, S., and Kennish, W. J., 1984. "Second Law Analysis of Solar Powered Absorption Cooling Cycles and Systems," *Journal of Solar Energy Engineering*, Vol. 106, August, pp. 291-298.

- Aphornratana, S. and Eames, I. W., 1995. "Thermodynamic Analysis of Absorption Refrigeration Cycles Using the Second Law of Thermodynamics Method," *International Journal of Refrigeration*, Vol. 18, No. 4, pp. 244-252.
- Arh, S., 1994. "Absorption Heat Pump/Transformer Cycle for Simultaneous Heating and Cooling," *Proc. of the International Absorption Heat Pump Conference*, New Orleans, LA, AES-Vol. 31, ASME, pp. 251-266.
- ARI, 1992. "Standard for Absorption Water Cooling and Water Heating Packages," ARI Standard 560, Arlington, Va.
- ASHRAE, 1997. *ASHRAE Handbook of Fundamentals*, American Society of Heating, Refrigerating, and Air-conditioning Engineers, Atlanta, Georgia.
- Bejan, A., Tsatsaronis, G., and Moran, M., 1996. *Thermal Design and Optimization*, John Wiley, New York.
- Best, R., Islas, J., and Martinez, M., 1993. "Exergy Efficiency of an Ammonia-Water Absorption System for Ice Production," *Applied Energy*, Vol. 45, pp. 241-256.
- Bosnjakovic, F., Knoche, K. F., and Stehmeier, D., 1986. "Exergetic Analysis of Ammonia/Water Absorption Heat Pumps," ASME Winter Annual Meeting, *Computer-Aided Engineering of Energy Systems, Vol. 3--Second Law Analysis and Modeling*, AES-Vol. 2-3, pp. 93-104.
- Cane, R. D. and Clemes, S. B., 1996. "Industrial Heat Pump Operating Experiences in North America," *Industrial Heat Pumps*, IEA Heat Pump Centre Workshop Proceedings, Report No. HPP-AN21-4, pp77-90.
- Carmody, S. A. and Shelton, S. V., 1993. "Analysis of Generator-Absorber Heat Recovery for an Ammonia/Water Absorption Cycle," The 1993 ASME Winter Annual Meeting, New Orleans, LA, Nov. 28-Dec. 3, *Thermodynamics and the Design, Analysis, and Improvement of Energy Systems*, AES-Vol. 30/HDT-Vol. 266, ASME, pp. 33-38.
- Carmody, S. A. and Shelton, S. V., 1994. "Direct Second Law Analysis of Advanced Absorption Cycles Utilizing an Ideal Solution Model," *Proc. of the International Absorption Heat Pump Conference*, New Orleans, LA, AES-Vol. 31, ASME, pp. 369-374.
- Cheng, C.-S. and Shih, Y.-S., 1988. "Exergy and Energy Analyses of Absorption Heat Pumps," *Int. J. Energy Research*, Vol. 12, pp. 189-203.

- Ciambelli, P. and Tufano, V., 1988a. "On the Performance of Advanced Absorption Heat Transformer Part I. The Two Stage Configuration," *Heat Recovery Systems & CHP*, Vol. 8, pp. 445-450.
- Ciambelli, P. and Tufano, V., 1988b. "On the Performance of Advanced Absorption Heat Transformer Part II. The Double Absorption Configuration," *Heat Recovery Systems & CHP*, Vol. 8, pp. 451-457.
- Davidson, W. F. and Erickson, D. C., 1986. "New High Temperature Absorbent for Absorption Heat Pumps," Final Report, ORNL/Sub/85-22013/1, Oak Ridge, TN.
- DeVault, R. C., 1988. "Triple Effect Absorption Chiller Utilizing Two Refrigeration Circuits," U.S. Patent No. 4,732,008.
- DeVault, R. C. and Biermann, W. J., 1993. "Triple-Effect Absorption Refrigeration System with Double-Condenser Coupling," U.S. Patent No. 5,205,136.
- Dorgan, C. B., Leight, S. P., and Dorgan, C. E., 1995. *Application Guide for Absorption Cooling/Refrigeration Using Recovered Heat*, American Society of Heating, Refrigerating, and Air-conditioning Engineers, Atlanta, Georgia.
- Egrican, N., 1988. "The Second Law Analysis of Absorption Cooling Cycles," *Heat Recovery Systems & CHP*, Vol. 8, No. 6, pp. 549-558.
- Eisa, M. A. R., Chaudhari, S. K., Paranjape, D. V., and Holland, F. A., 1986. "Classified References for Absorption Heat Pump Systems from 1975 to May 1985," *Heat Recovery Systems & CHP*, Vol. 6, No. 1, pp. 47-61.
- Eisa, M. A. R. and Holland, F. A., 1986. "A Study of the Operating Parameters in a Water-Lithium Bromide Absorption Cooler," *International Journal of Energy Research*, Vol. 10, pp. 137-144.
- El-Sayed, Y. M. and Evans, R. B., 1970. "Thermoeconomics and the Design of Heat Systems," *Journal of Engineering for Power*, January, pp. 27-35.
- Erickson, D. C., 1991. "Branched GAX Absorption Vapor Compressor," U.S. Patent No. 5,024,063.
- Erickson, D. C., 1992. "Vapor Exchange Duplex GAX Absorption Heat Pump," U.S. Patent No. 5,097,676.
- Franck, P. Å., 1996. "Industrial Heat Pump Screening Software," *Industrial Heat Pumps*, IEA Heat Pump Centre Workshop Proceedings, Report No. HPP-AN21-4, pp53-66.

- Garimella, S., Christensen, R. N., and Lacy, D., 1994. "Performance Evaluation of a Generator Absorber Heat Exchange Heat Pump," *Heat Pump and Refrigeration Systems Design, Analysis and Applications*, AES-Vol. 32, ASME, pp. 11-21.
- Garimella, S., Christensen, R. N., and Lacy, D., 1996. "Performance Evaluation of a Generator-Absorber Heat-Exchange Heat Pump," *Applied Thermal Engineering*, Vol. 17, No. 7, pp. 591-604.
- Garland, P. W., DeVault, R. C., and Zaltash, A., 1998. "United States Department of Energy large commercial absorption chiller development program," *Proceedings of the ASME Advanced Energy Systems Division*, AES-Vol. 38, pp. 271-275.
- Gommed, K. and Grossman, G., 1990. "Performance Analysis of Staged Absorption Heat Pumps: Water-Lithium Bromide Systems," *ASHRAE Transactions*, Vol. 96, Pt. 1, pp. 1590-1598.
- Granryd, E., 1996. "Heat Pumping Technologies," *Proceedings of the 5<sup>th</sup> International Energy Agency Conference on Heat Pumping Technologies*, Toronto, Ontario, Canada, Sep. 22-26, Vol. 1, pp. 7-15.
- Grossman, G., 1982. "Adiabatic Absorption and Desorption for Improvement of Temperature-Boosting Absorption Heat Pump," *ASHRAE Transactions*, Vol. 88, Pt. 2, pp. 359-367.
- Grossman, G., 1985. "Multi-stage Absorption Heat Transformers for Industrial Applications," *ASHRAE Transactions*, Vol. 91, Pt. 2b, pp. 2047-2061.
- Grossman, G., 1994. "Modular and Flexible Simulation of Advanced absorption systems," *Proc. of the International Absorption Heat Pump Conference*, New Orleans, LA, AES-Vol. 31, ASME, pp. 345-351.
- Grossman, G., DeVault, R. C., and Creswick, F. A., 1995a. "Simulation and Performance of an Ammonia-Water Absorption Heat Pump Based on Generator Absorber Heat Exchange (GAX) Cycle," *ASHRAE Transactions*, Vol. 101, Pt. 1, pp.
- Grossman, G. and Gommed, K., 1987. "A Computer Model for Simulation of Absorption Systems in Flexible and Modular Form," *ASHRAE Transactions*, Vol. 93, Pt. 2, pp. 2389-2428.
- Grossman, G. and Michelson, E., 1985. "A Modular Computer Simulation of Absorption Systems," *ASHRAE Transactions*, Vol. 91, Pt. 2b, pp. 1808-1827.
- Grossman, G. and Wilk, M., 1994. "Advanced modular simulation of Absorption Systems," *International Journal of Refrigeration*, Vol. 17, No. 4, pp. 231-244.

- Grossman, G., Wilk, M., and DeVault, R. C., 1994. "Simulation and performance analysis of triple-effect absorption cycles," *ASHRAE Transactions*, Vol. 100, Pt. 1, pp. 452-462.
- Grossman, G., Zaltash, A., and DeVault, R. C., 1995b. "Simulation and Performance Analysis of a Fourth-Effect Lithium Bromide-Water Absorption Chiller," *ASHRAE Transactions*, Vol. 101, Pt. 1, pp.
- Gupta, C. P. and Sharma, C. P., 1976. "Entropy Values of Lithium Bromide-water Solutions and Their Vapors," *ASHRAE Transactions*, Vol.82, Part 2, pp. 35-46.
- Herold, K. E. and Moran, M. J., 1985. "A Thermodynamic Investigation of an Absorption Temperature Boosting Heat Pump Cycle," The Winter Annual Meeting of ASME, Miami Beach, FL, Nov. 17-22, *Analysis of Energy Systems--Design and Operation*, AES-Vol. 1, ASME, pp. 81-88.
- Herold, K. E. and Moran, M. J., 1987. "Recent Advances in the Thermodynamic Analysis of Absorption Heat Pumps," The Fourth International Symposium on Second Law Analysis of Thermal Systems, Rome, Italy, May 25-19, *Second Law Analysis of Thermal Systems*, ASME, pp. 97-103.
- Herold, K. E., Radermacher, R., Howe, L., and Erickson, D. C., 1991. "Development of an Absorption Heat Pump Water Heater Using Aqueous Ternary Hydroxide Working Fluid," *International Journal of Refrigeration*, Vol. 14, May, PP. 156-167.
- Herold, K. E., Radermacher, R., and Klein, S. A., 1996. *Absorption Chillers and Heat Pumps*, CRC Press, Boca Raton, FL.
- Howe, L. A. and Erickson, D. C., 1990. "260°C Absorption Working Pair Ready for Field Test," *IEA Heat Pump Center Newsletter*, Vol. 8, No. 4, pp. 7-9.
- Hufford, P. E., 1991. "Absorption Chillers maximize Cogeneration Value," *ASHRAE Transactions*, Vol. 97, Pt. 1, pp. 428-433.
- Hufford, P. E., 1992. "Absorption Chillers Improve Cogeneration Energy Efficiency," *ASHRAE Journal*, Vol. 34, No. 3, pp. 46-53.
- IEA, 1995. "Industrial Heat Pumps: Experiences, Potential and Global Environmental Benefits," IEA Heat Pump Centre, Report No. HPP-AN21-1, Sittard, The Netherlands.
- Inoue, N., Iizuka, H., Ninomiya, Y., and Watanabe, K., 1994a. "COP Evaluation for Advanced Ammonia-Based Absorption Cycles," *Proc. of the International*

- Absorption Heat Pump Conference*, New Orleans, LA, AES-Vol. 31, ASME, pp. 1-6.
- Inoue, S., Yamamoto, S., Furukawa, T., Wakiyama, Y., and Ochi, K., 1994b. "Improvement of High-Temperature Application and Compactness of a Unit of an Absorption Heat Pump," *Heat Recovery Systems & CHP*, Vol. 14, No. 3, pp. 305-314.
- Irvine, T. F., Jr. and Liley, P. E., 1984. *Steam and Gas Tables with Computer Equations*, Academic Press, New York.
- Ishida, M. and Kawamura, K., 1982. "Energy and Exergy Analysis of a Chemical Process System with Distributed Parameters Based on the Enthalpy-Direction Factor Diagram," *Ind. Eng. Chem. Process Des. Dev.*, Vol. 21, pp. 690-695.
- Iyoki, S. and Uemura, T., 1990. "Performance Characteristics of Water/Lithium Bromide-Zinc Chloride-Calcium Bromide Absorption Refrigerating Machine, Absorption Heat Pump and Absorption Heat Transformer," *Int. J. Refrigeration*, Vol. 13, May, pp. 191-196.
- Koehler, W. J., Ibele, W. E., Soltes, J. and Winter, E. R., 1987. "Entropy Calculations for Lithium Bromide Aqueous Solutions and Approximation Equation," *ASHRAE Transactions*, Vol. 93, Part 2, pp. 2379-2388.
- Kotas, T. J., 1985. *The Exergy Method of Thermal Plant Analysis*, Butterworth, London.
- Lide, D. R., 1991. *Handbook of Chemistry and Physics*, 72th edition, CRC Press, Boca Raton, FL.
- McNeely, L. A., 1979. "Thermodynamic Properties of Aqueous Solution of Lithium Bromide," *ASHRAE Transactions*, Vol. 85, Pt. 1, PP. 413-434.
- Meacham, H. C., Cook, F. B., and Christensen, R. N., 1993. "Optimization of a Ten Ton Double-Effect Absorption Heat Pump," The 1993 ASME Winter Annual Meeting, New Orleans, LA, Nov. 28-Dec. 3, *Heat Pump and Refrigeration Systems Design, Analysis, and Applications*, AES-Vol. 29, ASME, pp. 65-73.
- Miyoshi, N., Sugimoto, S., and Aizawa, M., 1985. "Multi-Effect Absorption Refrigeration Machine," U.S. Patent No. 4,551,991.
- Modahl, R. and Hayes, F., 1992. "Development and Proof Testing of Advanced Absorption Refrigeration Cycle Concepts," ORNL/Sub/86-17498/1. Oak Ridge, TN.

- Mohanty, B. and Paloso, G., Jr., 1995. "Enhancing Gas Turbine Performance by Intake Air Cooling Using an Absorption Chiller," *Heat Recovery Systems & CHP*, Vol. 15, No. 1, pp. 41-50.
- Moore, W. J. 1972. *Physical Chemistry*, 4th edition, Prentice-Hall, Eaglewood Cliffs, New Jersey.
- Moran, M. J., 1989. *Availability Analysis: A Guide to Efficient Energy Use*, ASME Press, New York.
- Nerves, N. D., 1982. "The Second Way to Use the Second Law," *Chem Tech*, May, pp. 306-317.
- Oouchi, T., Usui, S., Fukuda, T., and Nishiguchi, A., 1985. "Multi-Stage Absorption Refrigeration System," U.S. Patent No. 4,520,634.
- ORNL, 1995. *ABSIM-Modular Simulation of Absorption Systems, User's Guide and Reference*, ORNL. Oak Ridge, TN.
- Ouimette, M. S., 1993. *Performance Modeling of a Triple Effect Absorption Chiller*, MS Thesis, University of Maryland, College Park.
- Patil, K. R., Chaudhari, S. K., and Katti, S. S., 1991. "Thermodynamic Design Data for Absorption Heat Transformers-Part III. Operating on Water-Lithium Iodide," *Heat Recovery Systems & CHP*, Vol. 11, No. 5, pp. 361-369.
- Perez-Blanco, H. and Grossman, G., 1981. "Cycle and Performance Analysis of Absorption Heat Pumps for Waste Heat Utilization," ORNL/TM-7852, Oak Ridge, TN.
- Peter, S., 1979. "Thermodynamics of Multicomponent Systems a Basic for Physical-Chemical Separation Process," *Int. Chem. Eng.*, pp. 410-418.
- Petrucchi, R. H., 1989. *General Chemistry*, 5th edition, Macmillan Publishing Company, New York.
- Porneala, S., Manole, D. M., and Lage, J. L., 1993. "Resorption and Absorption Systems for Recovery of Low Temperature Wasted Energy," The 1993 ASME Winter Annual Meeting, New Orleans, LA, Nov. 28-Dec. 3, *Thermodynamics and the Design, Analysis, and Improvement of Energy Systems*, AES-Vol. 30/HDT-Vol. 266, ASME, pp. 425-435.
- Rame, M. V. and Erickson, D. C., 1994. "Advanced Absorption Cycle: Vapor Exchange GAX," *Proc. of the International Absorption Heat Pump Conference*, New Orleans, LA, AES-Vol. 31, ASME, pp. 25-32.



- Rivera, W., Best, R., Hernandez, J., Heard, C. L., and Holland, F. A., 1994a. "Thermodynamic Study of Advanced Absorption Heat Transformers--I. Single and Two stage Configurations with Heat Exchangers," *Heat Recovery Systems & CHP*, Vol. 14, No. 2, pp. 173-183.
- Rivera, W., Best, R., Hernandez, J., Heard, C. L., and Holland, F. A., 1994b. "Thermodynamic Study of Advanced Absorption Heat Transformers--II. Double Absorption Configurations," *Heat Recovery Systems & CHP*, Vol. 14, No. 2, pp. 185-193.
- Sawada, N., Tanaka, T., and Mashimo, K., 1994. "Development of Organic Working Fluids and Application to Absorption Systems," *Proc. of the International Absorption Heat Pump Conference*, New Orleans, LA, AES-Vol. 31, ASME, pp. 315-320.
- Siddiqui, M.A., 1993. "Optimum Generator Temperatures in Four Absorption Cycles Using Different Sources of Energy," *Energy Conversion and Management*, Vol. 34, No. 4, pp. 251-266.
- Siddiqui, M.A., 1994. "Economic Analysis of the Operating Costs in Four Absorption Cycles for Optimizing the Generator and Condensing Temperatures," *Energy Conversion and Management*, Vol. 35, No. 6, pp. 517-534.
- Summerer, F., 1996. "Evaluation of Absorption Cycles with Respect to COP and Economics," *International Journal of Refrigeration*, Vol. 19, No. 1, pp. 19-24.
- Takada, S., 1982. *Absorption Refrigeration Machines*, Japanese Refrigeration Society, Tokyo, Japan (in Japanese).
- Tozer, R and James, R., 1994. "Thermodynamics of Absorption Refrigeration: Ideal Cycles," *Proc. of the International Absorption Heat Pump Conference*, New Orleans, LA, ASME Publication, AES-Vol. 31, pp. 393-400.
- Tozer, R. and James, R., 1995. "Absorption Chillers Applied to CHP Systems. *Building Services Engineering and Research Technology*, Vol. 16, No. 4, pp. 179-188.
- Tozer, R and James, R., 1997a. "Fundamental Thermodynamics of Ideal Absorption Cycles," *International Journal of Refrigeration*, Vol. 20, No. 2, pp. 120-135.
- Tozer, R. and James, R., 1997b. "Thermoeconomic Life-Cycle Costs of Absorption Chillers," *Building Services Engineering and Research Technology*, Vol. 18, No. 3, pp. 149-155.

- Trane 1989. "Single Stage Absorption Cold Generation," The Trane Company, ABS-DS-1, March 1989, La Crosse, WI.
- Tribus, M. and Evans, R., 1962. "The Thermoeconomics of Seawater Conversion," Report No. 62-63, University of California, Los Angeles, August 1962.
- Tsatsaronis, G., 1993. "Thermoeconomic Analysis and Optimization of Energy Systems," *Prog. Energy Combust. Sci.* Vol. 19, pp. 227-257.
- Valero, A., Tsatsaronis, G., von Spakovsky, M., Frangopoulos, C., Lozano, M., Serra, L. and Piza, J., 1994. CGAM Problem: Definition and Conventional Solution. *The International Journal of Energy*, Vol. 19, No. 3, pp. 279-286.
- Verma, S. K., Mekhjian, M. S., Sandor, G. R., and Nakada, N., 1999. "Corrosion Inhibition in Lithium Bromide Absorption Fluid for Advanced and Current Absorption Cycle Machines," *ASHRAE Transactions*, Vol. 105, Pt. 1, pp. 813-815.
- Vliet, G. C., Lawson, M. B., and Lithgow, R. A., 1982. "Water-Lithium Bromide Double Effect Absorption Cooling Cycle Analysis," *ASHRAE Transactions*, Vol. 88, Pt. 1, pp. 811-823.
- Waked, A. M., 1991. "Second Law Analysis of a Cogeneration Power-Absorption Cooling Plant," *Heat Recovery Systems & CHP*, Vol. 11, No. 2/3, pp. 113-120.
- Zemaitis, J. F., Clark, D. M., Rafal, M., and Scrivner, N. C., 1986. *Handbook of Aqueous Electrolyte Thermodynamics*, American Institute of Chemical Engineers, New York.
- Ziegler, F. and Alefeld, G., 1987. "Coefficient of Performance of Multistage Absorption Cycles," *International Journal of Refrigeration*, Vol. 10, September, pp. 285-295.
- Ziegler, F. and Alefeld, G., 1994. "Comparison of Multi-Effect Absorption Cycles," *Proc. of the International Absorption Heat Pump Conference*, New Orleans, LA, AES-Vol. 31, ASME, pp. 257-264.
- Zubair, S. M., 1994. "Thermodynamics of a Vapor-Compression Refrigeration Cycle with Mechanical Subcooling," *Energy*, Vol. 19, No. 6, pp. 707-715.

## BIOGRAPHICAL SKETCH

Shun-Fu Lee was born on March 7, 1966, in Sha-Lu, Taiwan. He completed his bachelor's degree in mechanical engineering from Tamkang University, Tamsui, Taiwan, in 1988, and received his master's degree in mechanical engineering from National Sun Yat-Sen University, Kaohsiung, Taiwan, in 1990. After that, he became an instructor in the Department of Electrical Engineering, Chin-Yi Institute of Technology and Commerce, Taichung, Taiwan. During his two years of teaching, he offered many courses in the field of thermodynamics, refrigeration, air-conditioning, fluid machinery, and automatic control. He enrolled in the doctoral program in the Department of Mechanical Engineering at the University of Florida in Fall, 1992. He is also a registered professional engineer (PE) in refrigeration and air-conditioning engineering in Taiwan.

I certify that I have read this study and that in my opinion it conforms to acceptable standards of scholarly presentation and is fully adequate, in scope and quality, as a dissertation for the degree of Doctor of Philosophy.



S. A. Sherif, Chairman  
Associate Professor of Mechanical  
Engineering

I certify that I have read this study and that in my opinion it conforms to acceptable standards of scholarly presentation and is fully adequate, in scope and quality, as a dissertation for the degree of Doctor of Philosophy.



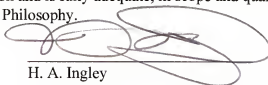
D. Yogi Goswami  
Professor of Mechanical  
Engineering

I certify that I have read this study and that in my opinion it conforms to acceptable standards of scholarly presentation and is fully adequate, in scope and quality, as a dissertation for the degree of Doctor of Philosophy.



Chung K. Hsieh  
Professor of Mechanical  
Engineering

I certify that I have read this study and that in my opinion it conforms to acceptable standards of scholarly presentation and is fully adequate, in scope and quality, as a dissertation for the degree of Doctor of Philosophy.



H. A. Ingle  
Associate Professor of Mechanical  
Engineering

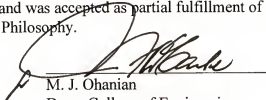
I certify that I have read this study and that in my opinion it conforms to acceptable standards of scholarly presentation and is fully adequate, in scope and quality, as a dissertation for the degree of Doctor of Philosophy.



C. Direlle Baird  
Professor of Agricultural and Biological  
Engineering

This dissertation was submitted to the Graduate Faculty of the College of Engineering and to the Graduate School and was accepted as partial fulfillment of the requirements for the degree of Doctor of Philosophy.

December, 1999



M. J. Ohanian  
Dean, College of Engineering

---

Winfred M. Phillips  
Dean, Graduate School